

PREDIS

Deliverable 6.6

Final Report on the Physico-chemical characterization of reconditioned waste form and stability testing

Date 30.8.2024 Final version

Dissemination level: Public

Emmi Myllykylä

VTT Technical Research Centre of Finland
Espoo, Finland

emmi.myllykyla@vtt.fi
tel. +358400261609



This project has received funding from the Euratom research and training programme 2019-2020 under grant agreement No 945098.

Project acronym PREDIS	Project title PRE-DISposal management of radioactive waste	Grant agreement No. 945098
Deliverable No. D6.6	Deliverable title Final Report on the Physico-chemical characterization of reconditioned waste for and stability testing	Version Final
Type Report	Dissemination level Public	Due date M47
Lead beneficiary VTT		WP No. 6
Main author Emmi Myllykylä (VTT)	Reviewed by Thierry Mennecart (SCK CEN)	Accepted by Maria Oksa (VTT) coordinator
Contributing author(s) Elena Torres Álvarez (CIEMAT), Eros Mossini and Andrea Santi (POLIMI), M. Cruz Alonso (CSIC), Raúl Fernández (UAM), Gianni Vettese (UH), Borys Zlobenko, Alla Rozko, Yuriy Fedorenko (SIIEG NASU) Karine Ferrand and Lander Frederickx (SCK CEN), H�el�ene Nonnet (CEA) Lucy Mottram and Russell J. Hand (USFD)		Pages 78

<p>Abstract</p> <p>This report describes the experiments and characterizations, which have been conducted to evaluate the disposability of candidate waste forms for radioactive solid organic waste (RSOW). The investigated candidate waste forms were geopolymers/ alkali activated materials, cements (CEM I, CEM II, CEM III), glass and ceramic materials. Partners contributing to this research were SIIEG NASU, UAM, CSIC, CIEMAT, POLIMI, UH, VTT, SCK CEN, USFD and CEA.</p> <p>WP6 "Innovations in solid organic waste treatment and conditioning" of the PREDIS project focused on the investigation and development of innovative technologies for volume reduction of RSOW by different methods and immobilization of reconditioned waste into solid matrices. In task T6.6 "Physicochemical characterization of reconditioned waste forms and stability testing" the research consisted of; short- and long-term leaching experiments, chemical characterization of leachants and analyses of possible changes in solid samples in leaching or immersion experiments. One of the main aims was to produce comparable results in the end of the project. Thus, common leaching protocol was created for the experiments and calculation of the results was also unified to achieve harmonized results.</p>
<p>Keywords</p> <p>Radioactive solid organic waste, RSOW, long-term performance, formulation, metakaolin, blast furnace slag, fly ash, material behaviour, MSO, ceramics, glass</p>

<p>Coordinator contact</p> <p>Maria Oksa VTT Technical Research Centre of Finland Ltd Kivimiehentie 3, Espoo / P.O. Box 1000, 02044 VTT, Finland E-mail: maria.oksa.@vtt.fi Tel: +358 50 5365 844</p>
<p>Notification</p> <p>The use of the name of any authors or organization in advertising or publication in part of this report is only permissible with written authorisation from the VTT Technical Research Centre of Finland Ltd.</p>
<p>Acknowledgement</p> <p>This project has received funding from the Euratom research and training programme 2019-2020 under grant agreement No 945098.</p>

TABLE OF CONTENTS

LIST OF ACRONYMS.....	6
1 INTRODUCTION.....	8
1.1 Background.....	8
1.2 Objectives.....	8
1.3 Methodology and harmonization of the results.....	9
2 CSIC, CIEMAT, AND UAM CONTRIBUTIONS.....	12
2.1 Sample preparation.....	12
2.1.1 Waste.....	12
2.1.2 Matrix.....	13
2.1.3 Waste encapsulation protocol.....	13
2.2 Leaching protocols.....	15
2.3 Results.....	16
3 POLIMI'S CONTRIBUTION.....	25
3.1 Samples preparation.....	25
3.1.1 Waste.....	25
3.1.2 Matrix.....	26
3.1.3 Waste encapsulation protocol.....	26
3.2 Ageing protocols.....	27
3.3 Leaching protocols.....	28
3.4 Results.....	28
4 VTT AND UNIVERSITY OF HELSINKI CONTRIBUTIONS.....	33
4.1 Sample preparation.....	33
4.1.1 Waste.....	33
4.1.2 Matrix.....	33
4.1.3 Waste encapsulation protocol.....	34
4.2 Leaching protocols.....	34
4.3 Results.....	36
5 SIIEG NASU CONTRIBUTION.....	38
5.1 Samples preparation.....	38
5.1.1 Waste.....	38
5.1.2 Matrix.....	39
5.1.3 Waste encapsulation protocol.....	39
5.2 Ageing protocols.....	40
5.2.1 Durability test after immersion.....	40
5.3 Leaching protocols.....	41

5.4	Results.....	42
6	SCK CEN CONTRIBUTION	45
6.1	Sample preparation.....	45
6.1.1	Waste	45
6.1.2	Matrix.....	46
6.1.3	Waste encapsulation protocol	47
6.2	Carbonation protocol	47
6.2.1	Results of carbonation	48
6.3	Leaching protocols	50
6.4	Results.....	50
7	CEA CONTRIBUTION.....	56
7.1	Samples preparation	56
7.1.1	Waste	56
7.1.2	Waste encapsulation protocol	56
7.2	Leaching protocols	57
7.3	Results.....	59
8	UNIVERSITY OF SHEFFIELD CONTRIBUTION.....	64
8.1	Samples preparation	64
8.1.1	Waste	64
8.1.2	Waste immobilisation protocol.....	64
8.1.3	Immobilised material.....	65
8.2	Leaching protocols	66
8.2.1	Sample preparation.....	66
8.2.2	Leaching protocols.....	67
8.2.3	Characterization.....	67
8.3	Results.....	68
9	SCK CEN CONTRIBUTION ON HIPED SAMPLES	73
9.1	Samples preparation	73
9.1.1	Waste	73
9.1.2	Matrix.....	73
9.1.3	Waste encapsulation protocol	73
9.2	Leaching protocols	73
9.3	Results.....	73
10	SUMMARY	76
	Remarks for future research	77
	REFERENCES	78

List of Acronyms

Alk _{tot}	Total alkalinity
ANSI	American National Standards Institute
ASTM	American Society for Testing and Materials
BFB	Bubbling fluidized bed
BSE	Back scattered electron
C3A	Tricalcium aluminate
CFL	Cumulative fraction leached
CEM	Cement
CH	Portlandite
CS	Compressive strength
CSH	Calcium silicate
D _e	Diffusion coefficient
DSC	Differential scanning calorimetry
DSW	Disposal site water
DTA	Differential thermal analysis
DW	Deionized water
EBS	Engineered barrier system
EC	European commission
EC	Electric conductivity
EDS	Energy dispersive spectroscopy
EDX	Energy dispersive X-ray spectroscopy
Eh	Redox potential
EWC	Evaporable water content
FA	Fly ash
FS	Flexural strength
FTIR	Fourier-transform infrared spectroscopy
GPO	Geopolymer
GW	Groundwater
HIP	Hot isostatic pressing
ICP	Inductively coupled plasma
ICP-MS	Inductively coupled plasma mass spectrometry
ICP-OES	Inductively coupled plasma optical emission spectrometry
IER	Ion exchange resin
ILW	Intermediate level waste
IXR	Ion exchange resin
LA-ICP-MS	Laser ablation Inductively coupled plasma mass spectrometry
LI	Leaching index
LLW	Low level waste
MAS NMR	Magic angle spinning Nuclear magnetic resonance
MCC	Materials Characterization Center
Micro-CT	Microtomography
MIP	Mercury intrusion porosimetry
MK	Metakaolin
MSO	Molten salt oxidation
NL	Normalized Loss
NMR	Nuclear magnetic resonance
OPC	Ordinary Portland Cement
Ph	Potential of hydrogen
PFA	Perfluoroalkoxy alkanes
PTFE	Polytetrafluoroethylene

rpm	rounds per minute
RSOW	Radioactive solid organic waste
RW	Radioactive waste
SA/V	Surface area per volume
SCW	Synthetic cement water
SEM	Scanning electron microscope
SIER	Spent ion exchange resin
TDS	Total dissolved solids
TG/DTA	Simultaneous Thermogravimetry and Differential Thermal Analysis
TOC	Total organic carbon
WP	Work package
WAC	Waste acceptance criteria
Wt%	Mass fraction
XAS	X-ray absorption spectroscopy
XANES	X-ray absorption near edge structure
XRD	X-ray diffraction
XRF	X- ray fluorescence

1 Introduction

The PREDIS project was a 4-year research act on “PRE-DISposal management of radioactive waste” granted by the European Commission’s (EC) Euratom Research Programme. The scope of the project included the development and improvement of activities for the characterisation, processing, storage and acceptance of different Low- and Intermediate-level (LLW/ILW) radioactive waste streams. In work package 6 (WP6) the focus was on treatment of Radioactive Solid Organic Wastes (RSOW) arising from nuclear plant operations, decommissioning and other industrial processes.

Work Package six (WP6) of the PREDIS project was focused on the treatment and conditioning of Radioactive Solid Organic Wastes (RSOWs). This document is presenting the achieved data on physicochemical characterisation and stability testing of different reconditioned waste forms investigated in WP6.

1.1 Background

Low and intermediate waste produced at nuclear power plants and industry. The activity inventory of RSOW is not necessarily high but the volume of the waste is relatively high in comparison to other waste types. The RSOW waste consists mainly of spent ion exchange resins (SIERs), operational waste (gloves, paper, fabric, etc.) produced in nuclear power plant operations (or decommissioning), and active waste from other industrial sources. [1]

So far, most of the waste that has been handled by binding the RSOW into matrices as bitumen and cement, and sealed into metallic barrels before removed disposal facility. [1]

PREDIS project was planned to help industry to screen various treatments methods and compare them. In WP6 geopolymers, cements with additives, glass and ceramic waste forms have been investigated for optional candidates for traditional waste forms for RSOW waste treatment methods.

Prior to the research on physico-chemical characterization and durability testing of created candidate waste forms there has been effort on volume reduction by thermal treatments and formulation of different waste forms. The more detailed results of these two subjects have been previously reported in Deliverables D6.1 [2] and D6.2 [3]

1.2 Objectives

To assess the safety of the repository, the behaviour and robustness of the candidate waste forms must be studied and understood. In this task, the focus is on physico-chemical behaviour, the performance of the final conditioned waste form. The disposability performance can be compared to “waste acceptance criteria” (WACs).

When disposed, the reconditioned RSOW waste forms might end up in contact with water during the lifetime of the repository. The interaction of waste matrix with leachant might lead to:

- Release of radionuclides from the conditioned waste form
- Degradation and chemical alteration of matrix under disposal conditions
- Changes in the physical properties of the waste matrix

Thus, the aim of the research in task 6.6 has been to study the chemical and mechanical durability of candidate waste forms produced in the previous tasks (6.3, 6.4 & 6.5)

This report introduces achievements of final task T6.6 in PREDIS WP6. Technical description starts with the descriptions of testing of geopolymer and cementitious materials, ends up to the contributions of research of glass and ceramic materials. Each contribution by partners, also contains background information about the waste and the reconditioned waste forms. However, the results of this report concentrate mainly on the achievements of leaching experiments, post-mortem

characterizations and comparison of different waste forms. There is a lot of data generated in task 6.6, more than we can present here in this report. Part that research has been already reported or published earlier. Some of the long-term experiments will continue and the results will be published later mainly in scientific publications.

1.3 Methodology and harmonization of the results

The thermal treated wastes, previously generated in Task 6.3 can be divided into 3 categories:

- Ashes produced from ion exchange resins (IER), which were tested by VTT, SIIEG, POLIMI, UAM, CSIC, and CIEMAT;
- IRIS ashes produced by CEA and tested by SCK CEN, POLIMI, and USFD;
- MSO residues produced CVRez and tested by SCK CEN and POLIMI.

In addition, some partners have added contaminants (Cs, Sr, Co, Ni, Ag, Ce, Nd, Eu, Th, U, B, Fe, Cr, Mn, Zn) into the surrogate waste before treatment, or alternatively doped the treated residues afterwards.

The matrices used for the encapsulation of the waste can be divided into the 3 different categories accordingly:

- Geopolymers or alkali activated materials based on metakaolin (MK), blast furnace slag (BFS) and fly ash (FA) tested by VTT, SIIEG, UAM, CSIC, CIEMAT, POLIMI, and SCK CEN;
- Cements (CEM I, CEM II, CEM III) tested by VTT, SIIEG, SCK CEN, UAM, CSIC, and CIEMAT;
- Glass and ceramic materials tested by, CEA, USFD and SCK CEN.

After curing, the samples of reconditioned waste were tested for short term leaching experiments (3 months) and long-term durability tests. Most of the partners used a PREDIS leaching protocol agreed by partners and End-user Group in the beginning of the project. The leaching solution is based on a synthetic cementitious water defined already in EURAD-ACED [4] for a generic ILW disposal cell. The chemistry of the selected leaching solution simulates the cementitious chemical environment, which will prevail in the most disposal facilities, if water intrudes into the drums and gets into contact with the waste form. The protocol included a series of key parameters, such as surface area to leachant volume ratio to guarantee the comparability of the results provided by different partners. Additionally, this protocol describes other experimental issues as sampling intervals and a common basic analyses of leachates and post-mortem characterization of solids. Table 1 gives the main perspectives of the PREDIS protocol, but the whole protocol is described more detail in Milestone report MS39 [5].

Several partners conducted additional leaching experiments according to their national interests. These studies included:

- CEA: glass monoliths leached according to ASTM Standard Test Method MCC-1 [6].
- CSIC-UAM-CIEMAT: cement- and geopolymer-based waste forms in national conditions (protocol based on ISO 6961:1982 and as leachants, ultrapure water and water sampled in the disposal platforms in the ILW-LLW facility)
- VTT & UH: geopolymer-based waste form in nationally relevant disposal site groundwater (both natural and synthetic)

For some experiments the ageing of the samples was accelerated either by freeze-thaw cycles or accelerated carbonation. These experiments are presented in Table 2.

Table 1. The main characteristics of the PREDIS leaching protocol

PREDIS Reference protocol		Additional information
Leachant	Synthetic cementitious water Composition for the leachant from EURAD. "CEM I + silica fume" synthetic water (without silica)	pH ~12.7 For 1 L: - 1.8858 g K_2SO_4 - 0.0774 g $CaSO_4 \cdot 2 H_2O$ - 50 ml 1 M KOH - 950 mL Milli-Q [®] water
Type	Semi-dynamic (each step refreshing the complete volume of leaching solution)	Changing frequency: 1st year 7 days, 14, 21, 28 d, and monthly there after 2nd year : 14, 16, 18 months and 2 years
Sampling intervals	Modified from ISO 6961-1982; Long-term leaching testing of solidified radioactive waste forms	1st year : 7 days, 14, 21, 28 d, and monthly there after 2nd year : 14, 16, 18 months and 2 years
Temperature	22 ± 2 ° C	Some partners will use also 40, 70 or 90 °C
Duration	At least 90 days (or until leaching rate has become constant) for short term studies AND 2 years for long-term studies	
Leachant/Specimen	Volume of the leachant / exposed " geometric " surface area of specimen" Ratio 0.10 ± 0.02 m (= 10 cm) between leachant volume and specimen external surface area.	Ratio means e.g. 10 cm ³ of solution per 1 cm ² of sample surface area. Ratio kept same, specimen geometry and size can vary

Table 2. Experimental conditions for the accelerated ageing of geopolymers and cement wastefoms

Organization	Accelerated degradation tests	Post-mortem characterization
SCK CEN	Accelerated carbonation for 3 months: 20°C, 60%RH, 1% atmospheric CO ₂	Expansion measurement, mechanical strength, carbonation depth by phenolphthalein spray, XRD, FTIR, SEM/EDX
POLIMI	Thermal cycling: -40 to 40°C, 1 month, 90%RH, ΔT>10°C/hour	Mechanical strength (compression strength)
POLIMI	Thermal cycling: -20 to 60°C, 5 days, 90%RH, instant temperature changes	Leaching following WP6 protocol and standard protocol [2]

The leaching experiments conducted by different partners are summarized in table 3.

Table 3. Description durability tests performed in the task 6.6.

Partner	Composition of matrix	Type of waste /contaminants of interest	Waste load %w/w	Ageing WP6 leaching protocol (Yes/No)	Leaching duration	Chapter
Geopolymer and alkali activated materials						
CSIC	MK+BFS+Na ₂ SiO ₃	Surrogates SIERS ashes. Contaminants: B, Cs, Sr and activation products (Fe, Co, Cr, Mn, Ni, Zn, Ag)	0 & 20	YES	24 months	2
UAM				YES, with ultrapure water		
CIEMAT				YES, with disposal site water		
POLIMI	Volcanic tuff, BFS, FA, NaOH and Na silicate	Surrogates SIERS ashes. Contaminants: Cs, Sr, Co, Ni, Ag, Ce, Nd, Eu, Th, U	0, 10 & 20	YES, with ultrapure water	18 months	3
	Volcanic tuff, BFS, steel slag, FA, NaOH and Na silicate	IRIS ashes (CEA) doped with contaminants: Cs, Sr, Co, Ni, Ag, Ce, Nd, Eu, Th, U	0, 20 & 30	Thermal ageing YES No, with ultrapure water	3 months 1 week	
		IRIS ashes (CEA) + Molten salts (MSO, CVRèz)	16/20 14/30	Thermal ageing YES No, with ultrapure water	3 months 1 week	
VTT & UH	MK+Na ₂ SiO ₃ /K OH	Surrogates SIERS ashes: Fe, Ce, Cs and Eu.	0, 15 & 50	Yes	24 months	4
SIIEG-NASU	MK+BFS+KOH+Na ₂ SiO ₃	Surrogates SIERS ashes: Cs, Sr, Ce	20	Yes Additionally with 0.1M NaOH	3 months	5
SCK CEN	MK+BFS+Na ₂ Si ₂ O ₅	Treated Molten Salts (MSO) (CV Rez): <i>no contaminants</i>	10 & 20	Carbonation No	3 months	6
Cement						
CSIC	CEM I/42.5 SR	Surrogates SIERS ashes. Contaminants: B, Cs, Sr and activation products (Fe, Co, Cr, Mn, Ni, Zn, Ag)	0 & 20	YES	24 months	2
UAM				YES, with ultrapure water		
CIEMAT				YES, with disposal site water		
VTT & UH	CEM I 42,5 N – SR3	Surrogates SIERS ashes: Fe, Ce, Cs and Eu	0, 15 & 50	Yes	24 months	4
SIIEG NASU	CEM II/A-LL 42,5-R	Surrogates SIERS ashes: Cs, Sr, Ce	20 & 30	Yes Additionally with 0.1M NaOH	3 months	5
SCK CEN	CEM III+BFS+FA+ Lime+limestone	Treated Molten Salts (MSO) (CV Rez): <i>no contaminants</i>	10 & 14	Carbonation No	3 months	6
Glass/ceramic						
CEA	HIPed	IRIS ashes	95	Yes Additionally MCC-1 standard [6]	3 months	7
USFD	HIPed, no additives versus NaAlO ₂ and Na ₂ B ₄ O ₇	IRIS ashes (CEA): <i>no contaminants</i>	95 & 100	Yes	24 months	8
SCK CEN	HIPed		95	Yes	24 months	9

2 CSIC, CIEMAT, and UAM CONTRIBUTIONS

2.1 Sample preparation

2.1.1 Waste

CIEMAT, CSIC and UAM used the same thermally-treated Spent Ion Exchange Resins (SIERs) surrogates in WP6. These surrogates consisted of a mixed bed IERs (Amberlite IRN-77 and IRN-78 in 50/50 ratio), that were doped according to the specifications provided by 2 of the Spanish end users. Exchange resins were saturated mainly with boron and traces of Sr, Cs and most relevant activation products (i.e. Co, Cr, Zn, Fe....).

The thermal treatment of the doped IER surrogates was performed in the fluidized-bed pilot plant in the "Waste-to-energy" technologies facility in CIEMAT Headquarters. Operational parameters were optimized in order to retain most part of the inventory in a highly-stable form. For that, a low temperature range ($450\pm 20^\circ\text{C}$) was selected in order to avoid the release of volatile elements, Cs and B mainly [2].

To assess the compatibility of the thermally-treated waste with the chosen conditioning matrices, a detailed physic-chemical characterization of the residue was carried out. Elemental analysis and minor components determinations were performed (Table 4 and Table 5).

Microstructural characterization of the obtained solid was done by means of FTIR, XRD, BET, SEM-EDS and LS particle size measurements. Complementarily, two leaching test series using ultrapure water (pH 7) and NaOH 1 M (~ pH 13, mimicking geopolymer porewater) were run in order to evaluate the ashes leaching behaviour and the impact that its degradation may have on the performance of the waste form.

Table 4. Elemental analysis (CNSH) and boron content of the SIERs prepared for Task 6.6.

Main elements (% wt.)	Carbon	Hydrogen	Nitrogen	Sulfur	Boron
	75	4	3	2	16

Table 5. Trace elements determined in the thermally-treated SIERs prepared for Task 6.6.

Traces (%wt.)	Co	Cr	Cs	Fe	Sr	Zn
	0.018	0.0018	0.15	0.0040	0.24	0.0048

The resulting waste exhibited a hygroscopic behavior with an initial water content of 3%wt. Ashes were an amorphous solid according to XRD patterns. FTIR spectra showed a partial thermally-induced degradation of the polymeric scaffold. Morphologically, the treated waste presented a granular morphology, with a mean particle size of 300- μm diameter (Figure 1). Results from the leaching showed a strong acidic behavior of the treated waste in both ultrapure water and NaOH 1M media.

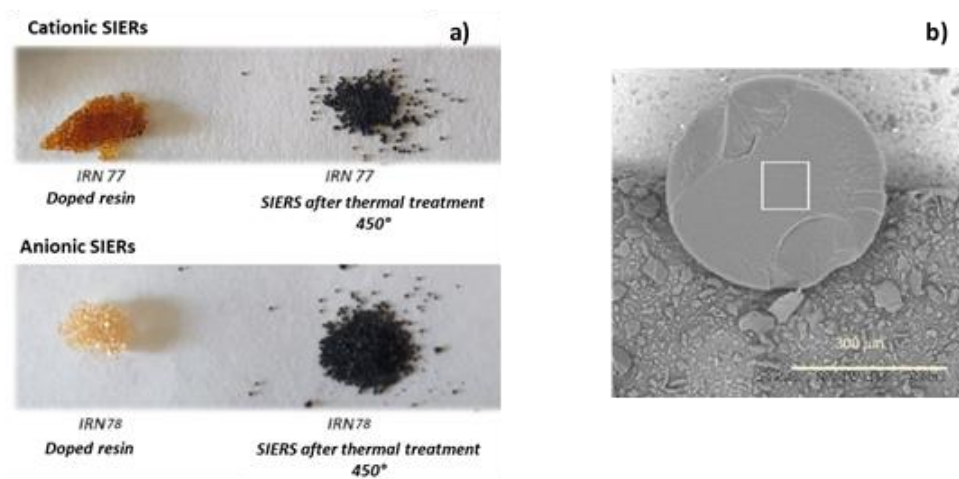


Figure 1. a) Photographs of SIERS surrogates before and after thermal treatment and b) SEM image of the thermally-treated SIERS bead.

2.1.2 Matrix

In task 6.6, three different matrices were used for the immobilisation of the surrogate SIERS described in the previous section: two types of Portland based cements and one geopolymer formulation, designed by CSIC in task 6.4.

As Portland cement systems, CEM I/42.5 SR, used as backfill in the national disposal facility, and CEM III/B 32.5, currently used for the conditioning of SIERS in Spain, were selected. The one-part geopolymer was based on metakaolin (MK) and blast furnace slag (BFS) as precursors, and $\text{Na}_2\text{SiO}_3/\text{NaOH}$ powders as the solid activators.

Chemical composition of the CEM I, CEM III, MK and BFS is shown in Table 6.

Table 6. Chemical composition (% wt. oxide, by XRF)

	SiO_2	Al_2O_3	Na_2O	MgO	CaO	K_2O	TiO_2	Fe_2O_3	SO_3	Others	LOI*
CEM I	17.4	4.7	0.2	1.8	60.3	0.3	-	5.0	3.2	2.9	4.2
CEM III	27.2	8.3	0.2	6.5	51.5	0.7	0.7	1.5	2.1	0.3	1.0
BFS	34.8	11.6	-	11.9	37.9	0.3	0.5	0.2	-	2.6	0.3
MK	55.9	38.9	-	0.1	0.1	0.5	1.6	1.2	-	0.3	1.4

*LOI: Loss of ignition $1000 \pm 5^\circ\text{C}$

2.1.3 Waste encapsulation protocol

The thermally-treated waste was incorporated in PC systems with a binder/cement ratio of 0.4, replacing 20% of the binder (%wt). In the case of the one-part AAC paste samples were prepared, in a first step, by the homogenisation of solid components, BFS/MK precursors, solid Na_2SiO_3 activator and SIERS surrogates in a high-shear mixer at 180 rpm for 2 min.

In all cases, after the homogenisation of the solids, water was added and all constituents were mixed at 1600 rpm for 3 min. Subsequently, the samples were cast in prismatic steel containers of $1 \times 1 \times 6 \text{ cm}^3$, and cured under controlled humidity conditions of 99% relative humidity and $22^\circ\text{C} \pm 2^\circ\text{C}$ until testing. Two sets of the specimens prepared for leaching tests in task 6.6 are shown in Figure 2.



Figure 2. Geopolymer specimens (a) without and (b) with thermally-treated SIERs prepared for leaching tests conducted in Task 6.6.

In Table 7, dosage used for the preparation of specimens tested in task 6.6 is displayed.

Table 7. Dosage of selected matrices for the fabrication of specimens for testing in task 6.6.

Component mass	Reference matrices			Matrices with the IER				
	One-part Geopolymer		CEM I	CEM III	One-part Geopolymer		CEM I	CEM III
CEM I 42.5 SR/MSR (g)		--	100.0	--		--	80.0	--
CEM III/B 32.5 N/SR(g)		--	--	100.0		--	--	80.0
Metakaolin (g)	42.5	60.7	--	--	34.0	48.5	--	--
Slag (g)	42.5	20.2	--	--	34.0	16.2	--	--
Solid Na ₂ SiO ₃ (g)	15.0	19.1	--	--	12.0	15.30	--	--
Waste IER (g)		--	--	--	20.0		20.0	20.0

Visual inspection of the prepared specimens did not detect major defects or surface chipping. All waste forms presented a good dimensional stability and homogeneous distribution of waste (Figure 3). Though addition of the treated waste resulted in a slight increase in porosity (Figure 4), in general, good waste-matrix cohesion was observed in all cases.



Figure 3. Prismatic specimens (1x1x6 cm) of CEM III and CEM III loaded with a 20 wt.% of thermally-treated IERs.

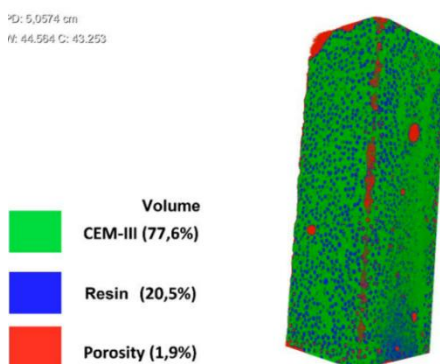


Figure 4. Porosity calculation based on micro-CT analyses performed in a CEM III prismatic specimen loaded with a 20 wt% of treated IERs.

2.2 Leaching protocols

The experimental programme planned by CIEMAT-CSIC-UAM for task 6.6. included a total number of 312 specimens to be tested. The three groups followed the experimental methodology defined in MS39 [5]. However, additionally and according to the Spanish national protocols, ultrapure water was used as leachant (UAM).

Disposability assessment has been a key issue in the contribution of the Spanish groups to task 6.6. For that purpose, water sampled from disposal vaults in El Cabril Facility was used for the leaching test series performed by CIEMAT. This Na-Ca-Mg-SO₄-HCO₃-type water presents a neutral pH (pH 7.2±0.2) and Electrical Conductivity (EC) values in the range of 520 ± 20 µS/cm.

Four leaching ages were selected, 3, 6, 12 and 18 months, in order to track degradation mechanisms of the waste forms and four replicates were tested per leaching age. In the case of CIEMAT experiments, the number of leaching tests had to be reduced due to the limited availability of water from the disposal site. A summary of the experimental conditions used is displayed in Table 8.

Table 8. Variables considered in the common leaching test programme defined by CIEMAT, CSIC and UAM.

Conditioning matrices	Waste loading (wt%)	Duration (months)	Leaching solutions	Replicates/leaching age
CEM I CEM III Geopolymer	0 - 20	3, 6, 12 and 24	Synthetic cementitious water (CSIC)	4
			Ultrapure water (UAM)	4
		6 & 24*	Water sampled in disposal vaults in El Cabril LILW facility (CIEMAT)	3*

*due to limited availability of water from site

An exhaustive characterisation of both, the solid and aqueous phases, was done co-ordinately by the 3 groups. For the pre-leaching and post-mortem characterisation of the tested specimens, analytical techniques proposed in the WP6 Leaching Protocol [5] were used, as well as additional ones, such as FTIR, TG/DTA, NMR or micro-CT. A list of the techniques used for the solid characterization and leachates analyses is shown in Table 9. Complementarily, and as part of the CIEMAT qualification testing protocol, mechanical resistance, water immersion and water-accessible porosity testing were performed.

Table 9. Analytical techniques for the pre-leaching and post-mortem characterization of solid and leaching solutions.

	Solid characterization	Leachates analysis
According to leaching protocol [5]	Mechanical testing (CSIC, CIEMAT, UAM)	Monitoring (pH, EC)
	XRD (UAM, CSIC)	Elemental analysis (ICP-OES / ICP-MS): <i>Indicators of matrix degradation: Al, Si, Ca, Na, K</i> <i>Immobilised elements: B, Co, Cr, Ni, Zn, Fe, Ag, Cs, Sr</i>
	BET (CIEMAT)	
	MIP (CIEMAT, CSIC, UAM)	
	SEM (UAM/CSIC/CIEMAT)	
Additional to leaching protocol	TG-DSC (CSIC)	E _n monitoring (CIEMAT)
	FTIR (CIEMAT, CSIC)	TOC (CIEMAT)
	Micro-CT (UAM, CSIC)	
	²⁹ Si and ²⁷ Al NMR (CSIC)	

2.3 Results

This paragraph summarizes most relevant results obtained in task 6.6. Additional information on the post-mortem characterization of tested specimens and leachates analysis are in [CIEMAT Data collection Task6 form.xlsx](#), [CSIC Data collection Task6 form.xlsx](#), [UAM Data collection Task6.6.xlsx](#) (available to PREDIS partners).

Qualification testing

Attending to results from qualification testing, in general, no significant differences were observed between CEM III (CEM III w/o 20%wt.RW), currently in use for SIERs conditioning in Spain, and geopolymer waste forms (GPO w/o 20%wt. RW) prepared for task 6.6.

Mechanical characterization of the studied waste forms (Figure 5) showed a slightly better performance of CEM III specimens compared to GPO samples for both, Compressive strength (CS) and flexural strengths (FS). However, in all cases, CS and FS values are far above the national mechanical WACs.

Similar results were obtained for water-accessible porosity (Table 10) and immersion tests performed (Figure 6). In the case of immersion testing, again CEM III waste forms exhibited moderately higher CS values after 90-day immersion in ultrapure water.

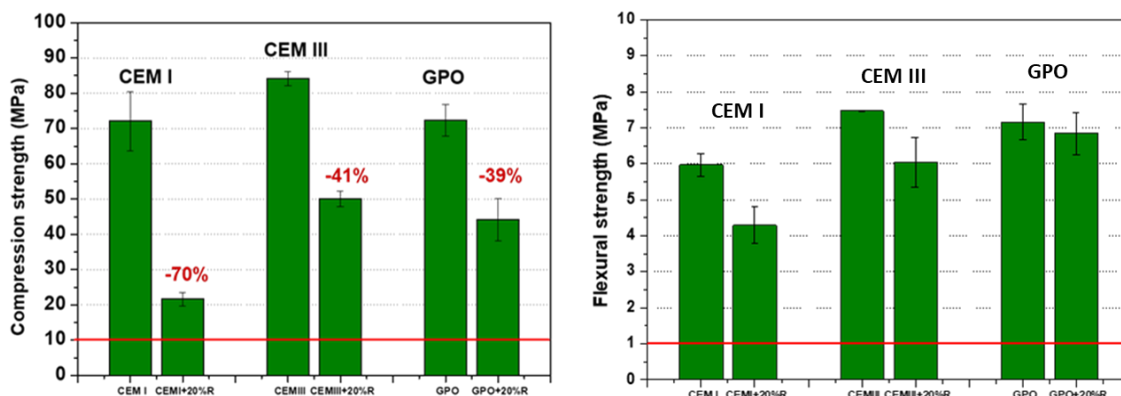


Figure 5. Mechanical characterization of tested wasteforms: (left) compression strength; (right) Flexural strength.

Table 10. Water-accessible porosity (%) measured for the tested waste forms.

	Water-accessible porosity (%)
CEM I	14.9
CEM I + 20%wt. RW	34.1
CEM III	12.9
CEM III+20%wt. RW	37.9
GPO	14.3
GPO20%wt. RW	25.9

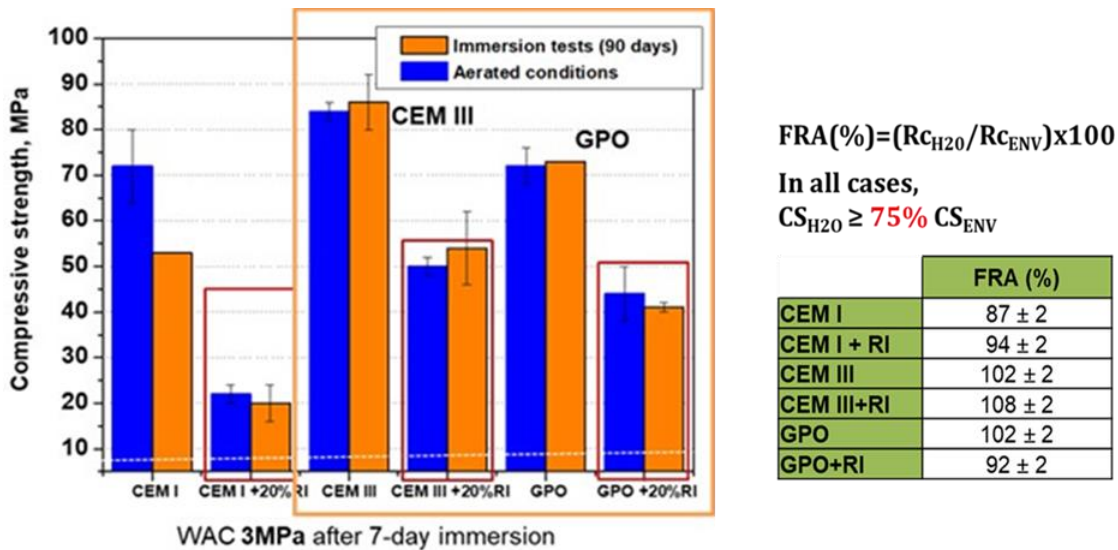


Figure 6. Compression strength measured after 90-day immersion testing in ultrapure water.

Post-mortem characterization

Mechanical characterization of the three types of waste forms was performed just after the dismantling of leaching tests (Figure 7). Results obtained showed no significant differences in Compression Strength (CS) values after leaching tests in the case of CEM I, CEM III and GPO specimens with immobilized waste. Despite the addition of the thermally-treated waste results in a decrease of CS, in all cases measured values were substantially greater than CS Spanish WAC (>10 MPa).

Similarly, according to MIP analyses, slight variations in total porosity were observed (Table 11). Regarding pore size distribution (Figure 8), pore diameter seems to decrease with increasing leaching time in the case of SCW, whereas in test where DSW was used, additionally to this refinement of the pore structure, an increasing proportion of pores >100µm was detected. The cause of this increase in macroporosity is uncertain and needs to be further studied and confirm at longer test ages of 24m.

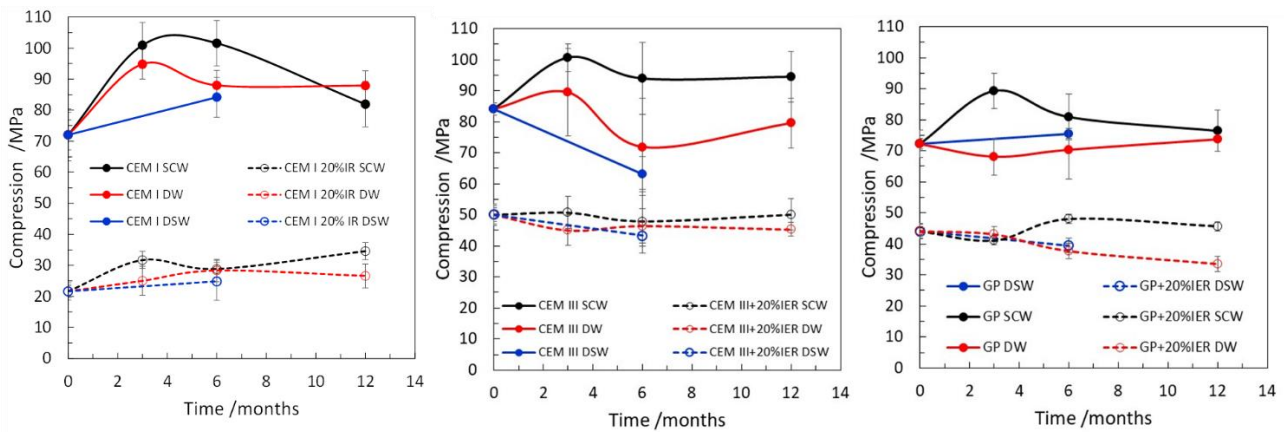


Figure 7. Post-leaching compression strength measured for the three leaching media.

Post-mortem characterization of the tested specimens, up to 1 year, confirmed that negligible microstructural changes have occurred in any of the tested wasteforms in any of the three leaching media used. XRD patterns showed a limited precipitation of crystalline phases such as, calcite (all wasteforms), portlandite and ettringite (OPC wasteforms) (Figure 9).

Table 11. MIP total porosity (%) measured after 6 month leaching tests in Synthetic Cement Water (SCW) and Disposal Site Water (DSW)

	MIP total porosity after 6 month-leaching tests		
	Pre-leaching porosity	Synthetic Cement Water (SCW)	Disposal Site Water (DSW)
CEM I	11.0	6.1	12.3
CEM I + 20%wt. RW	21.4	20.3	21.6
CEM III	9.8	6.1	8.1
CEM III+20%wt. RW	18.2	11.2	24.1
GPO	4.1	6.5	9.0
GPO20%wt+. RW	12.4	14.5	16.4

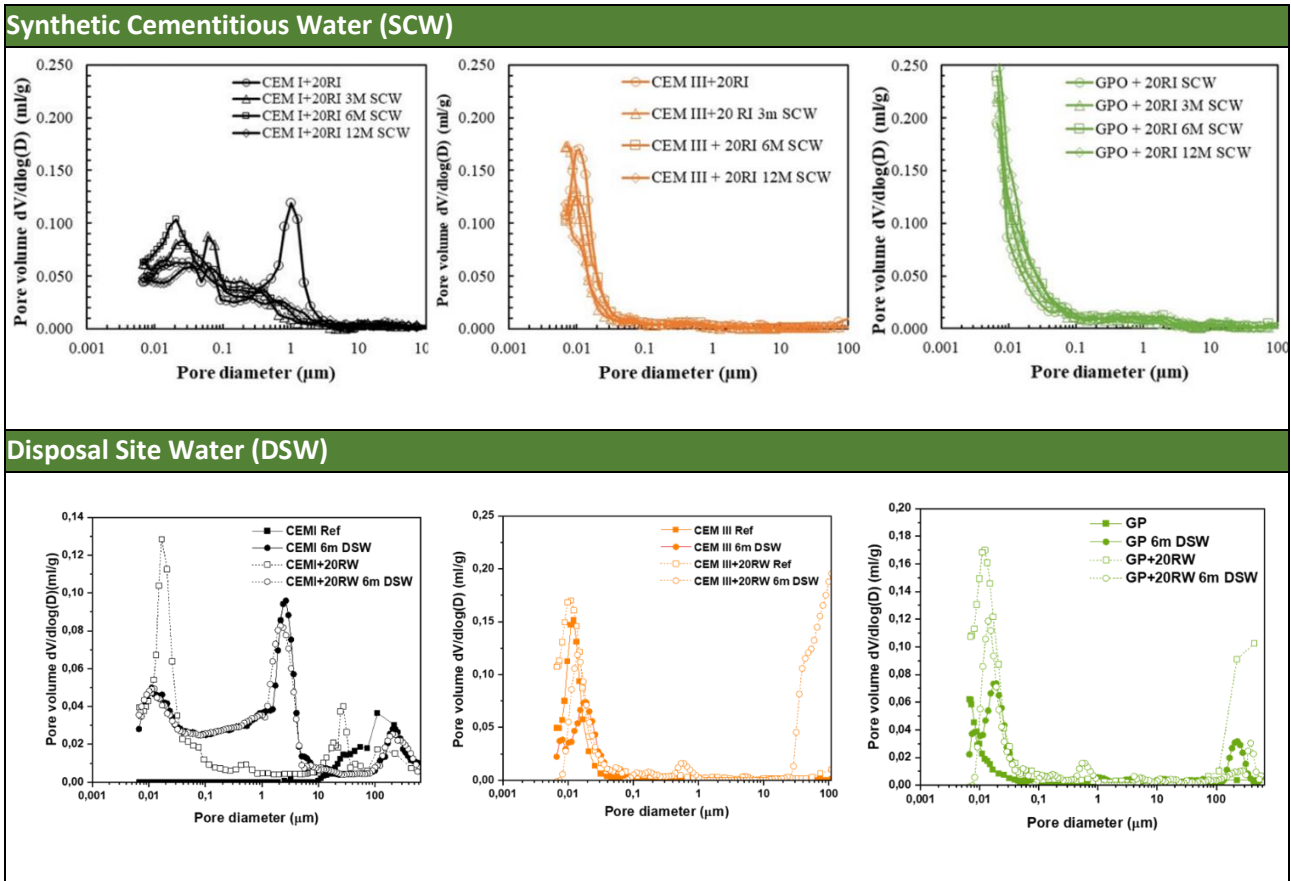


Figure 8. Pore size distribution determined for specimens tested in Synthetic Cementitious Water (SCW) and Disposal Site Water (DSW).

SEM-EDS analysis showed an enhanced Si and Al leaching the outer zones of the specimens, as well as a limited advance of the hydration front (Figure 10). Despite the extension of the alteration front was restricted to few hundreds of microns, it should be pointed out that the affected area was significantly greater in GPO waste forms (~450 μm after 12 months) than in CEM III-samples (~150 μm after 12 months).

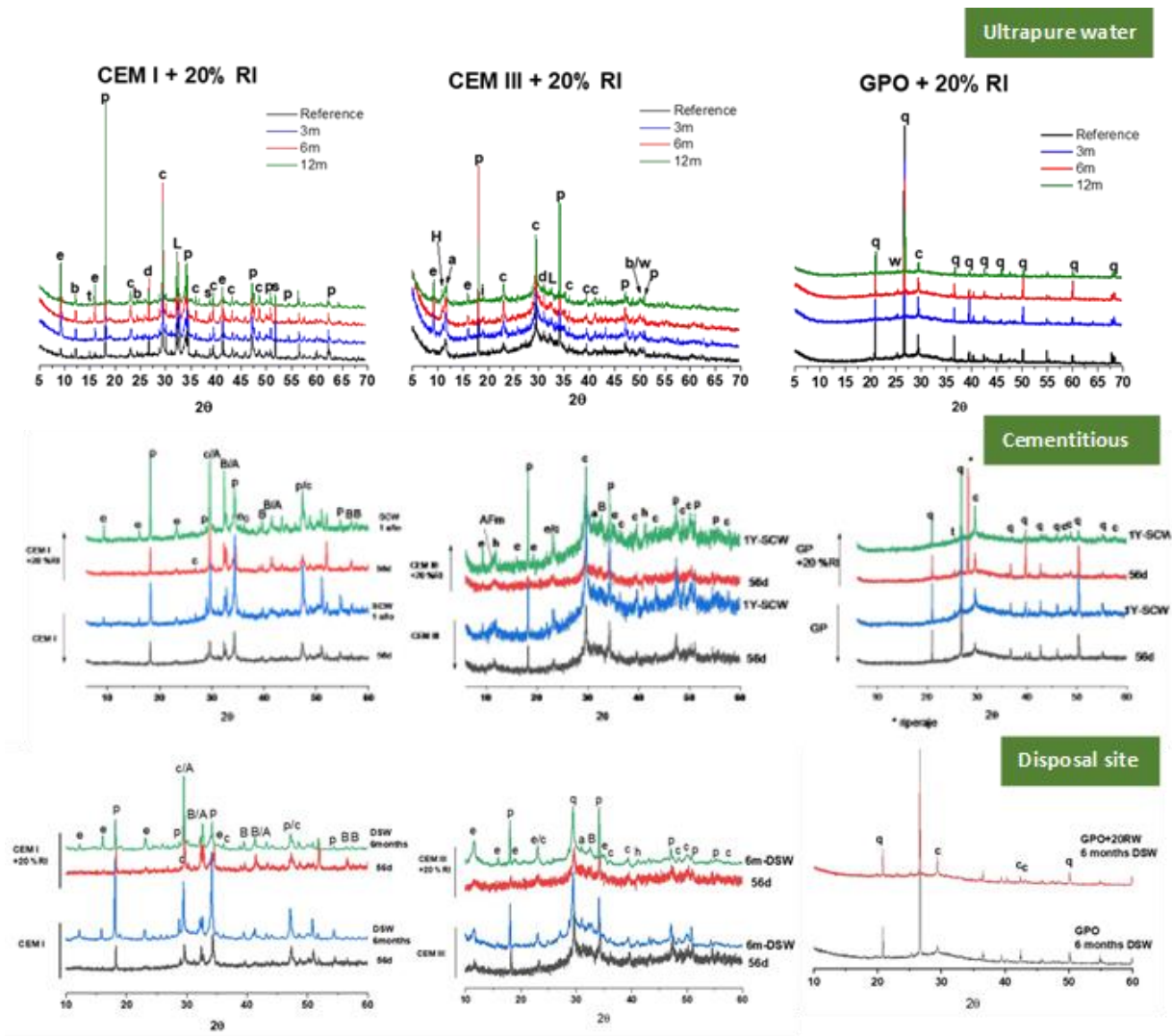


Figure 9. XRD post-mortem characterizations performed on tested specimens in Ultrapure water, Synthetic Cementitious Water and Disposal Site water.

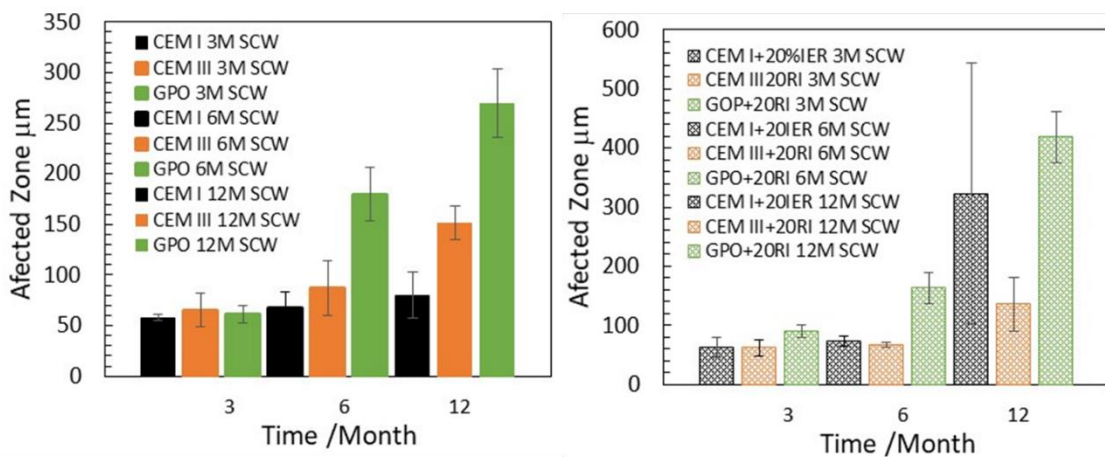


Figure 10. Extension of the alteration front in specimens tested in SCW, calculated on the basis of EDS analyses carried out on the samples.

Leachates analyses

Monitoring of pH and Electrical Conductivity (EC) confirmed the attenuation of leaching processes for all tested waste forms with increasing leaching time (Figure 11 and Figure 12). According to monitoring measurements, disposal site water exhibits a significant buffer capacity for all waste forms, which can turn out to be a positive aspect when considering disposability.

Normalized Losses (NLs) were calculated for main elements (Si, Al, Ca, Na) on the basis on ICP analyses of leachates. According to calculated NLs (Figure 13 and Figure 14), as expected, ultrapure water resulted the most aggressive medium for OPC-based waste forms, as it enhances Ca leaching. In the case of geopolymer waste forms, the synthetic cementitious water defined in the WP6 leaching protocol seems to favour Si and Al leaching from the matrix. This alkaline-induced dissolution may be of certain relevance for the assessment of the compatibility of GPO-based waste forms with existing cementitious EBS.

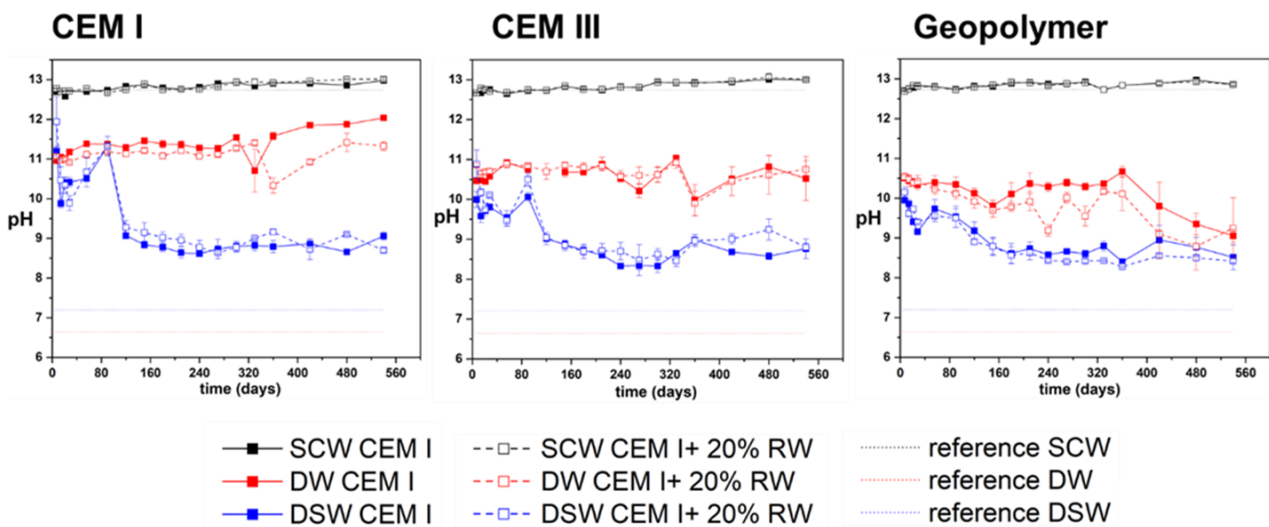


Figure 11. pH monitoring in the three leaching media.

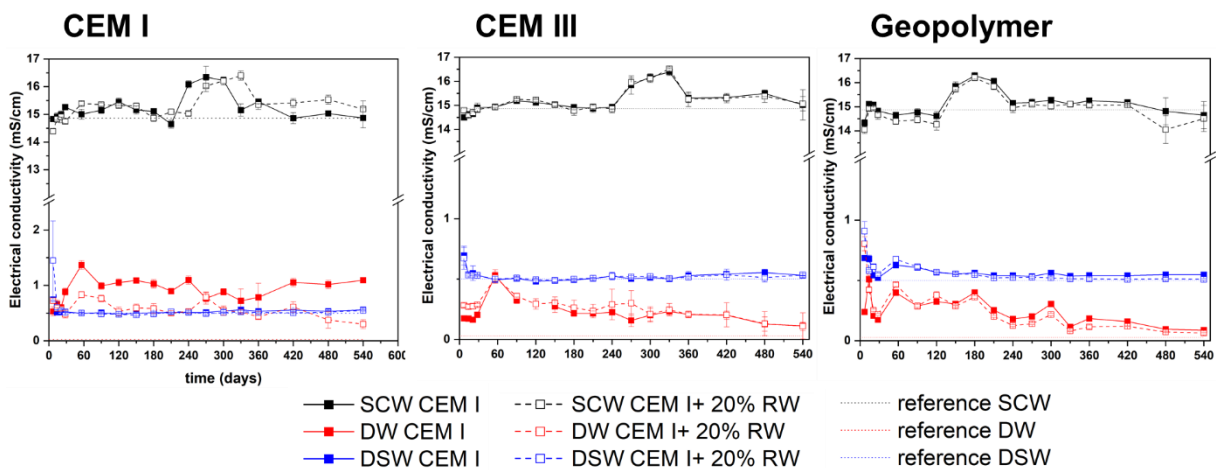


Figure 12. Electrical Conductivity monitoring in the three leaching media.

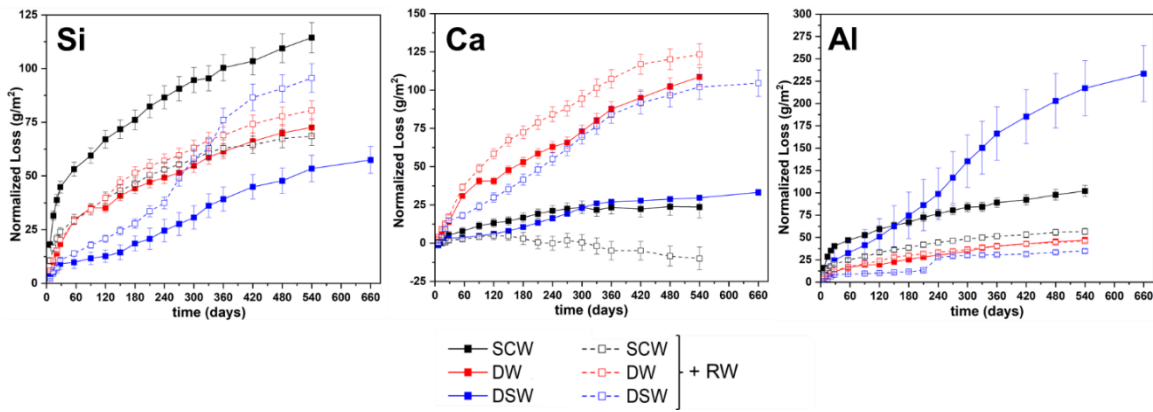


Figure 13. Normalized losses calculated for Si, Ca and Al for long-term leaching tests for CEM III specimens: a) SCW – Synthetic Cementitious Water; b) DW – Decarbonated ultrapure Water; c) DSW- Disposal Site Water

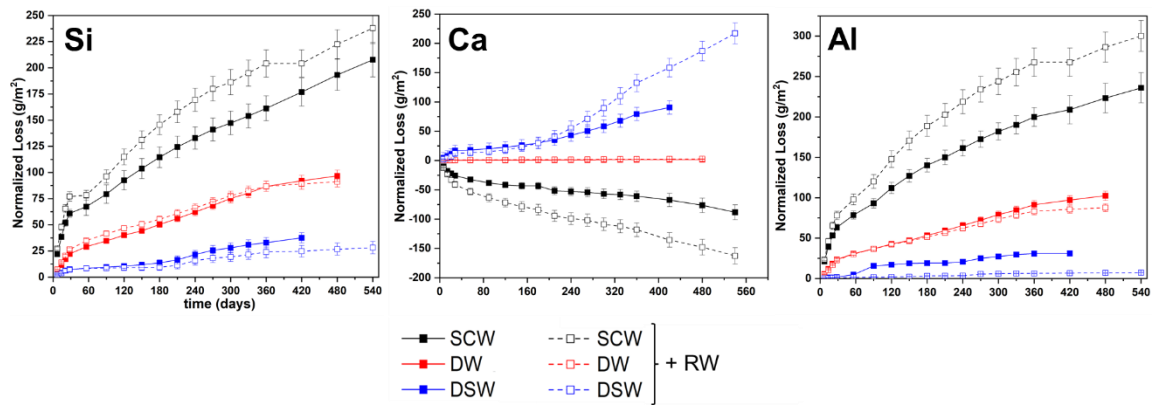


Figure 14. Normalized losses calculated for Si, Ca and Al for long-term leaching tests for GPO specimens: a) SCW – Synthetic Cementitious Water; b) DW – Decarbonated ultrapure Water; c) DSW- Disposal Site Water

Evaluation of the compatibility and stability of the immobilised waste in the novel conditioning matrices was a key issue of the contribution of the CIEMAT-CSIC-UAM groups. Apparently, thermally treated waste seems to be highly stable under alkaline conditions and exhibited an increased compatibility with all matrices studied if compared with the untreated SIERs. In this work, Boron values (Figure 15) as well as TOC measurements, were used as a tracer to assess waste degradation. TOC values (<5mgC/l) remained close to detection limit and thermally-treated waste did not seem to undergo significant alkaline-induced degradation processes in the temporal framework of PREDIS project.

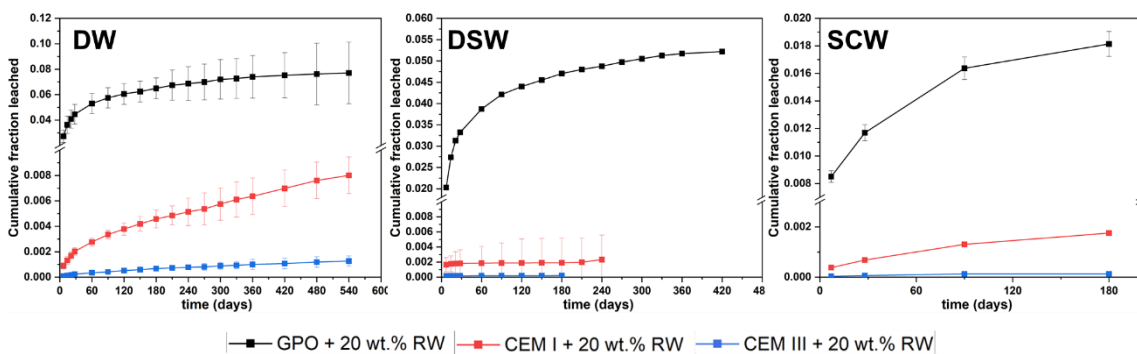


Figure 15. Cumulative Fraction Leached (CFL) of Boron in the three leaching media studied for CEM I, CEM III and GPO specimens with a 20%wt. waste loading.

Regarding leachability of the waste forms, Leaching Indexes (LIs) were calculated according to ANSI/ANS 16.1-2019 [7]. In the case of geopolymer waste forms, a significant improvement for Sr retention and similar leaching performance for Cs, compared to the current conditioning option (CEM III). Though, LIs calculated for geopolymer specimens were above the LI threshold defined by the standard (LI>6) for all doping elements (Cs, Sr and metallic elements), these waste forms presented unexpected drawbacks compared to conventional OPC matrices. Geopolymer waste forms exhibit a poorer leaching performance in alkaline medium. This fact is reflected on an increased Cs and Sr leachability and higher Si and Al Normalised Losses, as observed in Figure 14. Another issue that needs to be further studied is boron retention. Boron is retained to a lesser extent in the (C)-N-A-S-H network of geopolymer than in the CSH gels, where boron seems to be incorporated into the lattice.

In leaching tests where Disposal Site Water was used, precipitation of both, Cs and Sr, occurred due to their interaction with anions present in solution, i.e. carbonates, sulphates. These side reactions together with traces of Sr and Cs in the leachant do not allow to obtain a reliable LI value and have not included in the table below (Table 12).

Table 12. Leaching Indexes calculated for Cs and Sr for Decarbonated Ultrapure Water and Disposal Site Water (DSW)

LIs - 6 months	Cs		Sr	
Leachant	Ultrapure	Cement	Ultrapure	Cement
GPO+20RW	12.3	8.1	13.1	11.4
CEM III+20RW	11.9	12.4	7.7	10.1
CEM I+20RW	10.3	10.5	7.4	11.4
LIs - 18 months	Cs		Sr	
GPO+20RW	12.4	---	13.1	---
CEM III+20RW	12.2	----	7.7	----
CEM I+20RW	10.6	----	7.4	----

As a summary of all work done in Task 6.6, it should be pointed out that GPO matrix degradation was not significant after 1 year and a half and had a negligible influence on mechanical and physico-chemical characteristics. CEM III and GPO wastefoms exhibited similar mechanical and chemical performances. However, GPO-based matrices present some additional drawbacks compared to conventional CEM III specimens:

- The leaching response is highly dependent of the leachant composition.
- Poorer leaching performance in alkaline medium in comparison to ultrapure water, resulting on an increased Cs, although some higher retention for Sr leachability. This may be of certain importance for disposability assessment.
- Lower boron retention than OPC-matrices, which could be an issue of concern for boron-rich waste streams.
- In all cases the leachability indices are above the threshold of 6.0. Longer time spans are needed to assess long-term-performance.

On the basis of PREDIS results, three main research lines are planned to be address in the future projects:

- *Microbial degradation*: TOC values detected in leachates seem to be associated to the presence of biofilms. This fact together with the presence of high sulphide contents in BFS in CEM III and GPO may favour microbial growth as well as, enhance corrosion of metallic drums.

- *Compatibility of waste with GPO chemical environment:* GPO porewater (pH 13.2) is highly-aggressive for organic-based materials and may favour their alkaline-induced degradation. This could lead to the release of organics, which may have an impact on radionuclide re-mobilisation during disposal.
- *Ageing and durability assessment under disposal conditions* in order to extrapolate experimental results to representative time scales.

3 POLIMI's CONTRIBUTION

3.1 Samples preparation

Residues of organic wastes downstream of four different treatment processes have been encapsulated in the tuff-based matrix developed within the WP6: the ashes downstream of oxidative pyrolysis of cation-exchange resins developed at the Politecnico di Milano (POLIMI); the sludges coming from the treatment via Fenton-like wet oxidation varied out at POLIMI; the ashes from the IRIS incineration process managed by the French Atomic Energy Commission (CEA); the residues from the molten salt oxidation (MSO) pilot plant managed by the Centrum Výzkumu Řež (CVRez).

3.1.1 Waste

The oxidative pyrolysis is being developed at POLIMI and consists of a thermal treatment in which the resin beads are mildly heated up to 800 °C in a furnace to decompose the organic content while avoiding the volatilisation of contaminants. To work with representative conditions, the resin beads were loaded with stable isotopes of common fission and activation products, such as Cs, Sr, Co, Ni, Nd, and Eu. Downstream of the process, the ashes were characterized by means of XRD, Raman spectroscopy and ICP-MS, and comprise sulphates and oxides of the elements.

During the Fenton-like wet oxidation of cation-exchange resins, the organic content in the beads is oxidized by a reaction with hydrogen peroxide and iron ions provided by a catalyst. Downstream of the process, a liquor, rich in sulphuric acid and minor soluble organics, is evaporated into a sludge to reduce its volume.

The IRIS ashes were provided by CEA and comprise inorganic residues rich in aluminium and silicon oxides, with oxides of sodium, potassium and calcium as subordinate phases. Prior to encapsulation, the batches of IRIS ashes have been blended to break the particle clusters and obtain a fine powder, and characterized by means of X-ray powder diffraction (XRD) and inductively-coupled plasma mass spectrometry (ICP-MS) and optical emission spectroscopy (ICP-OES). (see paragraph 7.1.1)

The residues from MSO were provided by the colleagues from CVRez in three distinct batches with minor differences in terms of chemical and mineralogical compositions between each other. Prior to encapsulation, the batches were characterised via XRD, ICP-OES, and ICP-MS and blended to break the particle clusters and obtain a fine powder.

3.1.2 Matrix

Three recipes of the tuff-based matrix were employed to immobilise the treated wastes. The quantities of each component are reported in Table 13. The volcanic tuff is Zeolite Fertenia from Fertenia S.r.l. and is a micronized powder (0-5 μm). Fly ash (FA) and blast furnace slag (BFS) were provided by Buzzi Unicem and are powders with fineness of 0-100 μm and 0-300 μm , respectively. Steel slag is a byproduct of electric arc furnaces and was provided in the range 0-250 μm . Aluminium oxide was analytical grade (Merck). Sodium hydroxide (Martens) pellets and sodium silicate solution (35 wt.%, Chimitex) are technical-grade reagents. Sand (Axton) is in the range 0-2 mm and is mainly quartz, with traces of carbonates. All the reagents were employed with no further processing; only the sand was washed with de-ionized water and dried at 50 °C to remove excess humidity.

Table 13: Reference recipes for the tuff-based matrices.

Formulation	Material	Composition (wt.%)
Recipe 1	Volcanic tuff	11
	Fly ash	18
	Blast furnace slag	18
	Aluminium oxide	8
	Sodium hydroxide	8
	De-ionized water	37
Recipe 2	Volcanic tuff	23
	Fly ash	20
	Blast furnace slag	21
	Aluminium oxide	3
	Sodium hydroxide	5
	Sodium silicate solution	2
Recipe 3	De-ionized water	26
	Volcanic tuff	18
	Fly ash	16
	Blast furnace slag	16
	Aluminium oxide	2
	Sodium hydroxide	4
	Sodium silicate solution	2
	Steel slag	8
Sand (0-2 mm)	12	
De-ionized water	22	

To synthesise the matrices, the powders were weighted and homogenised. Afterwards, the NaOH pellets, the sodium silicate solution and the water were added to the mixture. The fresh grout was mixed for 10 minutes at mid-low speed in a planetary mixer and then poured into moulds: 5-cm cubes and 3-cm equilateral cylinders. Demoulding was performed after 3, 7 or 14 days depending on the setting time of the matrix (or waste form), and the hardened specimen was cured in a water-saturated environment (relative humidity greater than 90%) until 28 days of overall curing. Testing and characterization followed thereafter.

3.1.3 Waste encapsulation protocol

In the case of IRIS ashes, the treated waste was directly added to the powdery precursors and mixed with them prior to the addition of water and the activators. The same procedure was followed to immobilise the waste treated via MSO. In this case, however, because of the strong interaction of the residues with the water in the fresh grouts, IRIS ashes were added to the recipe as well to delay the setting of the formulation and, thus, allow stabilisation of the carbonates within.

Downstream of the oxidative pyrolysis, due to the high volumetric reduction of the beads and to the small scale to which the process is being developed, relatively small amounts of ashes were found, not suitable to investigate their encapsulation in the matrix. To cope with this issue, surrogate ashes were prepared by mixing sulphates and oxides of Cs, Sr, Co, Ni, Nd, and Eu, coherently with the results from the characterisations. Eventually, the sludges downstream of the Fenton-like oxidation were encapsulated in the tuff-based matrix. Prior to immobilisation, the sludges were reacted with sodium hydroxide pellets to bring the pH in the interval 7-10. It was found that 0.4 g of NaOH per 1 g of sludge was enough. The neutralised sludge was then incorporated into the freshly activated matrix with a 5-minute mixing at mid-low speed in the planetary mixer. Because the catalysis of the Fenton-like treatment is carried out with fly ash, which is found downstream of the process in the sludge, the amount of fly ash in the matrix recipe was reduced by the amount of fly ash within the encapsulated sludge.

Overall, the waste encapsulation factor f was defined as follows:

$$f = \frac{m_w}{m_{wf}}$$

where m_w is the mass of the treated waste and m_{wf} is the mass of the waste form.

Table 14 reports the main pieces of information related to the investigated waste forms. Contaminants such as Ce, Ag, Ba, Th and U were added in the matrix at concentrations of approximately 100 ppm by means of multi-elemental ICP-MS/OES calibration standard solutions.

Table 14: Characteristics of the synthesised specimens.

Waste form	Matrix	Waste	Loading factor	Contaminants
001			0 wt.%	
IA1	Recipe 1	IRIS ash	10 wt.%	
IA2		IRIS ash	20 wt.%	
002			0 wt.%	
OP1	Recipe 2	Oxidative pyrolysis ash	10 wt.%	Cs, Sr, Co, Ni, Nd, Eu, Ag, Ce, Th, U
OP2		Oxidative pyrolysis ash	20 wt.%	Cs, Sr, Co, Ni, Nd, Eu, Ag, Ce, Th, U
003			0 wt.%	
WO1		Wet oxidation sludge	6 wt.%	
WO2		Wet oxidation sludge	12 wt.%	
IA3	Recipe 3	IRIS ash	20 wt.%	Cs, Sr, Co, Ni, Nd, Eu, Ag, Ba, Ce, Th, U
IA4		IRIS ash	30 wt.%	Cs, Sr, Co, Ni, Nd, Eu, Ag, Ba, Ce, Th, U
MS1		IRIS ash + MSO residue	16 wt.% + 20 wt.%	Cs, Sr, Co, Ni, Nd, Eu, Ag, Ba, Ce, Th, U
MS2		IRIS ash + MSO residue	14 wt.% + 30 wt.%	Cs, Sr, Co, Ni, Nd, Eu, Ag, Ba, Ce, Th, U

3.2 Ageing protocols

Waste forms loaded with IRIS ashes and MSO residues in recipe 3, namely specimens “003”, “IA2”, “IA3”, “MS1”, and “MS2”, underwent thermal ageing prior to lixiviation. Such an ageing was performed by putting the specimens in a sealed bag and by carrying out 5 cycles, 24 hours each, between two environments set at $-20\text{ }^{\circ}\text{C}$ and $+60\text{ }^{\circ}\text{C}$.

Other two ageing protocols, unrelated to lixiviation tests, were performed according to the Italian acceptance criteria:

- 1 month of thermal cycles between $-40\text{ }^{\circ}\text{C}$ and $+40\text{ }^{\circ}\text{C}$, at relative humidity greater than 90%, with temperature changes greater than $10\text{ }^{\circ}\text{C}/\text{hour}$;
- 3 months of static immersion in de-ionized water.

The criterion for these tests was a minimum compressive strength of 10 MPa downstream of the ageing.

3.3 Leaching protocols

Three lixiviation protocols were followed: the ANSI/ANS-16.1-2003 protocol (ultrapure water as leachant, 2 weeks of semi-dynamic immersion), ANSI/ANS-16.1-2019 protocol (ultrapure water as leachant, 5 days of semi-dynamic immersion), the latter being imposed by the Italian regulator, and one developed within the Work Package 6 (WP6) of the PREDIS project (synthetic cementitious water as leachant, 3 months of immersion, MS39 [5]). An extended version of the ANSI/ANS-16.1-2019 protocol was followed up to 1.5 years to simulate long-term behaviours. For the lixiviation tests, cylindrical specimens were employed. Prior to lixiviation, cubic specimens were tested for compressive strength and characterised by means of XRD. Analyses of the leachates was performed via ICP-MS and ICP-OES. In all the lixiviation tests, the amounts of Ag, Ba, Ce, Nd, Eu, Th, and U leached from the samples fell below the detection and quantification limits of the instrumentation and, therefore, the corresponding leachability indexed could not be computed.

3.4 Results

The IRIS ashes were successfully immobilised in the tuff -based matrix (recipe 1) up to 20 wt.% loading. A compressive strength greater than 10 MPa is obtained, even after a two-week immersion. The setting time increases from approximately 1 hour for the matrix to approximately 7 hours for the specimen loaded at 20 wt.%. As can be seen in Figure 16, the mechanical performances of the waste forms increase with increasing ash loading, indicating interaction of the waste with the matrix. This is confirmed by XRD, in which some diffraction peaks characteristic of the IRIS ashes, namely those of chlorapatite, diopside pyroxene, anhydrite, spinel and plagioclase, are absent or less intense in the diffraction patterns of the resulting waste forms. The increased compressive strength brought by the waste can be attributed to its reactive silica- and alumina-based species, which contribute to an improved Si/Al ratio in the matrix. Coherently, the degree of amorphousness in the waste forms increases, in agreement with the mineralogical structure of geopolymeric and alkali-activated materials. Concerning the lixiviation properties, the waste forms loaded at 10 and 20 wt.% exhibit greater releases of matrix constituents, such as Na, Al, Si, Ca, very comparable to each other. The leaching rates of those elements increase about a factor two when the ashes are concerned. Na is the most leached element, because of its mobility and the low selectivity of the zeolites in the tuff towards this element. Despite this, the high releases of Na suggest that the microstructure of the loaded forms is more of the alkali-activated type rather than geopolymeric, with open frameworks from which ions can leach more easily.

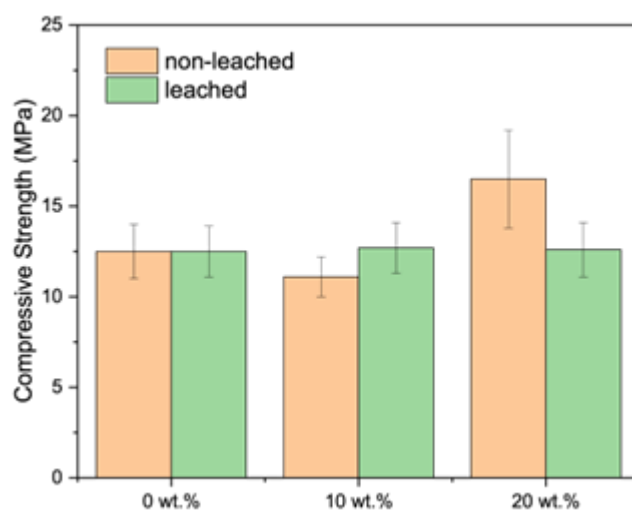


Figure 16: Compressive strength of waste forms synthesised with IRIS ashes in recipe 1.

When the IRIS ashes are immobilised in the tuff-based matrix (recipe 3), less interaction of the waste with the matrix is observed. Indeed, even though the third recipe is endowed with improved compressive strength and retention with respect to the first one, when the waste replaces part of the matrix the performances drop. This can be understood from the compressive strengths of the waste forms synthesised with the third recipe, which are reported in Table 15. With the first recipe, at 20 wt.% loading there is an increase in the strength, as outlined in Figure 16, while a drop of about a factor two is observed for the third recipe. This may be related to the lower alkalinity of the new formulation, which may be insufficient to promote activation of the IRIS ashes. The lower interaction of the waste in this case can also be deduced by the fact that the increase in the release rates of the matrix constituents is somewhat proportional to the amount of loaded ash. This can be explained, once again, with the substitution of the structural part of the matrix with a more inert one of the waste.

Table 15: Compressive strength values for the IRIS ashes immobilised in the third recipe.

Waste form	Waste loading	Compressive strength (MPa)
003	0 wt.%	18.9 ± 1.9
IA3	20 wt.%	9.2 ± 1.4
IA4	30 wt.%	2.9 ± 0.4

The specimens in Table 15 underwent thermal ageing for 1 week and subsequent lixiviation following the protocol from PREDIS WP6 and the ANSI/ANS-16.1-2019 protocol. For K and S, a different behaviour was observed between the two tests: these two elements were uptaken over time by the specimens when the synthetic cementitious water was employed, while were released in the ultrapure water when the other protocol was followed. Both these opposites behaviours are diffusion-driven, for release/uptake profile linearly evolve against the square root of time. For other elements, both matrix constituents and contaminants, a diffusion-driven release from the specimens was observed. Overall, a slight difference in the leachability indices of some contaminants can be appreciated between the two protocols, as reported in Figure 17. Because the leachability index increases with decreasing release of the species from the waste forms, the increased aggressiveness of ultrapure water (ANSI/ANS-16.1-2019) with respect to the synthetic cementitious solution (PREDIS WP6) is confirmed. Concerning the thermal ageing, it was observed that the performed ageing did not appreciably affect the retention properties of the species, as shown in Figure 17.

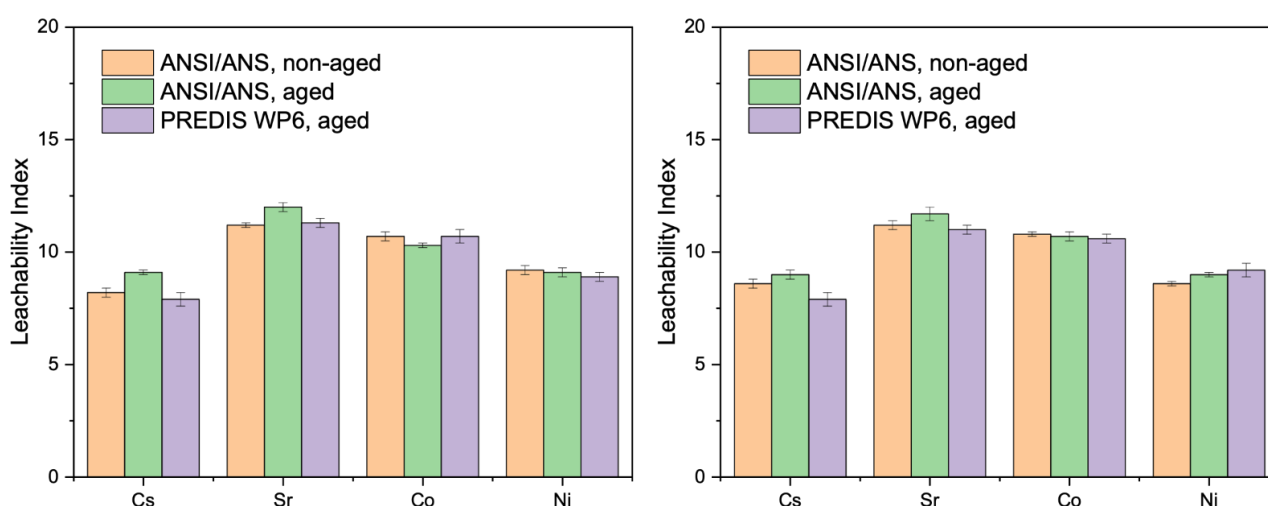


Figure 17: Leachability indices for specimens loaded with IRIS ashes, lixiviated according to PREDIS WP6 and ANSI/ANS-16.1-2019 protocols: 20 wt.% loading (left); 30 wt.% loading (right).

When ashes from oxidative pyrolysis are encapsulated in the tuff-based matrix (recipe 2), little drop in mechanical performances is observed. Indeed, the compressive strength drops from 23.7 ± 2.1

MPa of the matrix to 19.9 ± 2.0 and 21.5 ± 2.3 MPa of the waste forms loaded at 10 and 20 wt.%, respectively. The same occurs for the behaviour towards lixiviation (1.5 years). As reported in Figure 18, the leachability indices for the contaminants do not significantly vary with varying waste loading. Overall, the release of both matrix constituents and contaminants is diffusion-driven. For elements which are dominant in the matrix, such as Na and K, different diffusion coefficients can be derived over time, as depicted in Figure 19. This can be related to microstructural changes inside the matrix. For the aforementioned elements (Na and K), the released fraction is rather high. This suggests that the matrix is more of the alkali-activated type.

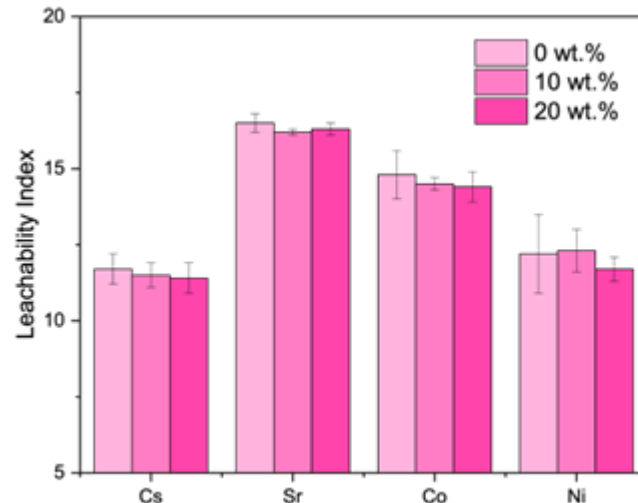


Figure 18: Leachability indices of some contaminants for specimens loaded with ashes from the oxidative pyrolysis treatment.

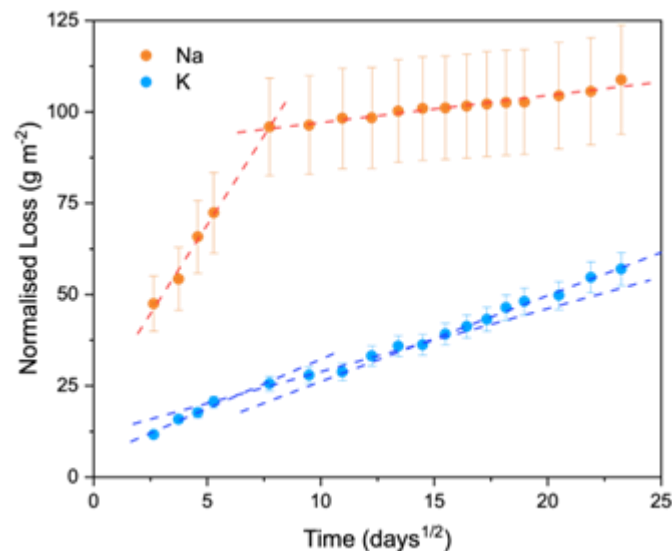


Figure 19: Cumulative releases of Na and K from waste forms loaded with ashes from oxidative pyrolysis.

The neutralization/alkalination of the sludges downstream of the Fenton-like wet oxidation treatment allows to obtain hardened waste forms with satisfactory properties in terms of compressive strength and resistance towards lixiviation-immersion. The diffraction pattern of the matrix exhibits peaks of zeolite chabazite, quartz, mullite and wuestite coming from the parental precursors, while peaks of calcite, mirabilite and larnite appear in the pattern of the specimens loaded with the sludges. During lixiviation, the release of matrix constituents is diffusion-driven. The diffraction pattern post-mortem exhibits peaks of quartz, zeolite chabazite, and wuestite which are preserved, while new peaks

related to vaterite and thenardite. The transformation of the mirabilite ($\text{Na}_2\text{SO}_4 \cdot 10 \text{H}_2\text{O}$) into thenardite (Na_2SO_4) allows to explain the high releases of sodium and sulphur from the waste forms, for a part of the mirabilite is easily dissolved by the leachant (ultrapure water).

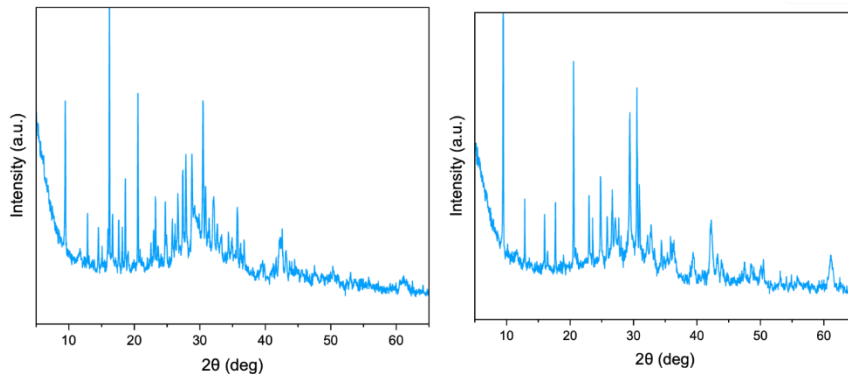


Figure 20: Diffraction patterns of the waste forms loaded with sludges from wet oxidation: before immersion (left), after lixiviation (right).

The encapsulation of residues from MSO returns waste forms with unsatisfactory properties. The addition of IRIS ashes as a setting retarder allows to stabilise the matrix towards environments with high humidity, but the dominant presence of natron ($\text{Na}_2\text{CO}_3 \cdot 10 \text{H}_2\text{O}$), thermonatrite ($\text{Na}_2\text{CO}_3 \cdot \text{H}_2\text{O}$) and gaylussite, coupled with a high replacement of the matrix with the wastes, namely IRIS ash and the MSO residue, still hinder the development of satisfactory performances in the hardened forms. Indeed, only the specimen loaded at 20 wt.% of MSO residues withstands one week of immersion, while the one at 30 wt.% loading dissolves in ultrapure water. This is coherent with the results from compressive strength, which are 12.4 ± 1.9 and 5.7 ± 0.9 MPa for 20 and 30 wt.% loading, respectively. When it comes to thermal ageing, none of the loaded specimens withstand the freeze-thaw cycles, and they easily dissolve when put in contact with both the ANSI/ANS and the PREDIS WP6 leachants within a couple of hours.

Specimens prepared by loading the IRIS ashes in the third recipe of the tuff-based matrix underwent ageing by immersion in de-ionised water for 90 days and freeze-thaw cycles between $-40 \text{ }^\circ\text{C}$ and $+40 \text{ }^\circ\text{C}$ at relative humidity greater than 90%. The two protocols do not significantly affect the mechanical properties of the matrix, as can be seen from Figure 21. This is not only related to the stability of the matrix towards these stimuli, but also to the progression of the curing and, therefore, to the simultaneous development of the strength of the matrix.

Additional information on the post-mortem characterization of tested specimens and leachates analysis is available in [POLIMI Data collection Task6.6.xlsx](#) (available to PREDIS partners).

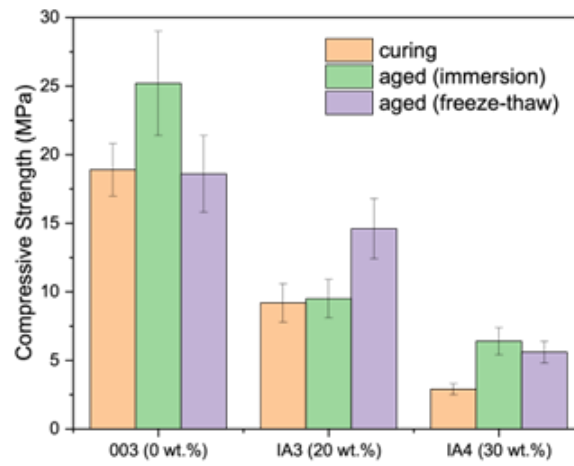


Figure 21: Compressive strength of specimens loaded with IRIS ashes downstream of the immersion and freeze-thaw ageing.

4 VTT and UNIVERSITY OF HELSINKI CONTRIBUTIONS

4.1 Sample preparation

4.1.1 Waste

The initial waste was unspent organic ion exchange resin (sulfonated styrene IXR). One resin batch was impregnated with Europium, Cerium and Cesium-(for test run PR-3) as analogues of actinides, (An^{3+} and An^{4+} species) and activation products, present in real L-ILW waste. For the test run PR-4, another IXR batch contained in addition to Ce, Eu and Cs also Fe_2O_3 (8 wt-% of dry IXR). Batches were gasified in test trials with an atmospheric pressure bench-scale Bubbling Fluidized Bed (BFB) gasifier (Figure 22) at Bioruukki - VTT's Piloting Center. The gasification of doped IXR (dry feed of 16.5 kg) resulted in 680 g filter dust in the test run PR-3. In the test run PR-4, 12.5 kg of dry doped IXR was reduced to 630 g filter dust, meaning that the amount of the waste was reduced ~95%. More detailed information of the gasification and related results can be found in PREDIS Deliverable 6.1 [2]. The elemental composition of produced dusts was analyzed from digested samples with ICP-OES and HR-ICP-MS. CHN and ash contents in the feed (IXR) and produced dusts were determined by Vario Max CHN-analyzer and by Leco TGA701 Thermogravimetric analyzer. In addition, the produced dusts were studied with XRD and SEM. After the gasification process, the produced dusts contained also other stable analogues for activation products, such as Sr, Cr, Co, and Ni.

In some cases, non-thermally treated resins were also used as a waste. For some formulations "blank ash" produced from same ion exchange resin type without any added dopants was also used.

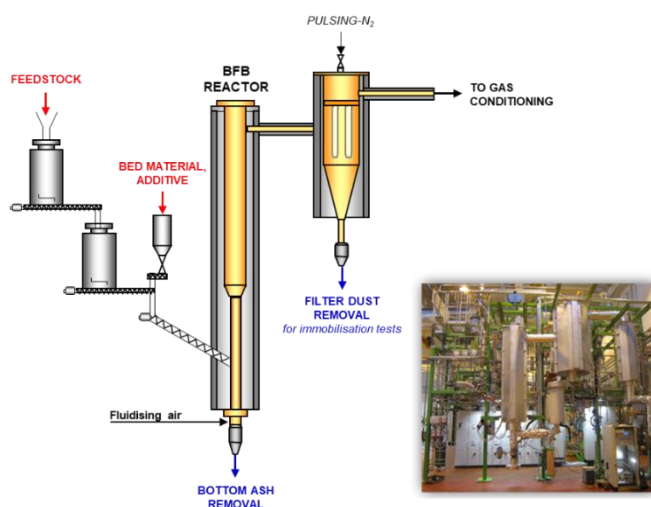


Figure 22. Bench-scale Bubbling Fluidized Bed gasification test rig.

4.1.2 Matrix

For immobilization primarily geopolymer based binders were used. Geopolymer precursors consisted of 3 different types Metakaolin with varying reactivity (Metastar, Argical, and MK40). A limited set of samples were also produced with ordinary Portland cement (sulfate-resistant CEM I 42,5 SR3. SR sementtti, Finnsementti). The used alkali activator was 10 M mixture of sodium silicate and potassium hydroxide solution, identical to one previously used in previous EU project THERAMIN [8]. Other components used in the preparation were de-ionized water and quartz sand (CEN Standard sand EN196-1, Normensand). Samples were stored in sealed conditions until de-molding (approximately one day), followed by one month of curing under 95% relative-humidity conditions at room temperature. Further details of the immobilization and related results can be found in PREDIS Deliverable 6.2 [3].

The produced waste forms; geopolymers and OPC references, were characterized primarily with SEM and XRD. On selected samples we also performed: Si/Al MAS NMR, FTIR and synchrotron based μ -XAS, XRF and XRD

Physical measurements consisted of:

- compressive strength, other mechanical testing;
- porosity measurements

4.1.3 Waste encapsulation protocol

Immobilization was primarily performed for dusts obtained from IXR gasification test runs -PR3 and PR4, but limited samples were also produced for following “waste forms”:

- One set of samples was produced with non-thermally treated resins;
- One set with “blank ash” (produced from non-doped resin) in which the Cs, Eu, Ce tracers were also added into the mixing water during geopolymer immobilization.

Alkali solution was pre-mixed and left to cool down to room temperature prior to addition to precursors. Waste ashes were included in amounts of 15% and 50% by weight (precursor replacement) in Argical-based geopolymers and OPC waste forms, while non-thermally treated resins were included at the 15% level. Mixing procedures followed were similar to those for preparation of standard mortars (SFS-EN 196-1), which were deemed already suitable for homogenization of fine particulates within the matrix.

4.2 Leaching protocols

Geopolymer and OPC samples were cut into size of 10 x 10 x 10 mm³ and polished. The cubic samples were leached according to PREDIS leaching protocol in synthetic cementitious water (pH ~12.7) at room temperature [5]. Experiments were run under anaerobic condition in argon glove box at room temperature. Liquid phase was replaced with fresh synthetic water after 7 days, 14, 21, 28 d, and then monthly during the first year of the experiments. The second year's water renewals were conducted at the time intervals of 14, 16, 18 months and 2 years. Every renewal was a sampling point for liquid samples for elemental analyses, and for pH and conductivity measurement. At time intervals 3 months, 6 months, 1 year and 2 years a solid sample from parallel leaching experiments was sacrificed for post mortem characterization purposes (e.g., XRD and SEM-EDS analyses) From leachates, bulk elements (Al, Ca, Fe, K, Na, S, Si) were analyzed with ICP-OES and the trace elements (Sr, Cs, Ce, Eu, Mg, Cr, Mn, Co, Ni) with HR-ICP-MS.-UH tested for colloids (Malvern NanoZS) at selected intervals although they did not find them at any detectable levels in any samples. Table 16 summarizes all the samples leached in leaching experiments by UH and VTT.

Table 16. List of samples included in the leaching experiments (the shaded samples were additionally leached in water sampled from the Olkiluoto disposal site for LILW).

Sample	Ash (wt. %)	Ash type	Cs, Eu, Ce (ppm)	Fe ₂ O ₃ (wt. %)
MK1	-	-	-	-
OPC	-	-	-	-
MK0 1-A1	1	A1	Cs [200]	-
MK1 15-A2	15	A2	-	-
MK1 50-A2	50	A2	-	-
MK1 50-A2 1k	50	A2	1000 in liquid	-
MK2 50-A2 1k	50	A2	1000 in liquid	-
OPC 50-A2 1k	50	A2	1000 in liquid	-
MK1 15-A3	15	A3	300, 50, 50	-
MK1 50-A3	50	A3	300, 50, 50	-
MK1 15-A4	15	A4	250, 50, 75	8
OPC 15-A4	15	A4	250, 50, 75	8
MK1 50-A4	50	A4	250, 50, 75	8
OPC 50-A4	50	A4	250, 50, 75	8
MK0 – metakaolin Metastar				
MK1 – metakaolin Argical				
MK2 – metakaolin MK40				
OPC – Ordinary Portland cement				

In addition, the reference geopolymer (MK1, 0%) and geopolymers with 15% and 50% loading of PR4 ash were leached in water sampled from the disposal site for low and intermediate level waste (at Olkiluoto Finland) for 3 months duration (Tables 16 and 17). These experiments were similar to 3 months short term experiments in synthetic cementitious water. In comparison also a simulant water representing these conditions was used in parallel test series. Experiments were run in anaerobic glove box (Ar), with similar sampling intervals to reference protocol described earlier. These experiments in simulated and real water from the site are continued for longer duration after the PREDIS project.

Table 17: Typical characteristics of Olkiluoto groundwater around -100 m, which slightly varies depending on the sampling time and point (left side), and composition of simulant groundwater also used in the leaching experiments (right).

GW characteristics		Olkiluoto simulant GW	
Location	Olkiluoto*	Salts	Water [g/L]
Depth [m]	97.5 – 156.5	NaCl	1.22
Water type	Brackish SO ₄	Na ₂ SO ₄	0.23
TDS [mg/L]	5224	KCl	0.0081
pH	7.74	NaHCO ₃	0.432
Alk _{tot}	1.87 meq/L	KBr	0.0052
HCO ₃ [mg/L]	131.08	KF	0.0015
		CaCl ₂ * 2H ₂ O	0.25
		MgCl ₂ * 6H ₂ O	0.25
		Na ₂ SiO ₃ * 9H ₂ O	0.032

*Finnish site for LILW repository

Helsinki University's post leaching characterization

Solid phase samples (i.e., starting materials and post-mortem samples) were analysed by FTIR, Si / Al MAS NMR, XRD, SEM and synchrotron based μ -XAS, XRF and XRD. Samples for FTIR, ²⁹Si / ²⁷Al MAS NMR, and XRD were ground to a fine powder before analysis. XRD samples were mixed with approximately 20%_{wt} pure zincite [ZnO] in order to determine the amount of amorphous material in the samples following Rietveld refinement. For SEM and synchrotron based μ -XAS, XRF and XRD, the samples were preserved in Spurr TM low viscosity epoxy resin via an already

established route that is designed to maintain the redox-state and texture at the point of sampling [9, 10] Synchrotron studies were carried out at Diamond Light Source, UK, beamline I18.

VTT's post leaching characterization

The samples containing ash A2 and were analysed with SEM-EDS, after 3 months leaching in synthetic cementitious water. The aim was to image the microstructure of the samples and see if it evolves with leaching time. The energy dispersive x-ray spectroscopy (EDS) allows to inspect how the elements distribute in the structure.

Solid state nuclear magnetic resonance, ^{29}Si / ^{27}Al -MAS NMR was used to samples prior, and 6 and 12 months after the leaching. The aim was to find the signs of potential loss of order, polymerization or formation of secondary products after the leaching experiments.

4.3 Results

Assessment of leaching behaviour of waste-form in repository conditions

Leaching experiments have been monitored for >1 year. UH and VTT are currently working together to find a suitable digestion method that can accurately determine the elemental compositions of the starting materials. Without these starting data interpretation of the data is limited; however, there are some things that can be stated. **(1)** The leaching / sorption of bulk components persists for the year but the rate of change is most significant in the first 30 days. Here, Si^{4+} and Al^{3+} leach into the solution, whereas Ca^{2+} is absorbed from the leachant into the solid phase in geopolymer samples. In OPC Ca leaches. **(2)** The rate of radionuclide release is most significant in the first 30 days. Currently, the data suggest that geopolymers retain a range of radionuclides relevant to LILW disposal equally as well as ordinary Portland cement (Figure 23). **(3)** The rate of radionuclide leaching does not increase linearly with ash loading; suggesting that the ash content of the geopolymers can still be optimised. **(4)** There was no evidence for colloids observed in leachate using dynamic light scattering.

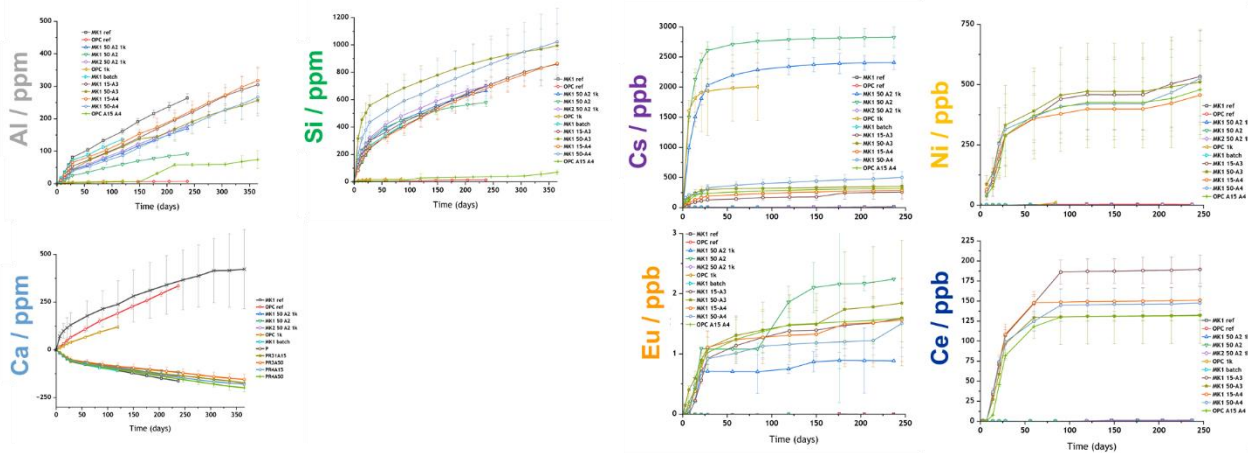


Figure 23: (Left 3 panels) cumulative leaching / absorption of bulk cations (Al, Si and Ca /ppm) in all experimental systems; and (right four panels) cumulative leaching of trace (Cs, Ni, Eu, and Ce /ppb) in all experimental systems.

Post-mortem characterisation of the properties of the leached geopolymer

Combined XRD, and ^{29}Si / ^{27}Al MAS NMR shows a decreasing degree of polymerisation following leaching and possible exchange of Na^+/K^+ for Ca^{2+} . Furthermore, XRD + SEM confirm CaCO_3 precipitation in some samples.

The synchrotron based $\mu\text{-XRF}$, -XRD and -XANES provided spatially resolved information on the contaminants (Cs, Ce, Eu, Ni), their bonding environments, its evolution and leaching mechanisms. As the data have only recently been collected the analysis is not yet complete. However, early analysis of the data suggests **(1)** following leaching in the OPC we can see clear changes in Ce speciation & oxidation state, these trends are not as distinct in the geopolymer samples. **(2)** Eu is most often found in co-location with Ce and Fe. As Ce was added in higher concentrations (and is easier to observe) we were able to locate areas with Ce but no Eu. **(3)** Cs present in amorphous areas (with e.g., geopolymer structure) and has long range (<5 Å) structure. Again, these data are still relatively new and require full analysis.

Additional information on the post-mortem characterization of tested specimens and leachates analysis is available in [VTT-HU Data collection Task6 form.xlsx](#). (available to PREDIS partners).

5 SIEG NASU CONTRIBUTION

5.1 Samples preparation

5.1.1 Waste

The combustion IER was carried out at different temperatures. The resulting ash was characterized by using IR spectroscopy, SEM and DTA to monitor the decomposition of organic matter. Previously, the DTA method established that a small sample mass is completely heated with a minimum temperature gradient over the sample volume. Incineration of significant volumes of spent ion-exchange resins can be problematic, also taking into account the uncertainty of the behavior of radionuclides depending on the temperature and duration of gasification. In Figure 24, the sequence of destruction of spherical particles of the cation IER during heat treatment is given. When heated, the particles of an IER crack from them, separating scales, and they decrease in size. In the future, cracking continues while the scales begin to burn out. At sufficiently high temperatures, particles of a spherical shape can be preserved in the samples. The presence of such particles in the samples significantly reduces the ultimate compressive strength of the geopolymer matrix, reducing their number in the samples of compounds, which is an urgent problem and requires a higher temperature after the first gasification.

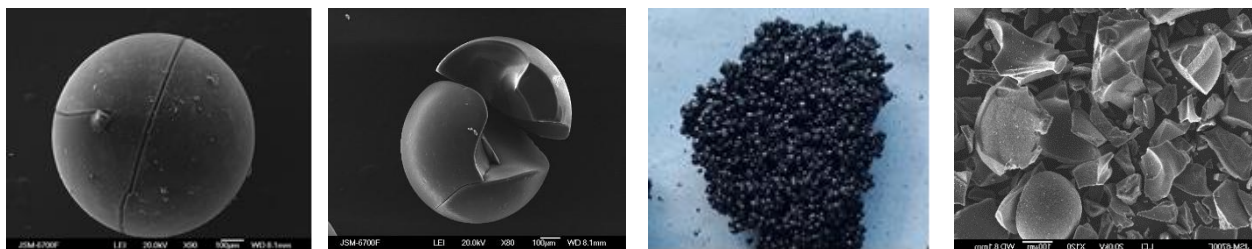
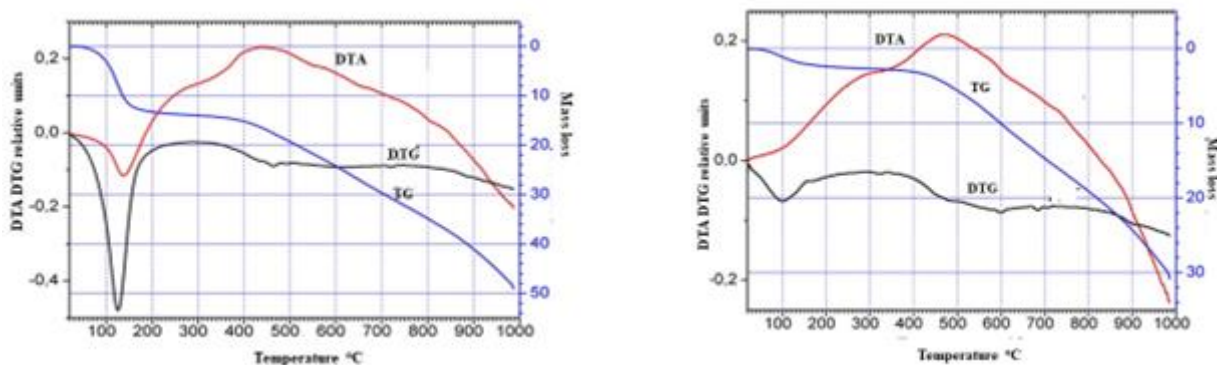


Figure 24. Destruction of IER under gasification.

At a temperature of about 900 °C, the mass sample decreases and remains at 13% of the initial (Figure 25 a). Repeated studies showed that complete decomposition (99%) can occur at a temperature of more than 1000 °C (Figure 25 b). After gasification, the ash was homogenized and mixed with the geopolymer.



a) DTA analysis of samples of IER of burnout b) DTA of samples ash after the burnout of IER.

Figure. 25. DTA analyses of samples of IER and ash.

These analyses suggest that the degradation of IER can be separated into three basic stages: weight loss between 25 and 150 °C is ascribed to dehydration. Most weight loss results from decomposing the functional groups from 250 to 350 °C for cationic exchange resins. The last stage (temperatures above 400 °C) is associated with the degradation of the organic matrix and its subsequent mineralisation. The cationic IER is characterized by releasing greater quantities of degradation products, mainly SO_2 .

5.1.2 Matrix

The main goal of this research is to perform a technical assessment of geopolymers and Cement II as an alternative agent OPC for the immobilisation of radioactive ash by evaluating the setting time and mechanical properties. Binder components for conditioning depend on the type of waste and are unsuitable for fine ash from solid radioactive waste. Waste form characterisations with ash were carried out using mechanical strength techniques and the leaching method. Several tests were done, including FTIR, XRD, and SEM.

SIIEG NASU development of geopolymer binder on base BFS with MK for matrices with ashes waste. Potassium hydroxide and sodium silicate solution have been used as activators. Due to the dependence of the ash fraction on processing IER waste, one of the main goals concerning the ash characterisation was to select those factors responsible for the compressive strength. For this purpose, the original ash sample has been fractionated by sieving. Measurement of the compressive strength after drying to constant weight showed that with an increase in the amount of ash fraction < 0.2 mm, in the amount of 16.6%, the strength was 10.5 MPa, and at increased to 29.6%, the strength decreased to 4.7 MPa. Compression tests of the hardened matrices conditioning of the IER ash were evaluated according to the ASTM C109/C109M standard. Compressive strength tests were performed at 7 and 28 days. The obtained matrix samples had a compressive strength of more than 25 MPa with a porosity of about 0.5%. Due to such low porosity, the samples dry slowly, and cracking occurs when a water concentration gradient occurs. To prevent this, metakaolin was added to the modified slag-alkaline binders, increasing the porosity to 15% and reducing the compressive strength to 19.3 MPa. For chemical durability, a leaching test was conducted. The strength indicators of the compounds primarily depend on the physical and mechanical properties of the ash.

Two commercial binders (CEM I-52,5R) and alkali-activated cement (CEMII/A-LL 42,5-R) were used for the experiments in the cementation of ash. The CEM I (OPC) specific surface was >3500cm²/g with the content of tricalcium aluminate (C3A) of no more than 8% by mass, and CEM II varied within the 3300-3500 cm²/g range. The most commonly used alkali-activated type of CEM II is slag cement. The high basicity modulus of slag (Mb = 1.1) improves microstructuring high hydrate Calcium silicate (CSH) stages. The chemical reaction binder of CEM II is slow at room temperature; adding alkali activators could enhance the reaction rate. As an alkaline activator for the cement, sodium silicate was a solution with silicate modulus Ms=2.87 and ρ=1300 kg/m³.

5.1.3 Waste encapsulation protocol

Preparation of geopolymer formulations

The MK/BFS geopolymer pastes were prepared with different Al:Si:Na/K: H₂O ratios. Using KOH as an activator led to higher compressive strength than NaOH. The optimal amounts of water, activator, MK, and BFS have been determined based on the literature study and experimentally. Geopolymer samples were produced: alkaline activation solutions were prepared by mixing appropriate quantities of sodium silicate solution, K/Na hydroxide pellets, deionised water and stirring to reach homogeneity. Solids content optimised for similar workability. Activator concentration is optimised to obtain suitable reactivity and mechanical stability for each material. The solution was mixed with powder components MK/BFS and added water until a 14-16 cm spreading cone was formed. The mixing operation was performed continuously at room temperature (600-800 rpm for 5-10 min). The geopolymer binder was measured on viscosity after mixing according to ASTM C1749 and set time based on EN 196-3. The setting time of geopolymer pastes should not be less than the duration of the technological cycle - the time from the beginning to the end of compounds mixing and pouring into moulds.

The high degree of variability in the physical properties and chemical composition of the BFS/MK used in producing alkali-activated binders is a significant problem in conditioning ash. The geopolymer grouts are cast in cube moulds (5 x 5 x 5 cm³ sides) and left in the moulds until the end of hardening. After the top layer was compacted, the moulds were vibrated to remove air bubbles for better compaction of the grouts. The negative effect of vibration compaction is the release of the liquid phase on the surface of the compound. The time of the end of hardening was determined by

the Vicat Needle, the cone of the device, which was filled at the same time as the forms. Each batch had 3 to 5 samples. After mixing components, the mixture was put into moulds for a grout set, which lasted from 40 minutes to 155 minutes or more. General view of the sample in Figures 26 a, b and c.

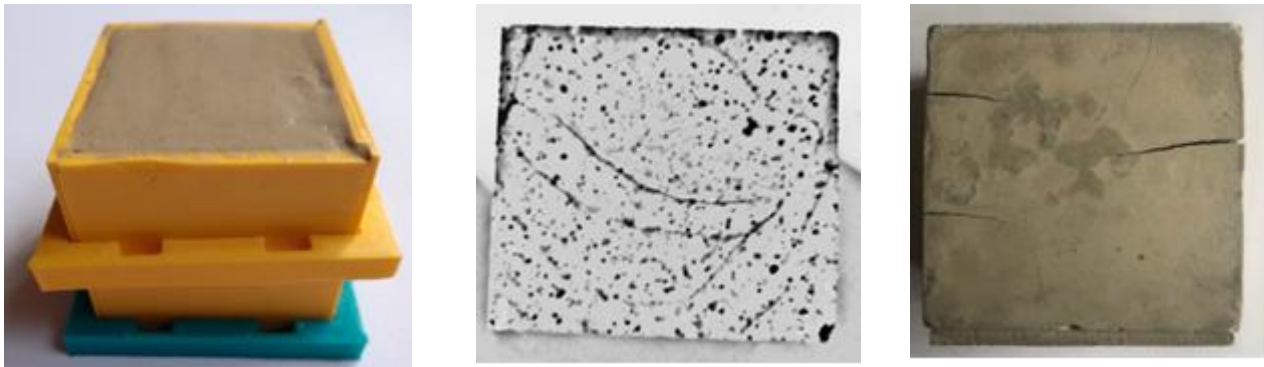


Figure 26 a) Geopolymer matrix samples (cubes moulds of the 5 x 5 x 5 cm side), b) Geopolymer compound with ash IER (WP6-54), and c) Geopolymer matrix with crack.

With low porosity, samples dry up slowly. When gradient distribution water in samples may occur, they crack (Figure 26 c). To prevent this, a modified slag-alkaline binder was added metakaolin, which increased porosity up to 15% and reduced limit compressive strength up to 19.3 MPa.

5.2 Ageing protocols

5.2.1 Durability test after immersion

The samples, the composition of which corresponded to two batches (#69 and #75), were used to carry out compressive strength tests. After the hardening period of 28 days, the samples were placed in a vessel with a capacity of 0.5 L and filled with 300 mL of synthetic without silica water (Figure 27). In the future, according to the duration, the water was drained from the cans, and the solution in the amount of 300 mL was again poured into the cans. The results of average measurements and calculations are presented in Table 18. The capacity of the developed matrixes to resist the structure release when immersed in a leaching solution was tested.

SAMPLE	#69	#69 AFTER	#75	#75 AFTER
CURING, DAYS	28	28	28	28
IMMERSION, DAYS	0	90	0	90
COMPRESSIVE STRENGTH, MPA	7.7	5.4	14.7	16.2



Table. 18. Evolution of compressive strength

Fig. 27. Durability immersed tests

5.3 Leaching protocols

Leaching experiments were carried out using the WP 6 “Reference protocol for short and long-term durability experiments” [5]. The leachates' measured concentrations of Al, Si, Ca, Ce, Cs, and Sr using inductively coupled plasma mass spectrometry (ICP-MS). The results of these tests are used to assess the leaching parameters by fitting the experimental data to graph models. Cerium (Ce) was selected as a surrogate element for U and Pu in cement mixtures for this work.

Procedure of leaching

The polypropylene containers, 100mL, were filled with two solutions.

1) **WP 6 Reference protocol for short and long-term durability experiments** [5]

NaOH/KOH/CaCl₂/Na₂SO₄, pH=12.7

2) **National SIIEG. Reference protocol for short-term durability experiments**

0.1 M NaOH, pH=11.73

- The solution amount was ten times the surface area of the sample, with a ratio of 1/10 g
- After certain intervals, as specified in the standard, the specimens were withdrawn from the containers and immediately transferred to the next leaching container filled with fresh leachate.
- All leached material was transmitted for analysis based on the ICP-MS.
- Leaching rate calculation of basic components Si, Al, Ca and Cs, Sr, Ce.
- Temperature: 20°C.
- Post-leaching characterisation

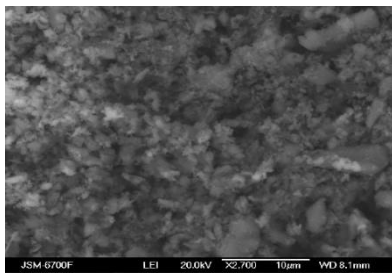


Figure 28. a) Use of the glovebox and N₂-purging of the headspace of the vials, and b) the polypropylene container, which were used for leaching.

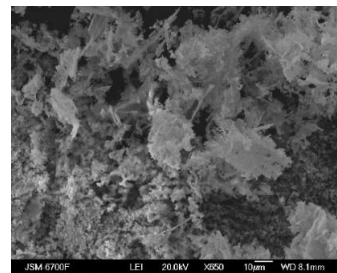
For leaching, samples were taken after 28 days of hardening in an atmosphere of saturated water vapour and dried for 10 days at room conditions. The surface of the sample has been cleaned of small particles or dust. The polypropylene containers were used for leaching, and the samples were suspended in containers filled with deionised water. The amount of deionised water was 10 times the specimen's surface area. After certain intervals, as specified in the standard, the specimens were withdrawn from the containers and immediately transferred to the next leaching container filled with fresh leachate. The used leaching containers containing all leached material have been closed and transmitted for analysis. Analytical data obtained for the leaching of the surrogate are based on ICP-MS results. To measure the leaching rate, it is necessary to know the total leaching from the samples. According to these results, the values of the leaching rate were calculated.

5.4 Results

Thus, it has been found that the most challenging issue when solidifying ash after thermal processing of IER is ash homogeneity in composition. From physical and mechanical properties, ash depends primarily on strength indicators compounds. Before the measurements, the ash samples were ground in an agate mortar. The microstructure and morphology of the ash fractions have been investigated on SEM (JSM-6490LV). As was indicated above, the presence of the sample's compounds of spherical particles significantly reduces their limited compressive strength, so decreasing the quantities in a sample of particles is a current problem. On the other hand, thermal processing IER to high values requires additional energy costs that may be impractical. The work has studied compounds obtained by solidification IER ash burned to 81% and 87%. Selected degree firing 80-90% proceeding shows that when the IER in the samples amounts spherical particles, many decreases, Figures 29 a and b.



a) processing at 600 °C



b) processing at 800 °C

Figure 29 Ash of IER after thermal processing.

Table 19. Properties of samples.

	WP6-26	WP6-54	WP6-55	WP6-56
Density, g/cm ³	2.3			
Porosity, %	0.5	14.0	-	-
Setting time, min	180	190	160	180
Compressive strength, MPa	51	4.4	9.6	10.9
Degree gasification of IER	-	0.81	0.87	0.81
Fraction ash	-	<0.3	<0.3	<0.3

Table 19 shows that the best strength was the sample WP 6-56, which used the ash fraction <0.3 mm, a degree of gasification of 0.81. The amount of ash in the compound was 22.7%, and the amount of liquid glass increased to 19.4%. All samples were prepared for test leaching according to the previously described method. The characteristics of the samples are given in Table 20. The stable Cs-133 has been used as doping nuclides for leaching from MK/BFS matrix samples.

Table 20. Characteristics samples for leaching

Sample number	Mass of the test sample, g	Mass of Cs, g	Area of the contact surface, sm ²
WP6-56 (1)	2.40	0.04	6.0
WP6-56 (2)	3.19	0.06	6.6

Analytical data obtained for the leaching of the surrogate Cs are based on ICP-MS results. To measure the leaching rate, the total leaching from the samples must be known. According to these results, the values of the leaching rate were calculated and presented in Figure 30. Concentrations of cesium measured in the solution were negligible after one month of leaching in both samples.

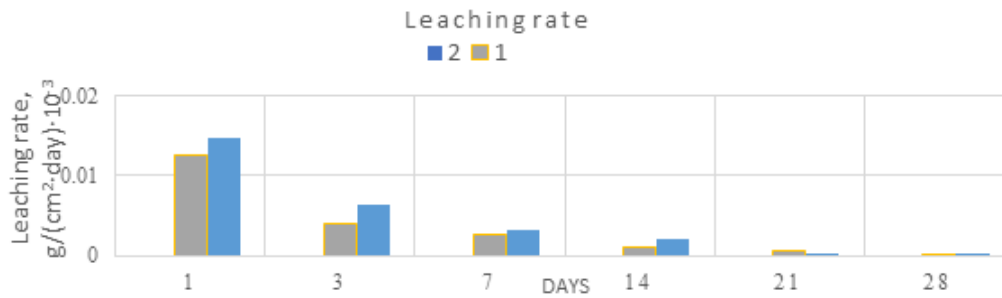


Figure 30. Leaching rate WP6-56 (1) and WP6-56 (2).

Leaching of cemented samples

Research has been done on the chemical resistance of the CEM II samples with ash by leaching in synthetic cement water with pH=12.7 (sample #WP6-69) and 0.1 M sodium hydroxide solution with (sample #WP6-75) pH=11.7. Batch leaching rates analysis of essential components in synthetic cementitious water compared to the test results in 0.1 M sodium hydroxide solution showed that the leaching rates for Al and Si were significantly lower.

Additional information on the post-mortem characterization of tested specimens and leachates analysis is available in [SIIEG Data collection Task6.6.xlsx](#) (available to PREDIS partners).

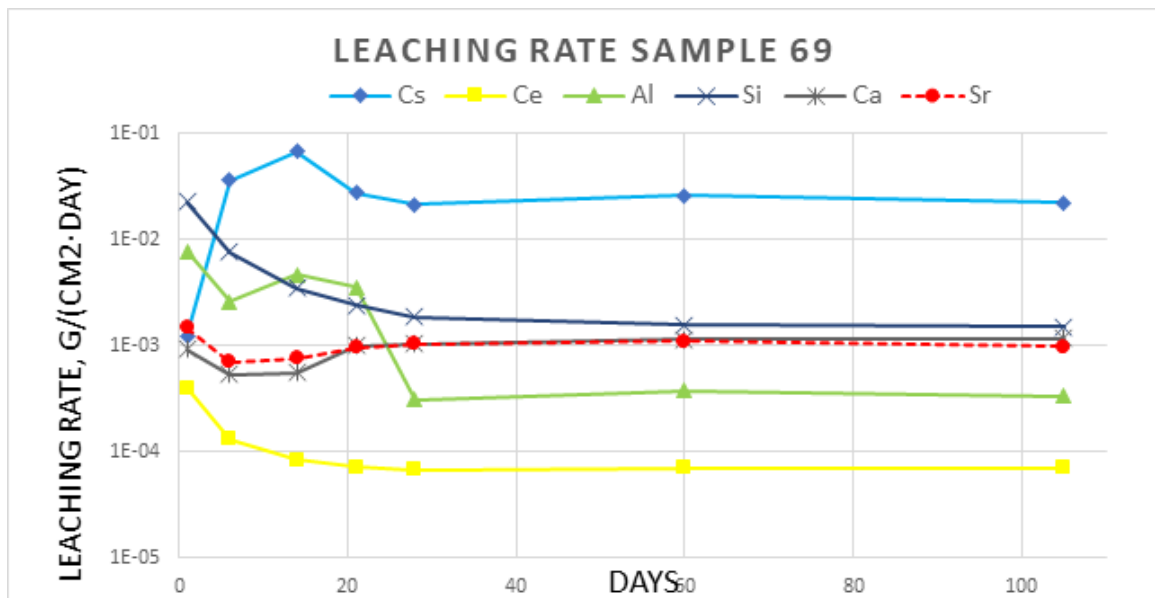


Figure 31. Leaching of sample #WP6-69, pH = 12,7 (NaOH/KOH/Na₂SO₄/CaCl₂).

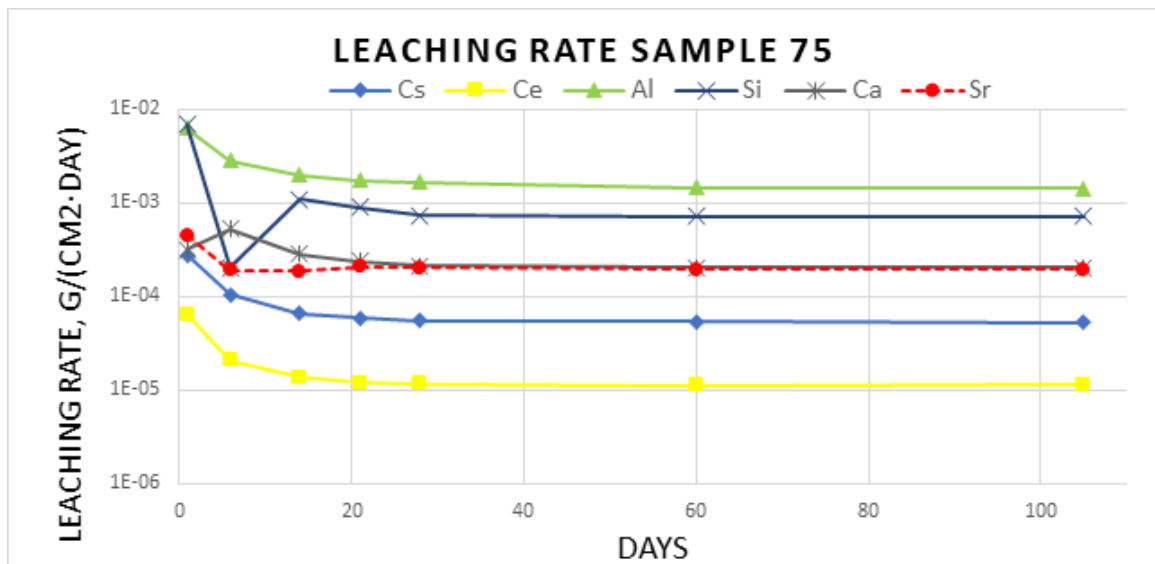


Figure 32. Leaching of #WP6-75, pH = 11.7 (0.1 M NaOH).

Table 21. Leaching results for two different protocols

	NaOH/KOH/CaCl ₂ /Na ₂ SO ₄ , pH=11.73	0,1 M NaOH, pH=12.7
L_i	13.3	12.1
D_e (cm ² s ⁻¹)	< 2.6·10 ⁻¹²	< 7.0·10 ⁻¹²

Conclusions

- Mechanical characterization of the waste forms was not performed after the dismantling of leaching tests, that used cub samples 1 x 1x 1 cm³, but reference protocol for compression test requires cubic samples 5 x 5x 5 cm³. As results obtained show significant differences in Compression Strength values for samples after leaching tests.
- The properties of binders' compositions of geopolymers intended to immobilise thermally treated organic wastes have been studied. The strength indicators of the compositions primarily depend on the physical and mechanical properties of the ash. It established that preliminary mechanical processing of precursors is necessary to increase the strength of the compounds to increase the efficiency of waste conditioning. The leaching test showed that the MK/BPS geopolymer compound has good leaching resistance and that the Cs leaching rate does not exceed the standard.
- Different formulations of the CEM II matrix base have been investigated at the laboratory scale as the more sustainable process for ash conditioning. The optimal formulation for CEM II with ash with the most acceptable properties was established. The hardened CEM II matrices have been characterised after curing time (setting time, density, porosity, and compressive strength). Research on the chemical resistance of the CEM II samples with ash leached in synthetic cement water with pH=12.7 and a 0.1 M sodium hydroxide solution with pH=11.7 has continued. Batch leaching rates analysis of essential components in synthetic cementitious water compared to the test results in 0.1 M sodium hydroxide solution showed that the leaching rates for Al and Si were significantly lower.

6 SCK CEN CONTRIBUTION

6.1 Sample preparation

6.1.1 Waste

The salt residues of the molten salt oxidation (MSO) process were received from CVRez. Visual inspection of the salt showed that it was water logged. Oven drying of the salt at 110°C indicated a water content of 52 wt.%. As the high water content of the salt may vary significantly with local atmospheric conditions, the choice was made to air-dry the salt. Remeasurement of the water content after air-drying resulted in a reduced value of 17 wt.%. To keep the water content as constant as possible, the air-dried salt was saved in an air-tight barrel.

The chemical composition of the salt was determined by CVRez (Table 22), which shows that it is dominated by Na, with minor contributions of K, S and Al.

Table 22: Chemical composition of two batches of salt produced by CVRez.

	Batch 1		Batch 2	
	Average	Stdev	Average	Stdev
Al ₂ O ₃	1.8	0.1	6.2	1.5
CaO	1.9	0.2	0.1	0.0
Cl	0.4	0.1	0.1	0.0
Fe ₂ O ₃	0.6	0.0	0.2	0.0
K ₂ O	4.2	0.4	1.7	0.1
MgO	1.8	3.4	0.3	0.0
Na ₂ O	83.8	4.7	84.5	2.9
NiO	0.6	0.0	0.2	0.0
P ₂ O ₅	2.1	0.2	0.0	0.0
SO ₃	0.4	0.0	0.2	0.0
SiO ₂	2.8	0.5	6.2	1.5

The mineralogical composition of the salt was determined twice: once on the original salt by CVRez and once on the air-dried salt by SCK CEN. The composition provided by CVRez showed a salt composed primarily of sodium carbonate (pentahydrate), complemented by smaller amounts of sodium chloride, sodium sulphate and sodium nitrate. Likewise, the air-dried salt is composed of sodium carbonate minerals of various hydration states: approximately 75 wt% of thermonatrite (Na₂CO₃·H₂O), 1 wt.% of natron (Na₂CO₃·10 H₂O) and 24 wt.% of trona (Na₂CO₃·NaHCO₃·2 H₂O).

Pretreatment of the salt

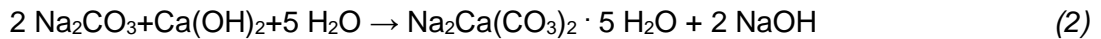
Extensive testing of direct immobilization of the air-dried salt in both alkali-activated and cementitious matrices revealed the main issue with the waste: its severe hygroscopic nature. The large range of hydration states (varying from monohydrate to decahydrate) of sodium carbonate represent a large volume change, with the molar volume increasing from 55 cm³/mol (thermonatrite) to 196 cm³/mol (natron). It is possible to produce waste forms with high mechanical strengths by directly immobilizing the salt, provided that curing occurs in sealed or otherwise dry conditions. The salt minerals which are not chemically transformed by incorporation into the matrix will partially hydrate depending on the available water. If the waste form created this way is exposed to variable humidity conditions (e.g. immersion in water, placing in a high humidity curing bench, oven drying), the salt minerals will (de)hydrate accordingly, resulting in catastrophic volume changes and associated cracking or liquefaction.

Therefore, two options are available regarding the immobilization of the salt. One path would still include direct immobilization, but limiting the waste loading in such a way that the salt does not significantly affect the microstructural and mechanical properties of the waste form. This approach would involve ensuring a full chemical bonding of the salt within the C-(N)-A-S-H gel, as free sodium

carbonate crystals could continue to negatively affect the durability of the waste form. Another path, explored in our work, involves transforming the salt into a non-hygroscopic form. After screening of reagents, the choice was made of reacting the sodium carbonate with slaked lime ($\text{Ca}(\text{OH})_2$), as this would result in the precipitation of CaCO_3 , which can be assumed to be inert and non-expansive:



An added advantage of this reaction for the immobilization in alkali-activated materials is the generation of NaOH, which can act as an additional activator. Testing of this conversion revealed that, in addition to the precipitation of calcite, an intermediate phase (gaylussite), was formed as well, according to following reaction:



Thermodynamic modelling has indicated that gaylussite is a metastable phase, with calcite being the thermodynamically stable end point, so it is likely that in time gaylussite will revert to calcite. While gaylussite does contain crystalline water, exposure of a waste form containing the converted salt to high/low humidity conditions did not result in any shrinkage or expansion, indicating that it is not readily released.

To promote the formation of the thermodynamically stable calcite over gaylussite, the pretreatment procedure was adjusted from simply adding $\text{Ca}(\text{OH})_2$ to a solution containing the waste salt, to slowly adding the waste salt to a $\text{Ca}(\text{OH})_2$ suspension. In the first approach, the available, i.e. dissolved, amount of Ca relative to Na is low, due to the low solubility of $\text{Ca}(\text{OH})_2$. In this case, the reaction to gaylussite is thermodynamically favoured. By slowly adding the salt to a $\text{Ca}(\text{OH})_2$ suspension, the concentration of Na relative to Ca is limited, thereby promoting the formation of calcite over gaylussite.

XRD analyses of the two pretreatments have shown that both types of pretreatments result in a full reaction of the sodium carbonate, with both gaylussite and calcite being formed. In the case of the slow addition of the salt to a $\text{Ca}(\text{OH})_2$ suspension, more calcite was formed than gaylussite.

Note on waste loading

Given the high initial water content of the waste salt and the pretreatment, there should be a clear definition of the waste loading. In the case of the SCK CEN waste forms, the waste loading is defined as the amount of air-dried salt, i.e. the salt containing 17 wt.% of water, relative to the total mass of the waste form. As it is likely that other partners will use a salt with a differing water content, any comparison would require a normalization to an equal water content of the salt.

6.1.2 Matrix

After extensive testing, two matrices were retained for immobilization of the air-dried salt and durability testing. On the one hand, a blended cementitious system including CEM III cement, blast furnace slag, fly ash, lime and limestone aggregate. On the other hand, an alkali-activated material based on blast furnace slag, activated by sodium disilicate ($\text{Na}_2\text{O} \cdot 2 \text{SiO}_2$) and NaOH produced by pretreatment of the salt. A mechanically performant metakaolin based waste form was also synthesized, but efflorescence was observed after curing, leading to the preferred focused on alkali-activated slag. The recipes can be found in Table 23 and Table 24.

Table 23: Recipes for the preparation of the cementitious waste forms. All figures are given as weight percentages.

Waste loading	CEM I	Lime	Blast Furnace Slag	Water	Limestone	Silica Fume	Fine Sand	Air Dried Salt	Ca(OH) ₂
10	4.5	1.9	20.7	27.8	5.7	4.9	18.8	10.0	5.7
14	3.9	1.6	17.9	27.1	4.9	4.2	18.3	14.0	8.0

Table 24: Recipes for the preparation of the alkali-activated waste forms. All figures are given as weight percentages.

Waste loading	Blast Furnace Slag	Na ₂ O·2SiO ₂	Water	Fine sand	Air Dried Salt	Ca(OH) ₂
10	38.6	1.3	23.5	21.0	10.0	5.7
20	27.6	0.9	21.0	20.0	19.6	10.9

6.1.3 Waste encapsulation protocol

All available free water was used in the pretreatment of the salt, to reduce the viscosity of the resulting slurry as much as possible. The slurry was then subsequently mixed together with the dry components (for alkali-activated slag: sodium disilicate, blast furnace slag and sand) in a planetary mixer prior to casting. Waste loadings considered for these waste forms are 10 and 14 wt.% (blended cementitious material) and 10 and 20 wt.% (alkali-activated slag). Due to the high viscosity of the salt slurry, setting of the mixtures was fast, especially on the high end of waste loadings (Table 25). If these recipes would be upscaled, superplasticizers could be considered to improve workability.

Table 25: Final setting time of each waste form considered in this work

	Alkali-Activated Slag		Cementitious	
Waste loading	10	20	10	14
Final Setting Time (h:m)	2:30	1:15	5:00	1:15

6.2 Carbonation protocol

After curing for 28 days, duplicates of each recipe were preconditioned at 20°C and at a relative humidity of 60% until a stable mass was attained. Afterwards, they were put into a climate chamber set to 20°C and 60% relative humidity with a 1% atmospheric CO₂ concentration to initiate accelerated carbonation. At regular intervals, selected samples were removed from the climate chamber for expansion measurement, determination of mechanical strength and determination of the carbonation depth by phenolphthalein spraying. Subsamples were also taken for destructive post-mortem analysis.

6.2.1 Results of carbonation

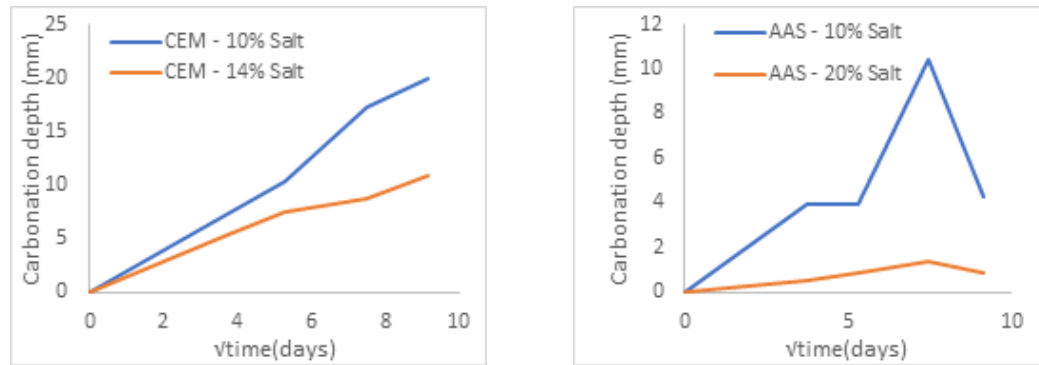


Figure 33: Carbonation depth of cementitious (left) and alkali-activated (right) waste forms determined by phenolphthalein spraying at set intervals after the start of the exposure to CO₂.

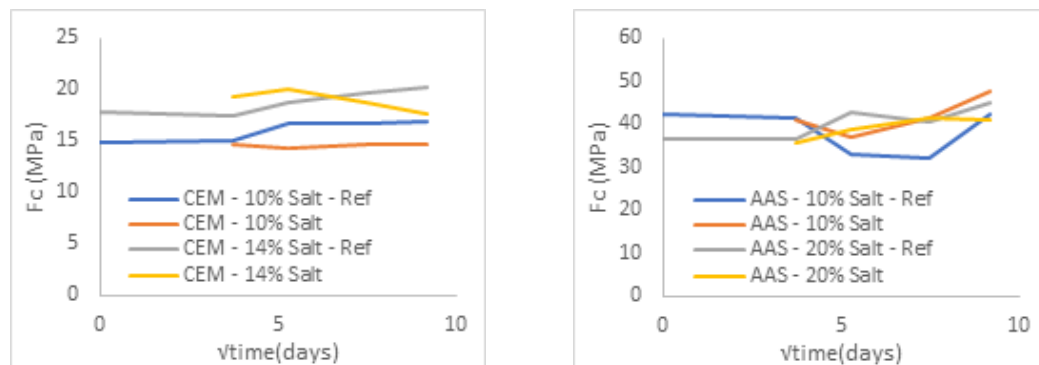


Figure 34: Compressive strength of cementitious (left) and alkali-activated (right) waste forms determined at set intervals after the start of the exposure to CO₂.

The extent of carbonation (Figure 33) of both type of waste forms is linked to the waste loading, with higher waste loadings correlated to lower carbonation depths. The extent of carbonation in the alkali-activated waste forms is markedly lower than that of the cementitious waste forms. Meanwhile, the compressive strength of the waste forms is not impacted by carbonation, with the carbonated waste forms not differing significantly from reference samples of a similar age (Figure 34). During the carbonation experiment, the alkali-activated waste forms on the one hand gained mass (1.3 and 0.4% respectively for 10 and 20% waste loading), which can be directly related to the sequestration of CO₂ in mineral form. They also display expansive behaviour, albeit limited to 0.1% for 20% waste loading and 0.02% for 10% waste loading. The cementitious waste forms on the other hand show a mass loss, which indicates that any mass gain due to CO₂ sequestration is offset by release of water from the matrix. This is also reflected in the length of the samples, as a shrinkage of -0.2 to -0.3% can be observed after 84 days.

These observations can best be framed within the mineralogical changes within the matrix of both waste forms. Quantification of the mineralogical composition (Figure 35) indicates that calcite is formed during carbonation and that its proportions increase during the experiment. The formation of calcite is more pronounced in the cementitious waste forms, which coincides with their greater carbonation depth. Notably, portlandite (CH) is present in the alkali-activated waste forms, a remnant from the preconditioning process. Its concentration goes down until it has completely disappeared after 56 days, indicating that CO₂ preferentially reacts with CH to form calcite before carbonating other phases. FTIR analyses of the alkali-activated waste forms (Figure 36) illustrate this process: in the case of the 20 wt.% waste loading sample, plenty of Ca(OH)₂ is available for carbonation. As a consequence, the structure of the C-N-A-S-H matrix (as shown by the Si-O stretching region at 1000 cm⁻¹ is unaffected). Meanwhile, in the 10 wt.% waste loading sample, the disappearance of Ca(OH)₂ leads to the carbonation of the C-N-A-S-H matrix and a change in its coordination from a

Q2 to a Q3 dominated system. The buffering effect of Ca(OH)_2 also explains the lower carbonation depth in the higher waste loading waste forms.

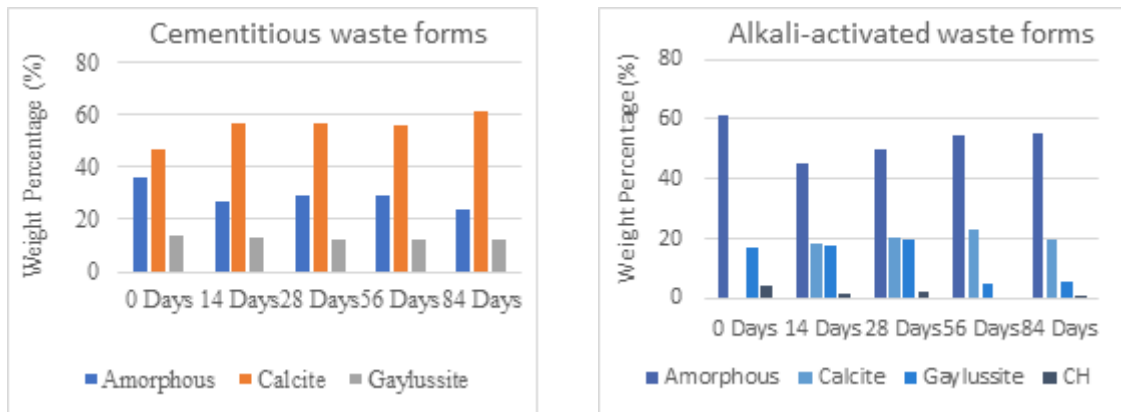


Figure 35: Quantified proportions of a selection of mineral phases in alkali-activated and cementitious waste forms containing 10 wt% of waste salt determined by Rietveld refinement of XRD diffractograms.

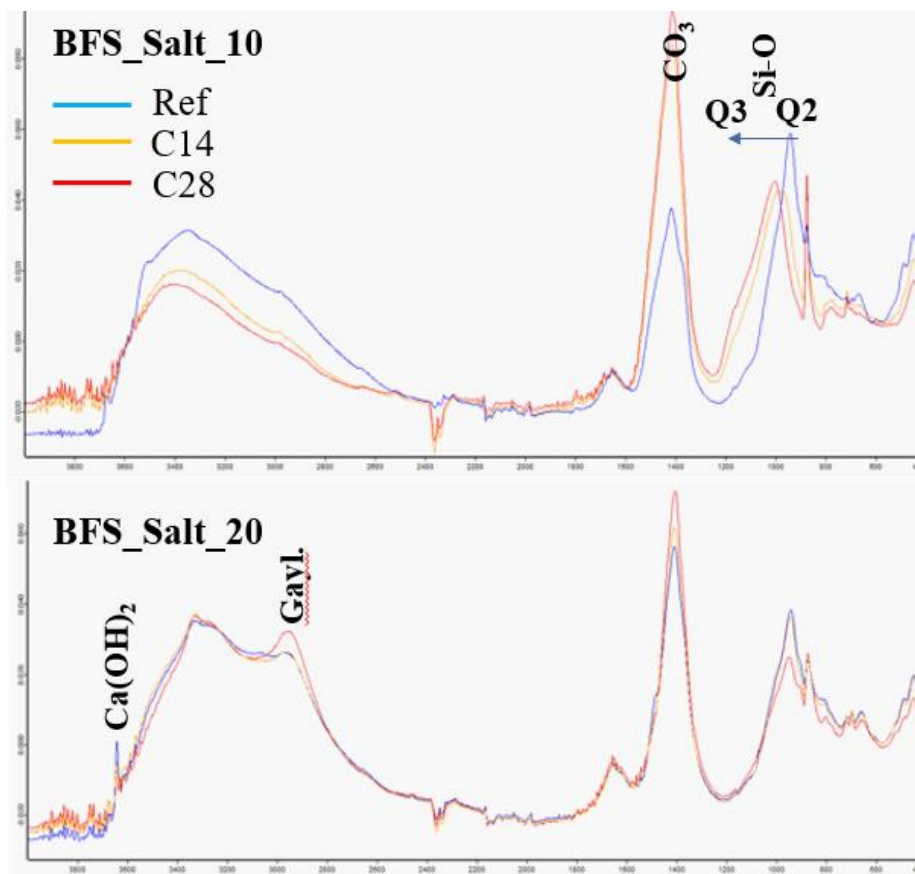


Figure 36: Comparison of the FTIR spectra of reference and carbonated alkali-activated waste forms.

6.3 Leaching protocols

For the leaching tests with the alkali-activated and leached samples, the reference protocol described in the milestone MS39 was used [5]. The elemental concentrations in the leachates were determined by ICP/MS. The unaltered and leached samples after 3 months were characterized by SEM-EDX and XRD.

6.4 Results

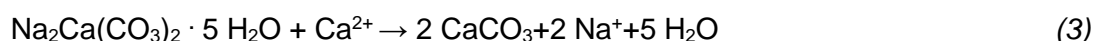
As requested in the reference leaching protocol, the temperature was constant at $22 \pm 2^\circ\text{C}$ throughout the tests. The pH was also constant at a value of 13.0 between two solution renewals. Concentrations of Si, Al, Ca, K, SO_4^{2-} and Na were monitored and used to calculate both the normalized mass loss (Figure 39) and the cumulative fraction leached (CFL) (Figure 40). Both the normalized loss and CFL for Na are high, reaching 50% after 3 months for the alkali-activated slags. The primary reason for this is the initial runoff of Na in the pore water of the waste forms in the first week of the leaching experiment.

As the preconditioning of the waste forms was not specified in the leaching protocol, the samples were preconditioned by exposure to 95% relative humidity until a stable mass was attained. In other studies, preconditioning is performed by soaking the sample in a solution with a pH similar to the eventual leachant to already capture the initial runoff prior to the start of the experiment. So, a comparison with other participants in the leaching study should include a critical comparison of the preconditioning.

After the high initial runoff, the leaching stabilizes, with a CFL of 10 to 14% from day 14 to 90 for Na. For the reference sample, the CFL in the same time interval is 4%. Similar trends can be seen for Si and Al, with the leaching rates stabilizing after an initial runoff. The CFL of K shows a variation around 0, indicating that the leaching of K is negligible. In the case of Ca, an uptake of Ca by the matrix is observed instead of leaching. This could be attributed to two phenomena. On the one hand, it is possible that Ca is taken up by the C-N-A-S-H matrix as a charge compensating ion, possibly replacing part of the leached Na ions. On the other hand, Ca can be used to react further with gaylussite to further precipitate CaCO_3 .

The observations for the cementitious waste forms (Figure 41, Figure 42) are similar for the most part, although the normalized losses and associated leached fractions are generally higher. It should be noted that for three elements (K, Si and S), the difference between the measured concentrations in the leachate and the blank are smaller than the uncertainty on the ICP measurement. Due to the cumulative nature of the calculation of both the CFL and the normalized losses, this may lead to seemingly high leaching rates, while in reality the leaching is non-existent. This is especially apparent for K, in which normalized losses of up to -25000 g/m^2 are calculated. If these elements are not taken into account, the trends in leaching are similar to the alkali-activated waste forms: high leaching of Na, somewhat compensated by uptake of Ca.

Despite the high fractions leached, the leachability indices (Table 26, Table 27) stay above the minimum value of 6 for each element in the alkali-activated waste forms, although the actual leaching of the matrix is itself expected to be lower than the values reported. For the cementitious waste forms, the minimum LI of 6 is generally not attained. The limited leaching from the matrix can be inferred from the limited effect of the leaching on the microstructure of the waste forms (Figure 37): the C-N-A-S-H matrix itself seems to be largely unaffected, with only a small number of microcracks appearing. There is evidence of dissolution in the high-brightness gaylussite crystals, which could be a major contributor to the observed release of Na in the leachant. The lack of accompanying leaching of Ca from the same mineral would support the hypothesis that after Na is leached, calcite reprecipitates taking up Ca from the leachant according to the following reaction mechanism:



The XRD diffractograms of the leached samples (Figure 38) support this hypothesis. Prior to leaching, gaylussite makes up the majority (exceeding 50%) of the carbonate minerals. However, after leaching, gaylussite only makes up 18 to 26% of the carbonate minerals (in alkali-activated slag waste forms). This is an indication that gaylussite has dissolved and/or that calcite has precipitated.

Additional information on the post-mortem characterization of tested specimens and leachates analysis is available in [SCK CEN AAM Cement Data collection Task6.6.xlsx](#) (available to PREDIS partners).

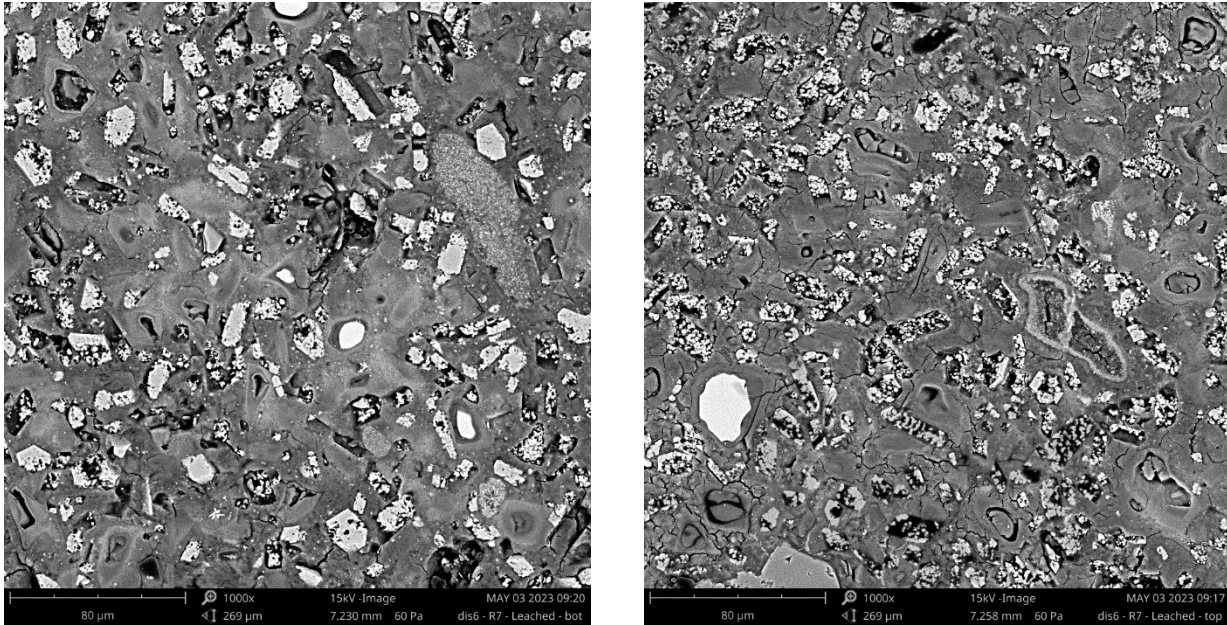


Figure 37: SEM photographs of the microstructure of an alkali-activated slag waste form containing 20 wt% of air-dried salt. On the left: unleached waste form after 3 months; on the right: leached waste form after 3 months.

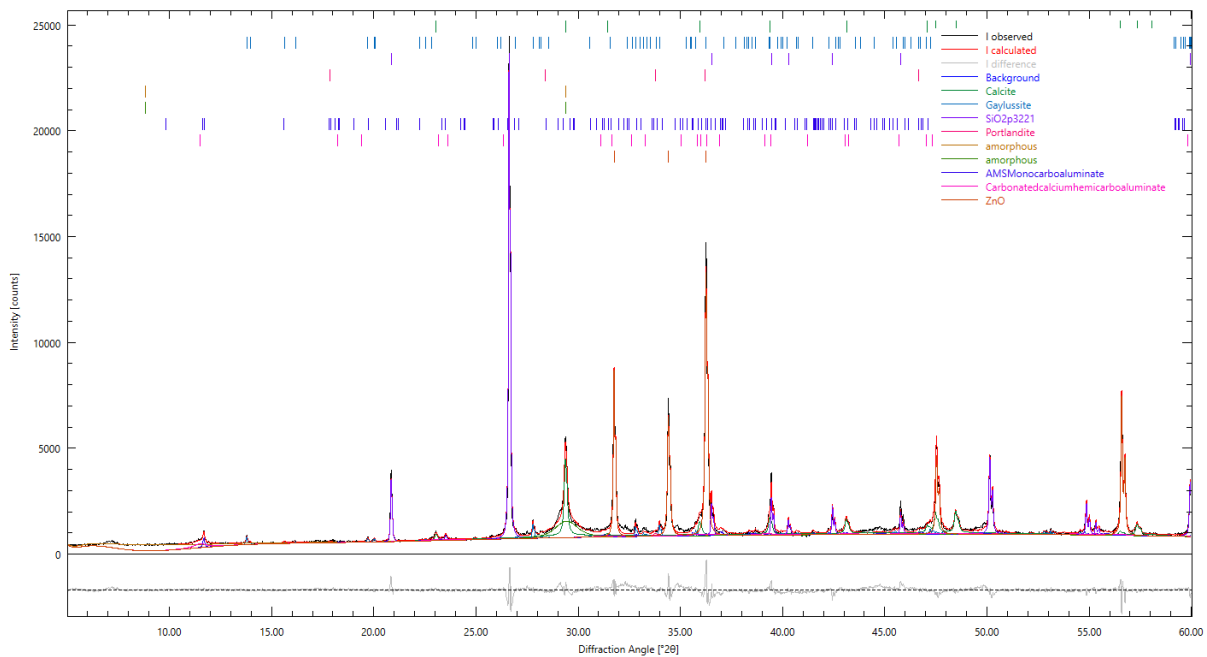


Figure 38: XRD diffractogram of an alkali-activated slag waste form containing 10% of air-dried salt.

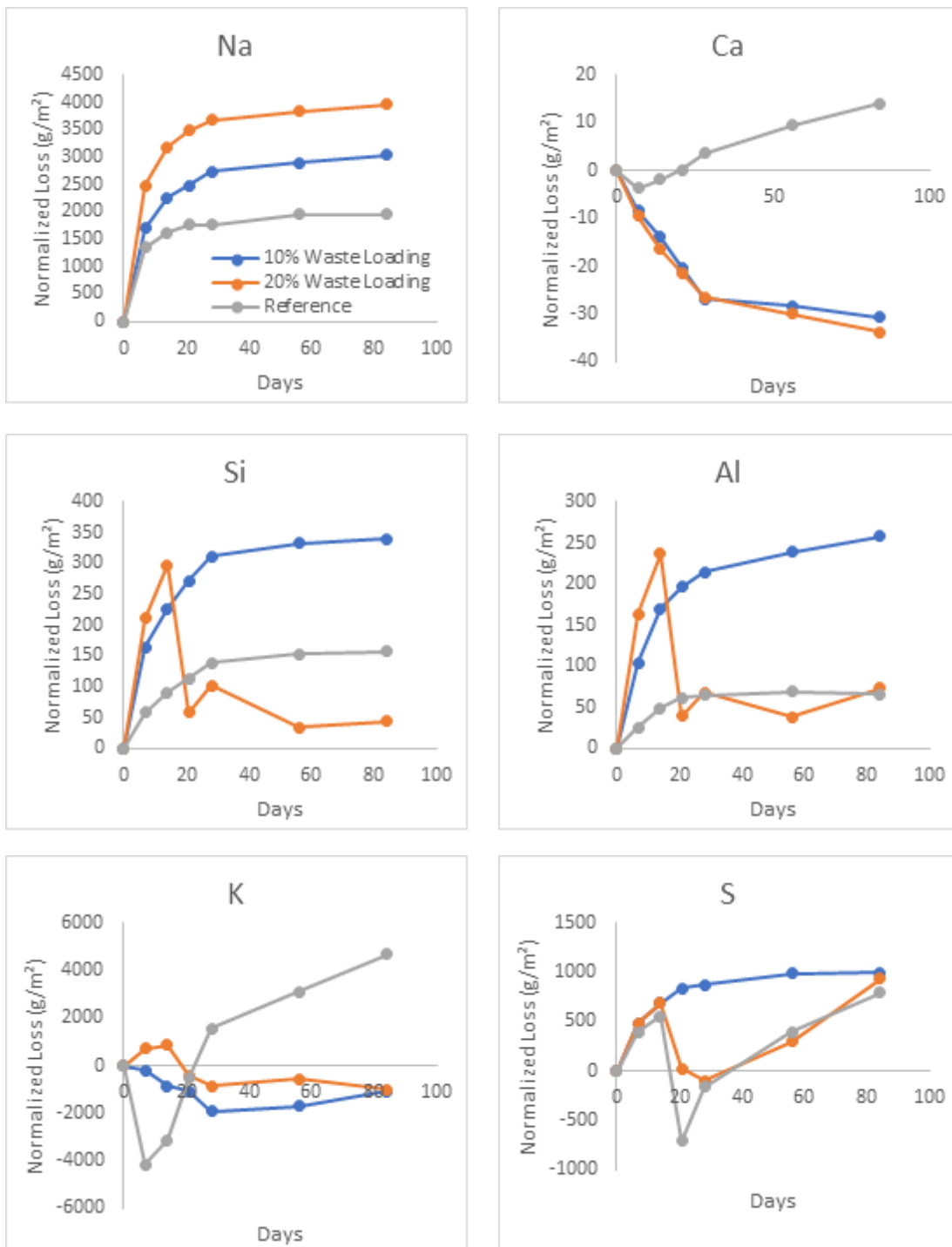


Figure 39: Normalized mass loss of Na, Ca, Si, Al, K and S in alkali-activated slag waste forms as a function of time.

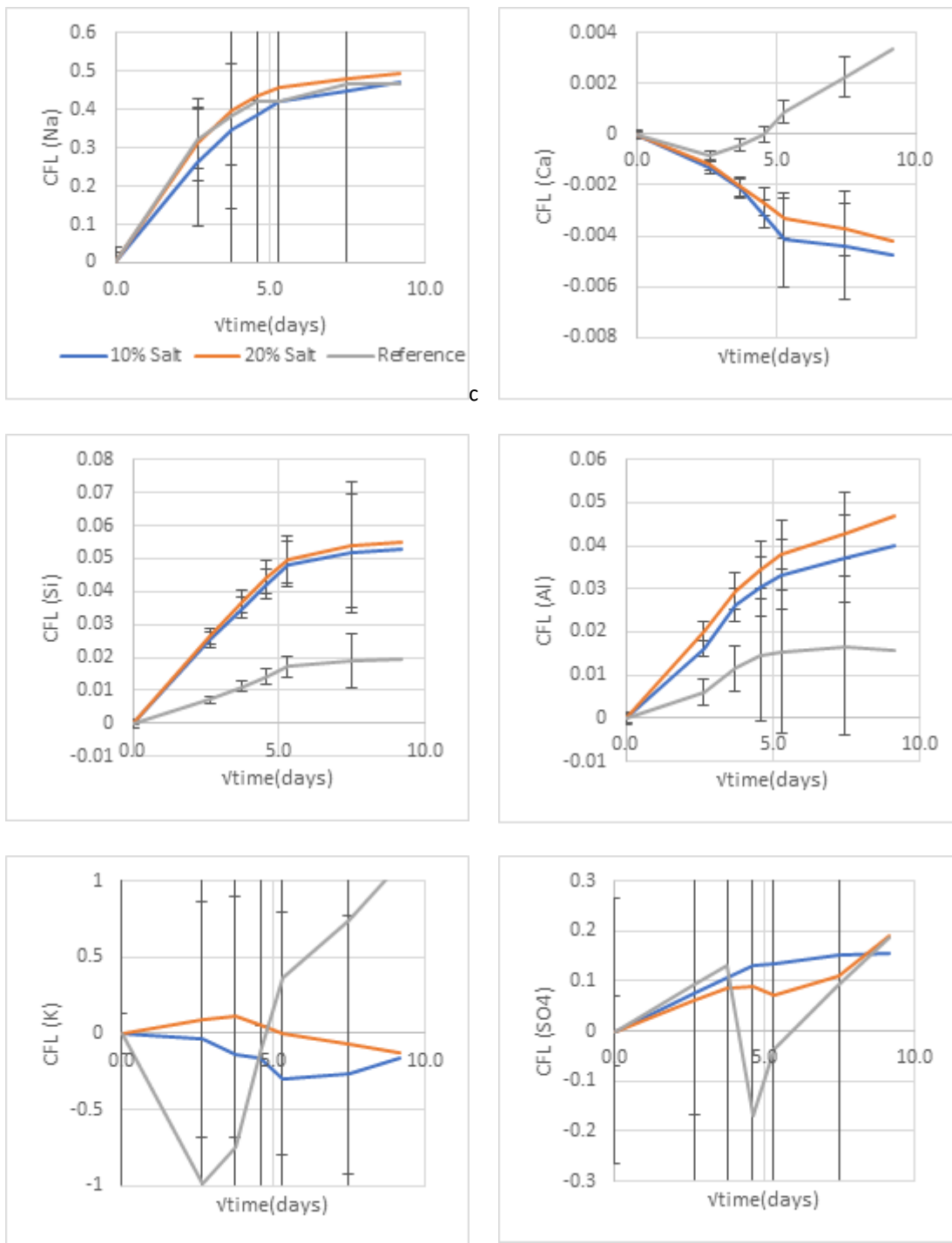


Figure 40: Cumulative fraction leached of Na, Ca, Si, Al, K and S in alkali-activated slag waste forms as a function of time.

Table 26: Leachability indices for all monitored elements for the alkali-activated slag waste forms. Values calculated from negative leaching rates are indicated in *italic*.

	Na	Ca	K	Al	SO ₄	Si
BFS – 10%	6	10	6	8	7	8
BFS – 20%	6	10	4	8	7	8
Reference	7	8	6	9	7	7

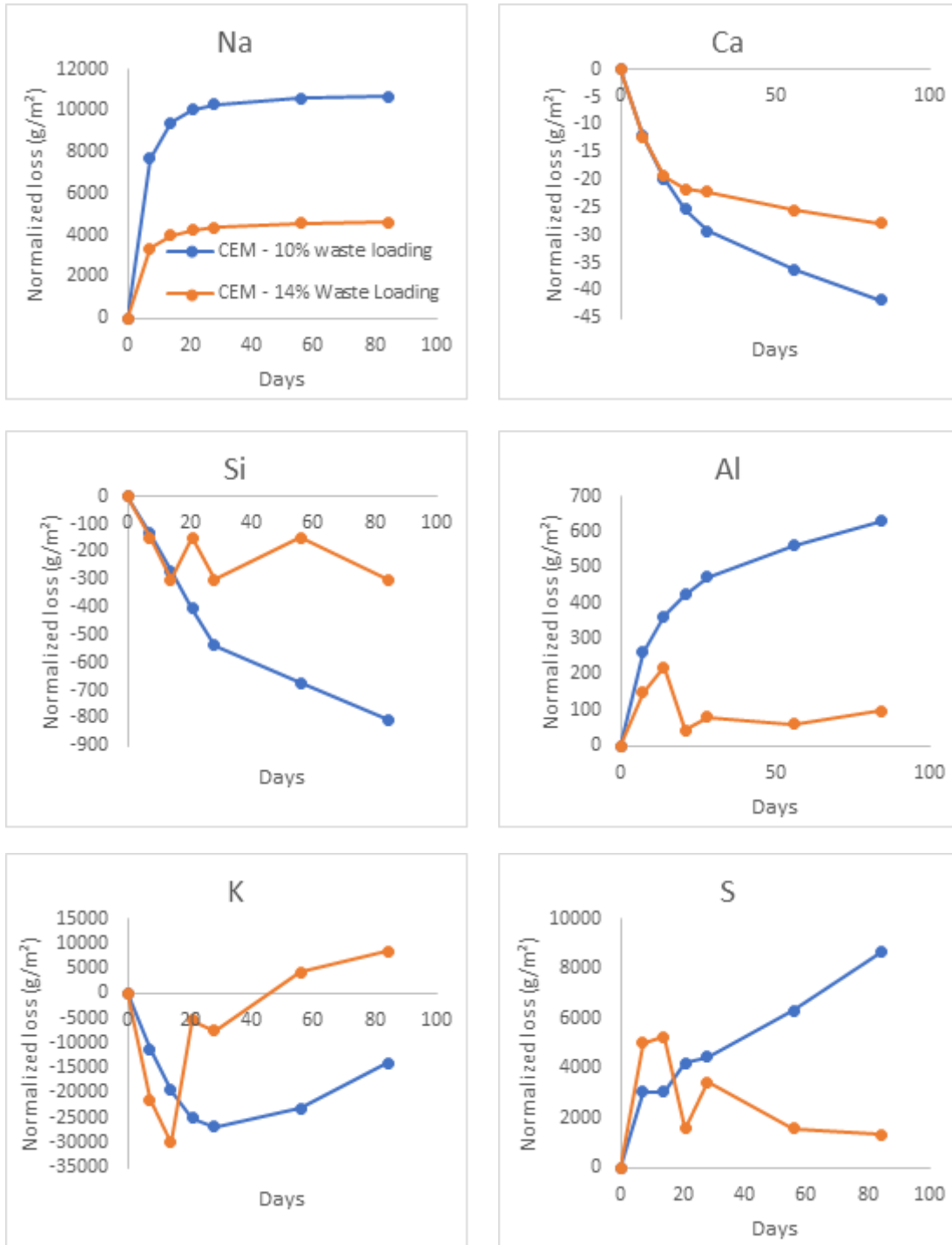


Figure 41: Normalized mass loss of Na, Ca, Si, Al, K and S in cementitious waste forms as a function of time.

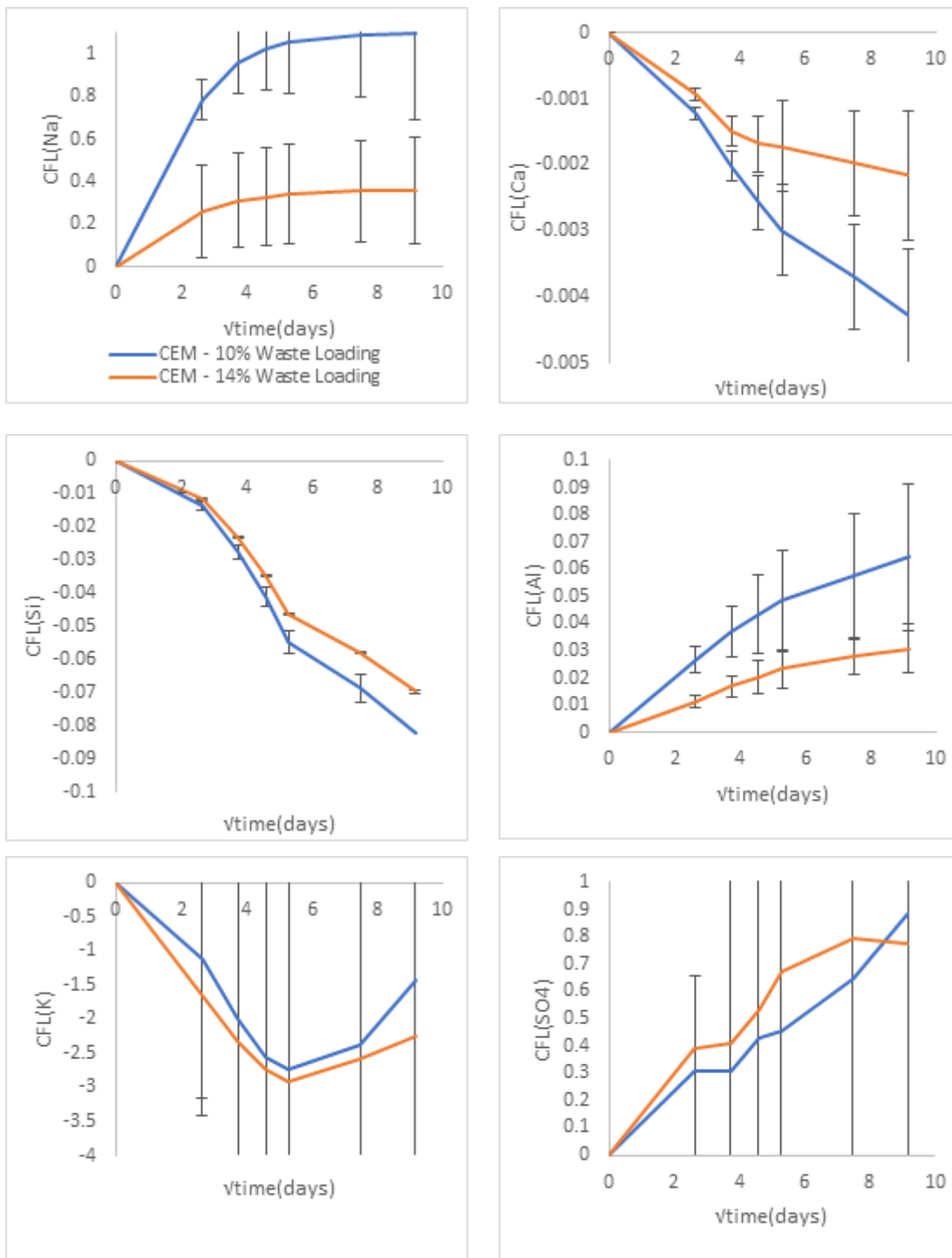


Figure 42: Cumulative fraction leached of Na, Ca, Si, Al, K and S in cementitious waste forms as a function of time.

Table 27: Leachability indices for all monitored elements for the cementitious waste forms. Values calculated from negative leaching rates are indicated in *italic*.

	Na	Ca	K	Al	SO ₄	Si
CEM – 10%	5	9	6	7	5	6
CEM – 14%	6	10	5	8	5	6

7 CEA CONTRIBUTION

7.1 Samples preparation

7.1.1 Waste

The waste studied is ash coming from the IRIS (Installation for Research on Incineration of Solids) pyrolysis/calcination incineration process installed at CEA Marcoule. This process is developed at CEA Marcoule for R&D support and devoted to the treatment of the organic waste contaminated by α -emitting actinides from glove boxes in the nuclear industry. This pilot is working exclusively under inactive environment, and the ashes produced come from the incineration of a mix of different organic solids and IER. This leads to achieve a volume reduction of the waste to about a 30 factor.

This is a three-stage process using rotating furnaces. The first stage consists of oxidizing pyrolysis at 550°C, producing a pitch which is then treated in a second calcination stage at 900°C in an oxygen-enriched atmosphere. The gases resulting from these thermal treatments include a fraction of volatile hydrocarbons, which are oxidized at 1100°C in an afterburner chamber.

The end-of-furnace waste is ash rich in silica, alumina and calcium oxide. The ashes have a high flying behaviour with a density of 0.2 g.cm⁻³ and their particle size is mainly between 0.1 to 1 mm.

SEM and structural characterizations show micro particles have a very porous aspect and are partially amorphous. The crystallized phase are composed of ringwoodite, anohrtite and chlorapatite Ca₅(PO₄)₃Cl [2].



Figure 43: (a) Ash optical scale, (b) SEM observations

7.1.2 Waste encapsulation protocol

Two types of samples were studied and characterized, from 2 different ways of conditioning ash from the IRIS incinerator, constituting the secondary waste from this heat treatment stage of mixtures of various solid organics (plastic mixtures and IER): 1) glassy samples containing an ash load of 30% by mass, and 2) pelletized, heat-treated ash samples for a densification stage.

Preparation of glassy samples (named V55-1)

The mixture of ash and glassy precursor (Si, Na, B base) is prepared in a proportion of 30% ash/70% glass. This intimate mixture is then slowly melted at low temperature (800°C) for 2 h and then slowly cooled. With these ash/glass proportions, this protocol enables ash conditioning with good dispersion in the matrix. In fact, it was found that above this proportion, the ashes aggregated on the surface and thus appeared less encapsulated. This was considered unfavorable for conditioning.

The glassy samples for the leaching tests were made from a square-section bar, which was then cut into parallelepipeds of around 10 x 10 x 3 mm³. These squares were then polished to grade 500.



Figure 44 : Preparation of glassy samples (named V55-1).

Preparation of pelletized ash samples (named V55-2)

The ash is mixed with an inorganic additive consisting of sodium silicate (5% by mass). This mixture is then compacted by a uniaxial press to obtain 10 mm diameter pellets. To consolidate these pellets, a heat treatment is then applied, at 1100°C for 3 hours. The pellets obtained after this treatment are slightly more compact, with an average diameter of 9 mm and a height of 3.6 mm.



Figure 45: Preparation of pelletized ash samples (named V55-2).

7.2 Leaching protocols

Two leaching media were tested in order to compare the obtained results: 1) PREDIS cement water as defined in the milestone MS39 [5], and 2) ultrapure water used in the MCC1 standardized tests [6].

1) The leaching protocol conditions for the cementitious “PREDIS” water are as follow:

- Savillex with screw cap (Teflon tape), 60 mL + baskets
- PREDIS synthetic cementitious water as defined in [5].

The solution was analyzed and the results are given in Table 28.

Table 28. Measured values for PREDIS leaching solution.

mg/L	K	Ca	SO42-	B	Na	Si	Al	Zn	pH
expected	2800	18	1083	/	/	/	/	/	12,7
measured	2782	15	1012	0,15	8,8	0,36	<0,05	<0,02	12,56

The experimental conditions were as follows:

- Oven 22°C ± 1°C;
- 1 sample V55-1 with Savillex change at 3, 7, 14, 21, 28, 56 days, stop at 91 days;
- 2 samples V55-2 under the same conditions as above.

The tests were doubled, with a modification of the deadlines (3, 14 and 28 days removed).

The conditions under which this test was carried out meant that the cementitious water had to be handled in a neutral atmosphere (N₂). Transfers of liquids (Savillex filling) and solids (during

container changes) were carried out under a hood. The latter is drawn under vacuum and then re-inflated with 99.99% dry nitrogen (repeated 2 times) before use:



Figure 46: Preparation of samples in a hood under a neutral atmosphere / Savillex 60 mL.

The cleanliness of the Savillex is tested prior to use by qualifying double-distilled water which has been left in the Savillex for 48 hours at 90°C (checking pH and conductivity). Pending use, Savillex filled with cementitious water are stored at a temperature of $22 \pm 1^\circ\text{C}$. The mass is checked before use to take account of any evaporation during this phase. When the Savillex is changed, the samples are gently grasped with Teflon tweezers and brought into contact with a sheet of cellulose (from below) to remove any excess liquid (hanging drop).

10 mL solution is filtered through a 0.45 μm Advantor filter and acidified with HNO_3 for chemical composition determination by ICP.

5 mL are filtered and stored for measurement of pH and silicon content by photometry. The rest of the solution is kept in its raw state.

After a cumulative 91 days, the tests are stopped; the samples are recovered, dried in an oven at 90°C for 48 hours and cooled before weighing.

The pH of the test solutions was measured according to the sampling intervals and results are given in Table 29.

Table 29. Measured pH values in experiments in different time intervals from 0 to 91 days.

pH	V55-1 essai 1	V55-1 essai 2	V55-2 essai 1	V55-2 essai 2
t0	12,56	12,56	12,56	12,56
3 j	12,68	X	12,69	X
7 j	12,66	12,68	12,67	12,68
14 j	12,72	X	12,68	X
21 j	12,71	12,72	12,69	12,7
28 j	12,72	X	12,67	X
56 j	12,69	12,73	12,68	12,68
91 j	12,86	12,83	12,86	12,82

2) The leaching protocol conditions for the ultrapure water are as follow:

- Savillex with screw cap with openings (Teflon tape), 180 mL, new, defluorinated and washed;
- Normaton-VWR ultrapure water Lot 9221090;
- Oven $90^\circ\text{C} \pm 1^\circ\text{C}$;

- V55-1 samples without change of Savillex and sampling at 1, 3, 7, 14, 21, 28, 56 days, stop at 91 days;
- V55-2 samples under the same conditions.

For the sampling for these tests:

- 5 mL of ultrapure water are taken using a syringe and preheated to 90°C;
- these 5 mL are injected into the Savillex through one of the openings, the body of the syringe is filled/injected four times in order to homogenize the solution in the Savillex;
- 5 mL of solution are taken, filtered 0.45 µm Sartorius and acidified HNO₃;
- pH of the leaching solution is only measured once at the end of the tests, and the pH results are reported in Table 30.

Table 30. Measured pH values in leaching experiments with ultrapure water.

pH	V55-1	V55-2
t0	6,03	6,03
91 j	9,56	8,75

7.3 Results

PREDIS test results

At the end of the tests, the weighing of the pellets makes it possible to obtain an average speed alteration.

The results are summarized in Table 31.

Table 31. Results of the sample weighing and average speed

	Test	Sample	Initial mass (g)	Final mass (g)	Average speed at 91d (g/m ² /j)
V55-1	V55-1-1	1	0,9370	0,9238	0,40
	V55-1-2	2	0,9452	0,9339	0,34
V55-2	V55-2-1	1	0,5121	0,5090	0,26 +/- 0,15
		2	0,4301	0,4227	
	V55-2-2	3	0,4833	0,4762	0,23 +/- 0,12
		4	0,5111	0,5079	

We note a significant variation in the average speed deduced from mass losses which can be due in particular to variations in the texture and heterogeneity of the samples. The post-leaching weighings are carried out after drying. The weathering film may be subject to deterioration (detachment, peeling, etc.) leading to a reading error. A photometric determination of silicon was carried out on each test portion. Considering the very basic leaching solution and loaded with different elements, these results are only qualitative (need for acidification, interferences).

The solutions of the V55-1 tests were measured by ICP. The results obtained in this case made it possible to trace the evolution curves of the mass losses for each element measured according to time:

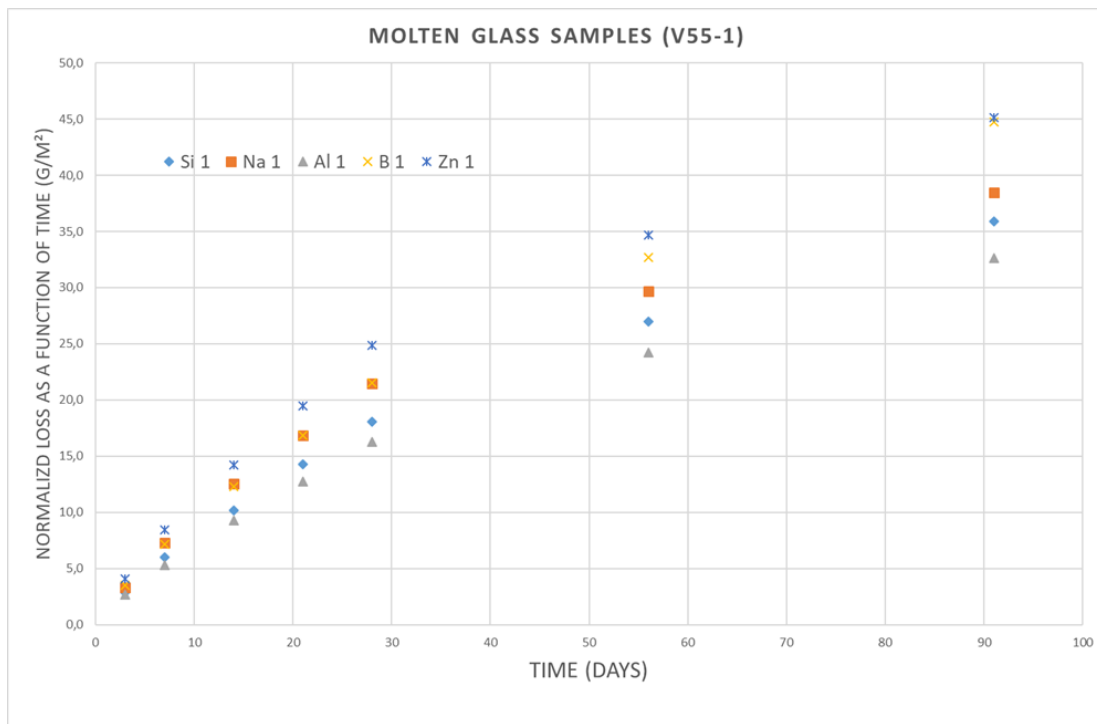


Figure 47: Normalized loss as a function of time, samples V55-1.

An additional calculation, makes it possible to draw a curve of the evolution of the altered thickness (in cm) as a function of the square root of time (in seconds). The parameters of the linear regression must make it possible to calculate a diffusion coefficient.

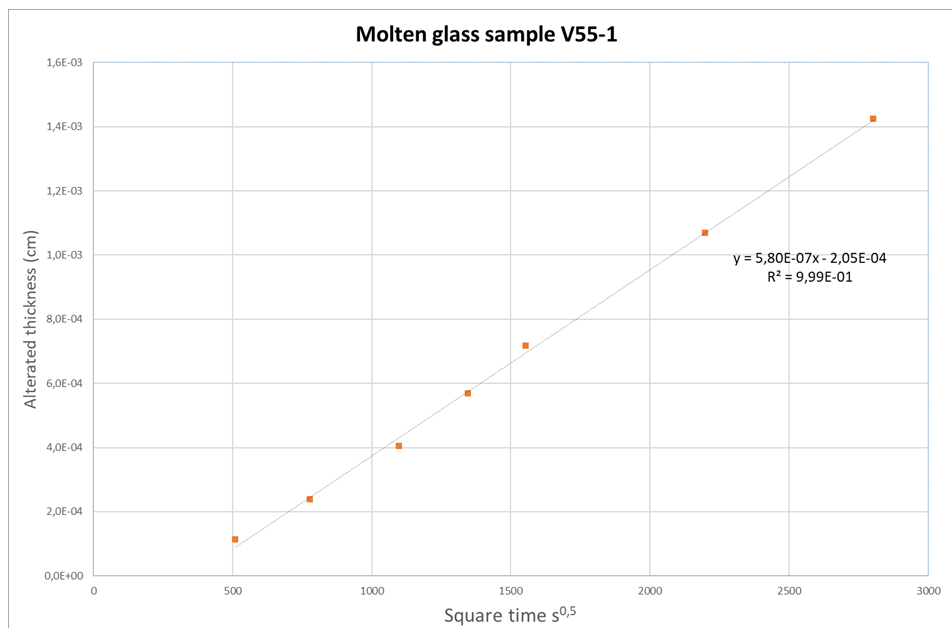


Figure 48: Altered thickness of the V55-1 sample.

MCC1 test results

At the end of the tests, the weighing of the pellets makes it possible to obtain an average speed alteration. The results are summarized in Table 32.

Table 32. Results of the sample weighing and average speed with alteration for MCC1 tests.

	Sample	Initial mass (g)	Final mass (g)	Average speed at 91d (g/m ² /j)
V55-1	3	0,9365	0,9227	0,49 +/-0,17
	4	0,9423	0,9316	
	5	0,9263	0,9025	
	6	0,9259	0,9086	
V55-2	5	0,4897	0,4876	0,09 +/-0,01
	6	0,4694	0,4675	
	7	0,5245	0,5225	
	8	0,5786	0,5765	
	9	0,6792	0,6773	
	10	0,6224	0,6201	

The alteration rate values in pure water at 90°C show a significant difference between the two materials.

The solutions of the V55-1 tests were measured by ICP. The results obtained in this case made it possible to trace the evolution curves of the mass losses for each element measured according to time:

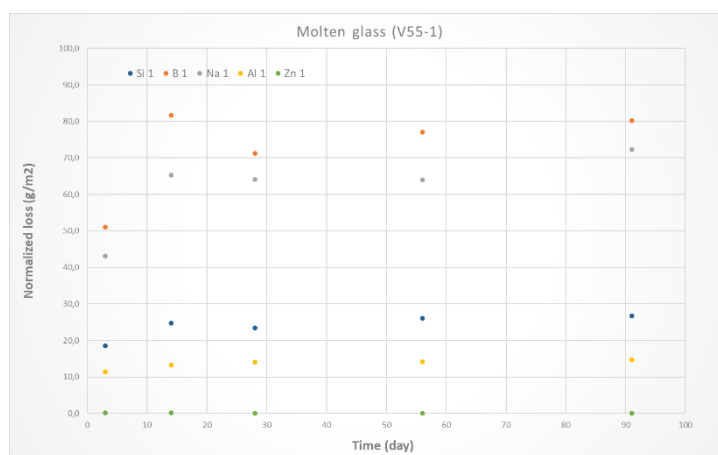


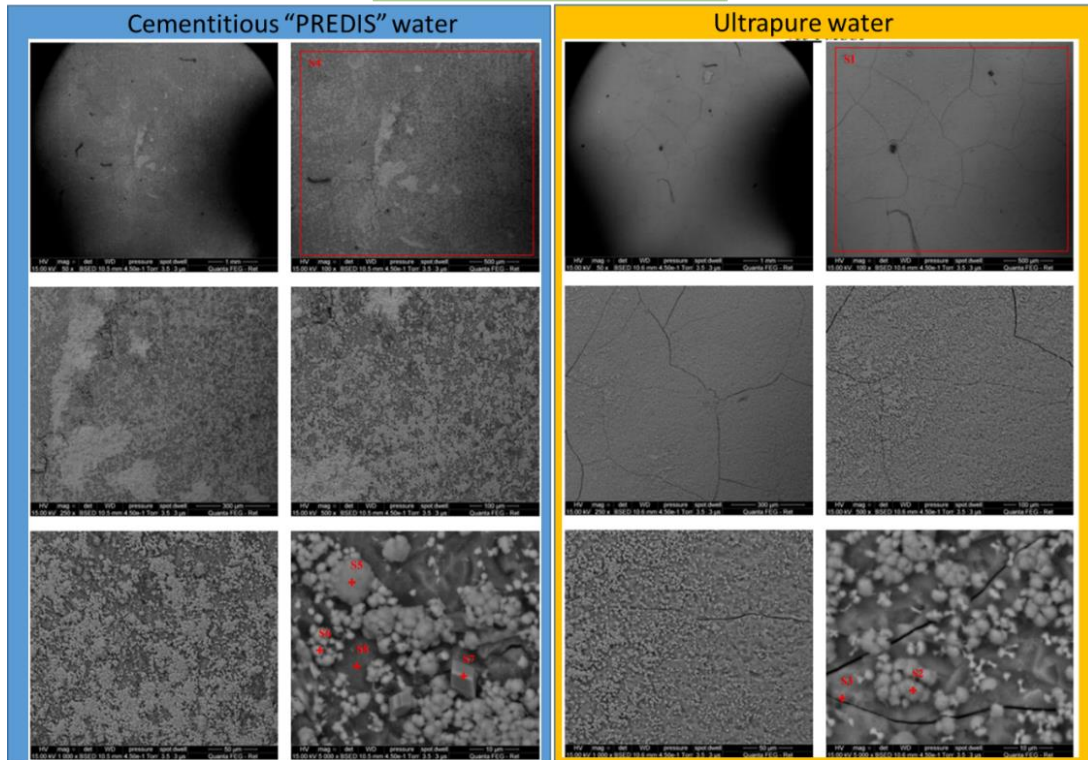
Figure 49: Normalized loss as a function of time, samples V55-1.

These curves show that saturation seems to appear quickly, probably due to a retroactive effect.

SEM observations of the sample surfaces after leaching were carried out. The results are shown in Figures 50 and 51.

Additional information on the post-mortem characterization of tested specimens and leachates analysis is available in [CEA Data collection Task6.6.xlsx](#). (available to PREDIS partners).

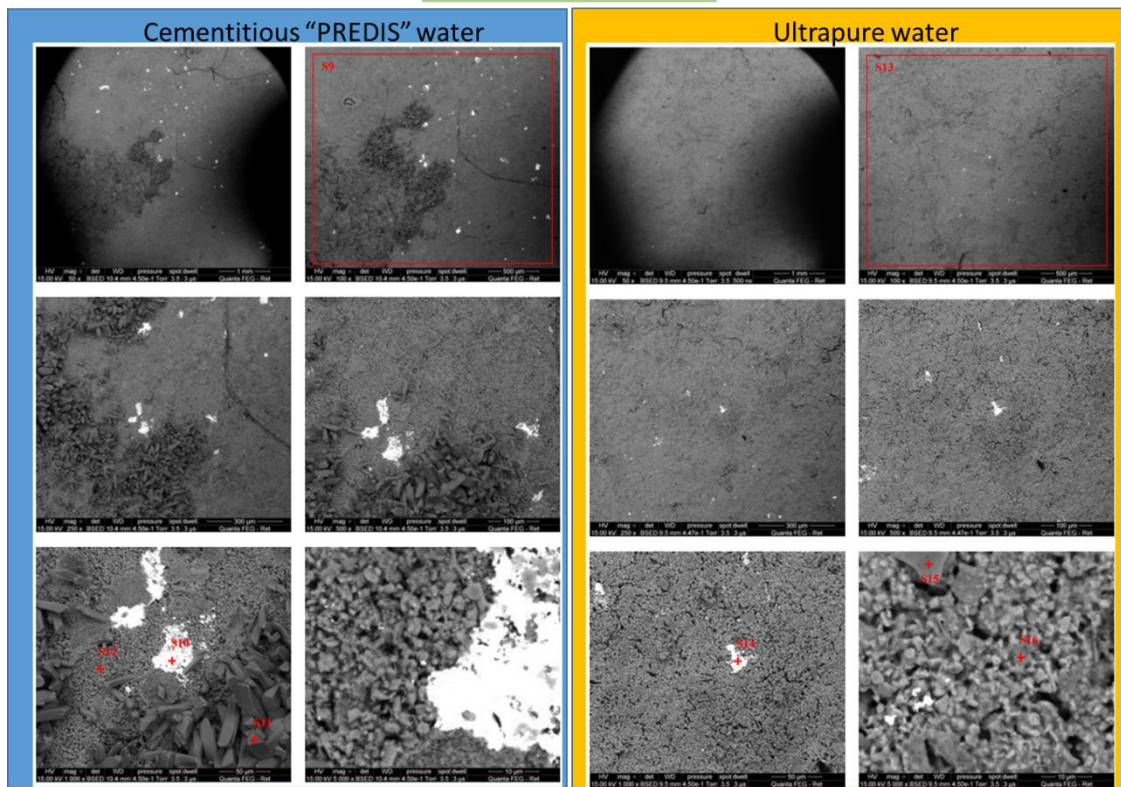
Molten glass samples (V55-1)



		C	O	Na	Mg	Al	Si	P	S	K	Ca	Ti	Fe	Zn	Hf	Ta	
V55-1	théorie		41,9	22,0	1,1	6,1	20,6	0,6		1,2	3,9	0,2	0,2	2,3			
	MCC1	S1	3,2	47,2	1,3	5,3	7,8	16,6	1,8	0,0	0,2	7,1	1,2	0,4	7,9	0,0	0,0
		S2	3,3	48,1	0,7	1,5	3,4	8,2	8,9	0,0	0,1	22,0	0,3	0,0	3,7	0,0	0,0
		S3	2,3	47,0	1,3	5,5	8,4	18,6	1,2	0,0	0,3	6,2	1,2	0,4	7,6	0,0	0,0
	PREDIS	S4	6,8	47,6	3,2	4,1	1,7	2,8	3,8	0,8	7,5	15,9	2,1	0,8	3,1	0,0	0,0
		S5	5,2	45,6	2,2	1,0	0,5	3,5	7,2	0,3	4,6	24,7	1,2	0,4	3,8	0,0	0,0
		S6	6,4	48,3	2,6	1,0	0,5	3,3	6,2	0,3	4,7	21,2	1,0	0,4	4,2	0,0	0,0
		S7	9,0	44,2	1,6	1,1	0,5	1,2	1,7	0,4	4,0	33,9	0,6	0,3	1,7	0,0	0,0
		S8	3,9	45,5	2,6	5,6	2,4	3,0	1,9	1,1	16,3	9,7	3,8	1,4	2,8	0,0	0,0

Figure 50: SEM pictures and results of analyzes expressed in % normalized elemental mass (excluding elements lighter than C).

Pellets samples (V55-2)



		C	O	Na	Mg	Al	Si	P	S	K	Ca	Ti	Fe	Zn	Hf	Ta	
V55-2	théorie		45,1	0,7	2,8	15,6	14,3	1,5		3,1	10,1	0,4	0,4	6,0			
	PREDIS	S9	4,5	40,4	1,5	3,1	15,5	9,9	1,6	0,2	2,9	12,9	0,7	0,4	6,5	0,0	0,0
		S10	3,9	19,9	0,4	0,4	3,5	0,0	0,2	0,0	0,8	4,5	0,3	0,0	1,5	59,5	5,2
		S11	13,0	50,5	0,0	0,4	1,9	1,1	0,2	0,0	0,4	31,0	0,2	0,2	1,1	0,0	0,0
		S12	3,5	41,0	1,3	2,5	14,0	13,0	1,9	0,2	3,4	12,4	0,7	0,2	4,8	1,1	0,0
	MCC1	S13	3,1	39,7	1,4	3,3	15,9	13,2	2,3	0,0	3,1	9,7	0,7	0,5	7,1	0,0	0,0
		S14	4,1	20,6	0,4	0,6	3,9	1,4	1,0	0,0	1,0	3,4	0,4	0,0	2,0	53,4	7,8
		S15	3,8	45,9	0,5	2,6	6,1	28,4	0,7	0,0	1,1	7,3	0,3	0,3	3,0	0,0	0,0
		S16	3,6	40,9	1,6	2,4	17,2	13,2	1,7	0,0	3,2	8,4	0,5	0,3	7,1	0,0	0,0

Figure 51: SEM pictures and results of analyzes expressed in % normalized elemental mass (excluding elements lighter than C).

In the absence of analyses on healthy pellets, the results obtained on altered pellets are compared to theoretical compositions.

Overall, we see that:

- The pellets having undergone the PREDIS test have a surface depleted in Si (especially V55-1);
- The surfaces present several a priori secondary crystallized phases (no trace polishing), certain constituent elements of these phases are potentially derived from the cement solution;
- Consistent with the solution analyses, the MCC1 test pellets show the conservation of less mobile elements (Al, Zn) and depletion of elements mobile (Na, K).

8 UNIVERSITY OF SHEFFIELD CONTRIBUTION

8.1 Samples preparation

8.1.1 Waste

Simulant IRIS ash was supplied to USFD by CEA. The material has a loose, light grey appearance, with significant particle heterogeneity (photograph in Figure 52 a). The ash weighed 305 g, and occupied a cylindrical space approximately 9 cm high by 12.5 cm wide (1104 cm³), resulting in a bulk density of 0.28 g/cm³.

Powder X-ray diffraction (XRD) analysis of the received ash is shown in Figure 52. This reveals a complex, diffraction pattern with both crystalline and poorly crystalline components. Phase matching determined the presence of crystalline anorthite (CaAl₂Si₂O₈), diopside (MgCaSi₂O₆), chlorapatite (Ca₅(PO₄)₃Cl), and anhydrite (CaSO₄), in addition to a minor contribution from gypsum (CaSO₄·2H₂O), and an unidentified poorly crystalline component at ~35 - 38° 2θ, as well as the broad background peak indicative of an amorphous component.

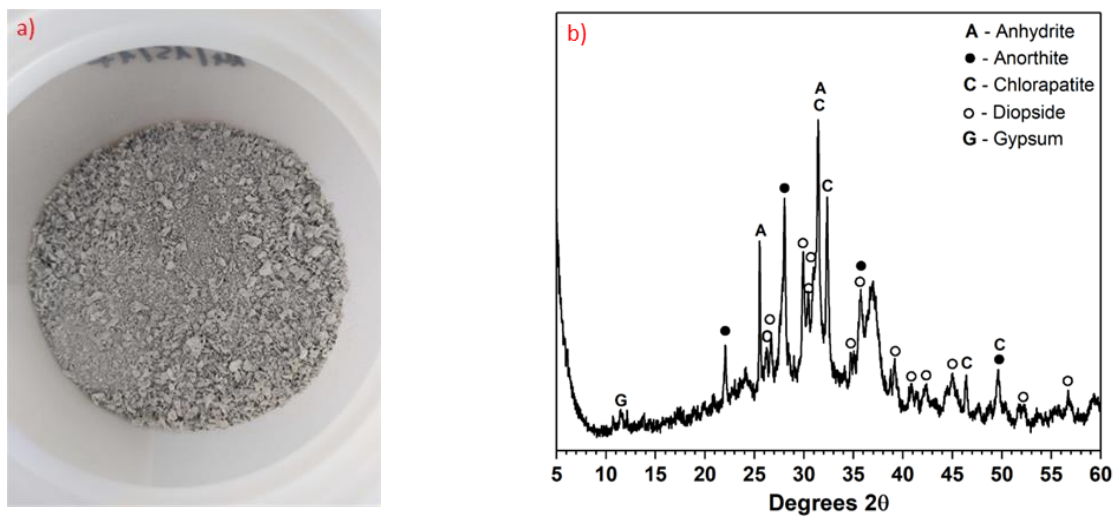


Figure 52. a) Photograph of as-received simulant IRIS ash. b) XRD pattern of as-received ash.

CEA supplied the ash chemical composition, as detailed in Table 33 ~75 wt. % of the material consists of SiO₂ + Al₂O₃ + CaO, with further contributions from P₂O₅, K₂O, ZnO, MgO. A number of minor components also exist.

Table 33. IRIS ash chemical composition provided by CEA.

Element	Al	Si	Ca	Zn	K	Mg	P	Cl	Na	S	Ni	Fe	Ti	Ba	Bi	Cr
Weight %	15.06	13.72	9.68	5.76	3.00	2.73	1.83	1.74	0.71	0.57	0.48	0.44	0.41	0.13	0.11	0.06

8.1.2 Waste immobilisation protocol

The simulant IRIS ash was treated using hot isostatic pressing (HIP). Prior to HIPing the simulant IRIS ash was ground by hand for five minutes, in a porcelain mortar and pestle. A total of three different formulations were attempted, (Table 34), firstly, the direct HIPing of the ground IRIS ash, to achieve a waste loading of 100 wt.% and then the HIPing of ash with glass forming additives were attempted. Two formulations with additives were produced, one with a 5 wt.% addition of sodium tetraborate and the other with a 5 wt.% addition of sodium aluminate; thus both have a nominal waste loading of 95 wt.%.

The same preparation and HIP conditions were performed for each formulation. Material was packed into a HIP can, welded, baked out at 300 °C for a minimum of 12 hours, and then sealed. HIP cans were then processed at 100 MPa pressure, heated to 1250 °C with a ramp up of 10 °C.min⁻¹ with a 2-hour dwell.

Table 34. HIPed IRIS ash target chemical compositions and waste loading.

Additive	Waste loading (wt.%)	Target composition (wt. %)																
		Al	Si	Ca	Zn	K	Mg	P	Cl	Na	S	Ni	Fe	Ti	Ba	Bi	Cr	B
None	100	15.06	13.72	9.68	5.76	3.00	2.73	1.83	1.74	0.71	0.57	0.48	0.44	0.41	0.13	0.11	0.06	0.00
Na ₂ B ₄ O ₇	95	14.31	13.03	9.20	5.47	2.85	2.60	1.74	1.66	0.68	0.54	0.46	0.42	0.39	0.12	0.10	0.05	0.01
NaAlO ₂	95	14.32	13.03	9.20	5.47	2.85	2.60	1.74	1.66	0.68	0.54	0.46	0.42	0.39	0.12	0.10	0.05	0.00

8.1.3 Immobilised material

Visual examination of HIP can cross sections cut from all three HIPed formulations found the samples to be heterogeneous, as can be seen in Figure 53. Heterogeneity was especially apparent between material in the centre of the HIP can, and material which was close to the HIP can wall. The latter material has been affected by chemical interactions between the HIP cans and the HIPed material, resulting in the incorporation of elements from the HIP can into the material during HIPing. Only material from the centre of each HIP can was collected for further analysis and leaching experiments.



Figure 53. Photographs of HIP can cross sections of HIPed a) ground ash b) ground ash + 5 wt.% Na₂B₄O₇ and c) ground ash + 5 wt.% NaAlO₂.

XRD data (Figure 54) were collected from material cut from the centre of each HIPed can (process described below). Analysis of the XRD patterns revealed that the HIPed ground ash and HIPed ground ash with additions of NaAlO₂ were highly crystalline, and both contained identified phases with the structure of anorthite (CaAl₂Si₂O₈), diopside (MgCaSi₂O₆), chlorapatite (Ca₅(PO₄)₃Cl), leucite (KAlSi₂O₆), and spinel ('MgAl₂O₄', but likely with Zn, Fe and Cr substitutions). However, in the XRD pattern collected from the ground ash + NaAlO₂ formulation, peaks attributed to C and S had a greater relative intensity. Unlike the other formulations, the XRD pattern collected from ground ash + 5 wt.% Na₂B₄O₇ only presented reflections associated with spinel ((Zn,Mg)(Al,Cr)₂O₄ and chlorapatite (Ca₅(PO₄)₃Cl), and there was a region of diffuse scattering present, indicating the formation of a glassy phase. The lack of any reflections associated with the crystalline silicate phases in the XRD pattern, which were present in the untreated ash, are evidence that wastefrom decomposition occurred to a greater extent in this formulation. None of the XRD patterns from any formulation presented reflections which could be attributed to anhydrite (CaSO₄) or gypsum (CaSO₄·2H₂O).

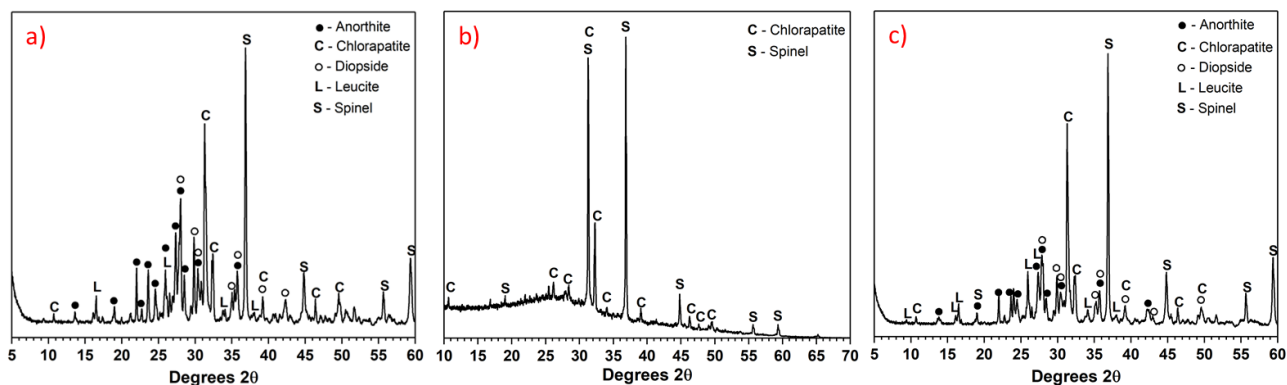


Figure 54. XRD patterns of HIPed a) ground ash b) ground ash + 5 wt.% $\text{Na}_2\text{B}_4\text{O}_7$ and c) ground ash + 5 wt.% NaAlO_2 .

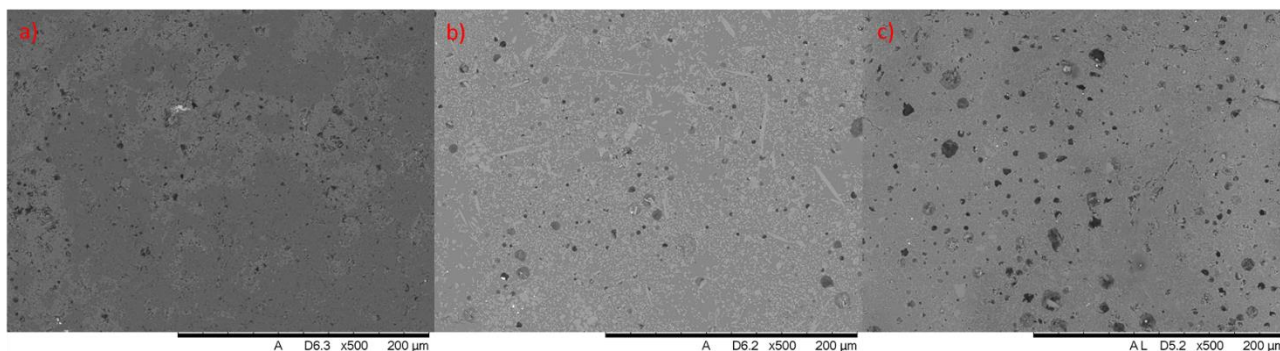


Figure 55. SEM BSE micrograph of HIPed a) ground ash b) ground ash + 5 wt.% $\text{Na}_2\text{B}_4\text{O}_7$ and c) ground ash + 5 wt.% NaAlO_2 .

SEM of the no additives formulation showed a heterogeneous product, with phase separation evident in the BSE micrograph (Figure 55 a), analysis of EDX data (not shown) revealed that Mg and Zn are anti-correlated with Si. Additions of $\text{Na}_2\text{B}_4\text{O}_7$ and NaAlO_2 resulted in more homogenous materials. Analysis of SEM (Figure 55 b) and EDX from HIPed ground ash + 5 wt.% $\text{Na}_2\text{B}_4\text{O}_7$ show a more homogenous sample, with glassy material containing large Ca and P rich crystals (chlorapatite), and smaller crystals which were assigned as spinel. The ground ash 5 wt.% NaAlO_2 also appeared more homogenous than no additions, however a lighter phase is apparent in the BSE micrograph (Figure 55 c), which EDX suggested was chlorapatite (Cl, Ca and P all associated in the lighter phase). EDX analysis also showed a variation in K concentration within the darker grey bulk phase.

Laser ablation ICP-MS (LA-ICP-MS) measurements were undertaken to attempt to confirm the composition of the formulations after HIPing. However, due to the highly heterogeneous nature of the samples and the relatively small measurement areas achievable with the instrumentation and sample available it was not possible to measure a representative composition. Notably all LA-ICP-MS measurements of all three formulations had consistently higher concentrations of Ba than the composition provided by CEA, by a factor of 2 to 3, so analysis of ICP-OES data shown later may overestimate the normalised mass loss of Ba.

8.2 Leaching protocols

8.2.1 Sample preparation

HIPed samples were sectioned to remove all faces in contact with the canister to ensure only the bulk sample was utilised (and not the canister-wasteform interaction zone), as demonstrated in Figure 56. The resulting cuboid was then cut in such a way as to produce a series of small cuboids for dissolution testing. Due to the small size of the HIP canisters, and the densification during HIP processing, very small cubes were required to maximise the number of samples that could be prepared from each canister. Between 9-12 cuboids were prepared from each canister, with sides

an average 4-5 mm length, and an average resulting surface area of 1.26 cm². Surfaces were not ground or polished further, and therefore retained the finish provided by the cutting blade.

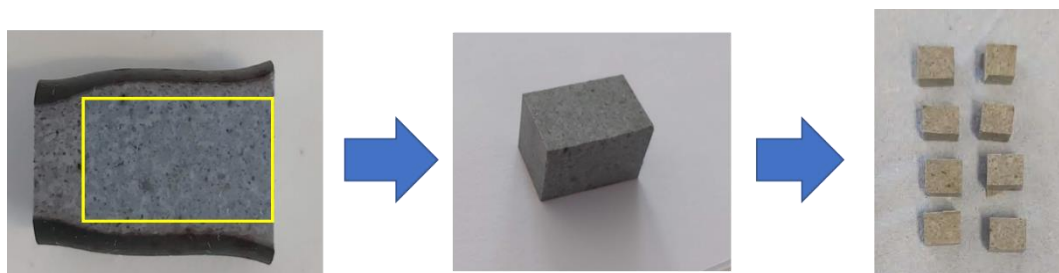


Figure-56. Photographs of HIPed ash size reduction stages (N.B. for this sample the cubes were further trimmed to ensure flat faces, and two further cubes were recovered from an off-cut piece).

8.2.2 Leaching protocols

A 24-month semi-dynamic periodic solution replacement leaching methodology was undertaken. Monoliths were placed on PFA support baskets in PFA PCT style vessels, and submerged in leachate. The volume of leachate was determined by monolith surface area, to ensure a fixed surface area (monolith) to liquid (leachate) ratio of 10 cm³ to 1 cm² (10 cm) was maintained. The leachate was a synthetic cementitious water which was prepared under anaerobic conditions, using degassed de-ionised Milli-Q[®] water, and reagents 1 M KOH, K₂SO₄ and CaSO₄ 2H₂O to produce a target ppm shown in Table 35, leachate was prepared in 1 L volumes and the pH was measured after preparation to confirm a target pH of 12.7 was achieved. Set up and sampling were undertaken under anaerobic/CO₂ free conditions, however to enable the maintenance of a temperature of 22 ± 2°C, which was not possible within the anaerobic chamber, the sealed vessels were then removed, placed into sealed tubs and stored in a Herathem IMC18 Incubator. Aliquots of leachate were removed for sampling and leachate was replaced at time points day 7, 14, 21 and 28, then every month until month 12 and then at months 14, 16, 18 and 24. Leachate was removed and filtered using a PTFE filter under anaerobic conditions.

Table 35. Target elemental concentrations in the synthetic cementitious water.

Component	K	Ca	SO ₄
Target composition (mg.L ⁻¹)	2800	18	1083

8.2.3 Characterization

After sampling the pH of leachate was measured using a Mettler Toledo fiveeasy pH meter which had been calibrated with pH 4.0, 7.0 and 10.0 standards. Samples were then acidified with 100 µmL ultrapure HNO₃ in preparation for ICP-OES. ICP-OES was performed on a Perkins Elmer Optima 5300.

Sacrificial samples were removed for post-mortem characterisation at months 3 and 12. The monoliths were immediately mounted in epoxy resin to preserve any alteration or precipitates on the surface of the monolith. Samples were then prepared for characterisation by grinding and polishing to a finish of 1 µm (using IPA and oil-based diamond suspensions), and then carbon coated. To enable comparison a set of pristine samples were also prepared using the conditions. SEM and EDX data were collected on a Hitachi TM3030, in EDX mode with an accelerating voltage and a working distance c.a. 8.3 mm. EDX measurements were performed on a Bruker Energy Dispersive X-Ray Spectrometer attached to the Hitachi TM3030, and EDX maps were all collected with 5 minutes scans. X-ray diffraction data were collected on a Malvern Panalytical Aeris diffractometer (Cu Kα, 1.5418 Å). Diffraction patterns were collected from 10° to 100° 2θ with a step size of 0.022°.

8.3 Results

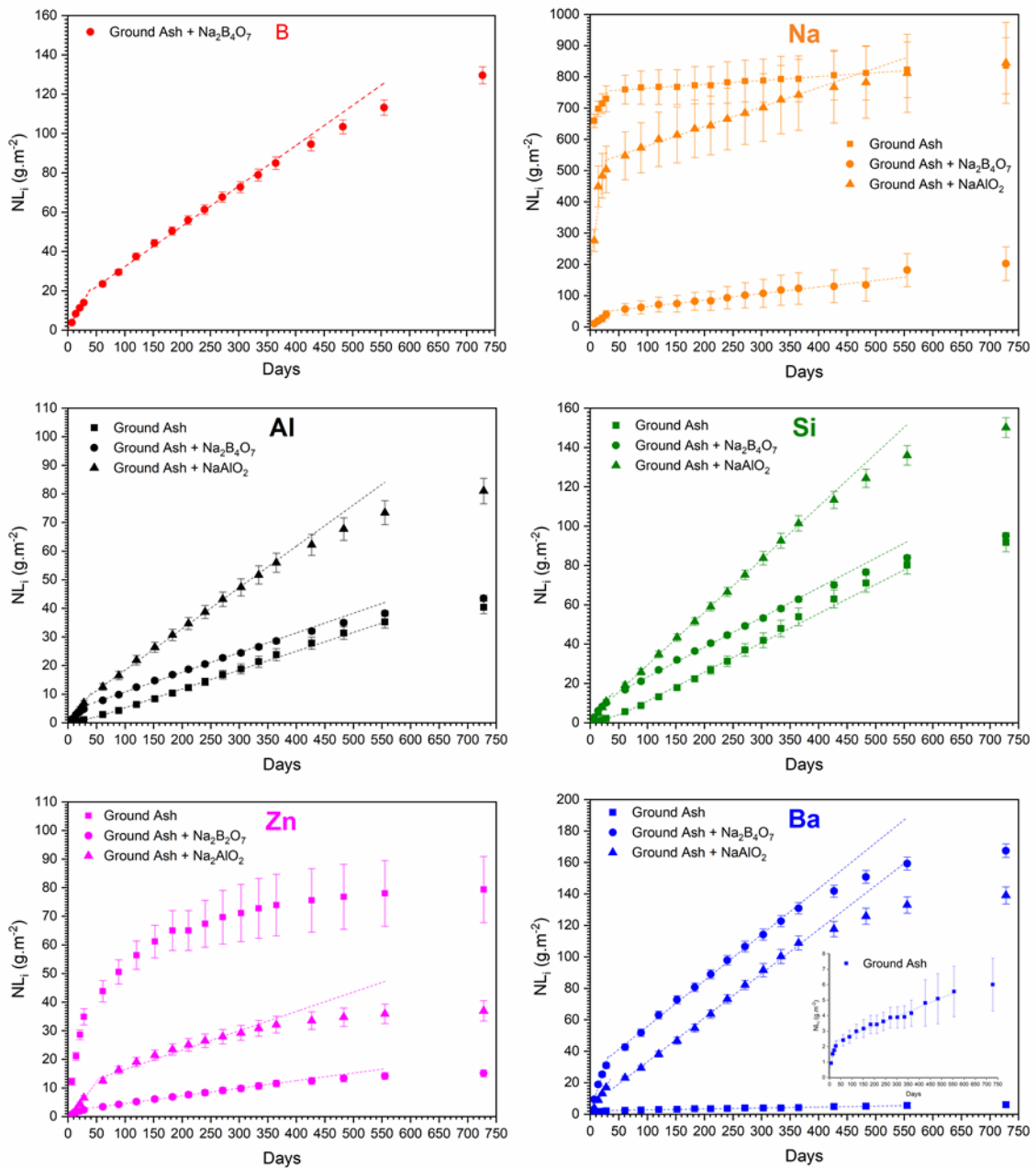


Figure 57. Normalised mass loss of B, Na, Al, Si, Zn and Ba from HIPed ground ash, HIPed ground ash + 5 wt.% $Na_2B_4O_7$ and HIPed ground ash + 5 wt.% $NaAlO_2$.

Overall trends

The normalised elemental mass loss (NL_i) for all elements in the two formulations (Figure 57) containing additions present a similar trend in release which can be described using two linear fits: an initial faster rate of release for days 7 to 28, and then a slower release for M2 (day 61) to M12 (day 365); which is followed by a further drop off in release in M14 (day 427) to M24 (day 728). The one exception to this is for Na in the ground ash + 5 wt.% $Na_2B_4O_7$ formulation where no drop off is observed. The parameters from these fits are shown in Table 36, the linear fits for M2 to M12 for each element have been projected to M18 to enable observation of the drop off in release.

The normalised elemental mass loss for elements from the no addition formulation do not all follow the trend described above. The normalised mass loss of Na, Al, Si and Ba can all be described by

two linear fits over the same two time periods, however Al and Si both display an increase in release rate from the (0.048 $\text{g}\cdot\text{m}^{-2}\cdot\text{d}^{-1}$ increasing to 0.066 $\text{g}\cdot\text{m}^{-2}\cdot\text{d}^{-1}$ and 0.091 $\text{g}\cdot\text{m}^{-2}\cdot\text{d}^{-1}$ to 0.148 $\text{g}\cdot\text{m}^{-2}\cdot\text{d}^{-1}$, respectively).

The addition of + 5 wt.% $\text{Na}_2\text{B}_4\text{O}_7$ resulted in an increase in the initial release rates of Al and Si (0.048 to 0.172 $\text{g}\cdot\text{m}^{-2}\cdot\text{d}^{-1}$ and 0.091 to 0.372 $\text{g}\cdot\text{m}^{-2}\cdot\text{d}^{-1}$ respectively) whereas the secondary release rates (calculated from M2 to M12) are very similar (0.065 and 0.069 $\text{g}\cdot\text{m}^{-2}\cdot\text{d}^{-1}$ of Al and 0.144 and 0.151 $\text{g}\cdot\text{m}^{-2}\cdot\text{d}^{-1}$ of Si for no additions and + 5wt.% $\text{Na}_2\text{B}_4\text{O}_7$ respectively). The formulation HIPed ground ash + 5 wt.% NaAlO_2 had greater normalised mass loss of Al and Si than the other two formulations, with a greater initial and secondary release rate for both elements. The similarity in the normalised elemental mass losses of Al and Si for these formulations suggests that the elemental loss of both elements is occurring from the same phase or phases where Al and Si are associated together, by the same mechanism or mechanisms. This suggests that the change in composition and waste loading affects the location of both Al and Si within phases in the samples in the same way.

The normalised elemental mass loss of Zn from the no additions formulation did not present a linear relationship with time unlike all other elements measured; attempts to apply a linear fit to the normalised mass loss of Zn when plotted against the square root of time were unsuccessful, demonstrating that the release of Zn was not purely diffusion based. Additions of glass formers resulted in a change in release rate from non-linear to two periods with a constant release rate, and a reduced loss of Zn, more significantly for the + 5 wt.% $\text{Na}_2\text{B}_4\text{O}_7$ formulation.

Table 36. A summary of the linear fits applied to normalised element mass loss data showing gradient (m), which is an estimate of release rate ($\text{g}\cdot\text{m}^{-2}\cdot\text{d}^{-1}$), and goodness fit (R^2) of linear fits 1 (day 7 to day 28) and 2 (M2 (day 61) to M12 (day 365)).

	Ground ash with no additions		Ground ash + $\text{Na}_2\text{B}_4\text{O}_7$		Ground ash + NaAlO_2	
	Linear fit 1 m ($\text{g}\cdot\text{m}^{-2}\cdot\text{d}^{-1}$)	Linear fit 1 R^2	Linear fit 1 m ($\text{g}\cdot\text{m}^{-2}\cdot\text{d}^{-1}$)	Linear fit 1 R^2	Linear fit 1 m ($\text{g}\cdot\text{m}^{-2}\cdot\text{d}^{-1}$)	Linear fit 1 R^2
Na	3.564(656)	0.936	1.331(77)	0.993	12.276(3330)	0.872
Ba	0.059(9)	0.955	1.090(95)	0.985	0.649(29)	0.996
Al	0.048(1)	0.998	0.172(15)	0.985	0.282(6)	0.999
B	-	-	0.521(50)	0.982	-	-
Si	0.091(3)	0.997	0.372(35)	0.983	0.444(7)	0.999
Zn	-	-	0.076(6)	0.989	0.265(12)	0.996
	Linear fit 2 m ($\text{g}\cdot\text{m}^{-2}\cdot\text{d}^{-1}$)	Linear fit 2 R^2	Linear fit 2 m ($\text{g}\cdot\text{m}^{-2}\cdot\text{d}^{-1}$)	Linear fit 2 R^2	Linear fit 2 m ($\text{g}\cdot\text{m}^{-2}\cdot\text{d}^{-1}$)	Linear fit 2 R^2
Na	0.115(7)	0.966	0.210(7)	0.989	0.622(16)	0.994
Ba	0.006(1)	0.959	0.292(5)	0.998	0.280(4)	0.998
Al	0.065(1)	0.995	0.069(1)	0.998	0.144(1)	0.999
B	-	-	0.205(4)	0.997	-	-
Si	0.144(4)	0.992	0.151(2)	0.998	0.269(1)	1
Zn	-	-	0.027(1)	0.999	0.068(4)	0.964

Additions of + 5 wt.% $\text{Na}_2\text{B}_4\text{O}_7$ and + 5 wt.% NaAlO_2 presented significantly higher losses of Ba than the no additions formulation. The + 5 wt.% $\text{Na}_2\text{B}_4\text{O}_7$ formulation had a higher initial release rate (1.090 $\text{g}\cdot\text{m}^{-2}\cdot\text{d}^{-1}$) than + 5 wt.% NaAlO_2 (0.649 $\text{g}\cdot\text{m}^{-2}\cdot\text{d}^{-1}$), however the secondary release rates for both formulations were very similar (0.292 and 0.280, respectively $\text{g}\cdot\text{m}^{-2}\cdot\text{d}^{-1}$).

Normalised mass loss for Na for both the no additions and + 5 wt.% NaAlO_2 formulations showed very high losses, initial release rates, and large uncertainties. This high initial loss may be caused by the presence of Na on the surface of the monoliths at the beginning of the leaching set up, but how two sets of samples could become contaminated with Na while the third did not is unclear. The presence of Na on the surface is in good agreement with the data for the no additions formulation, as the secondary release rate (0.124 $\text{g}\cdot\text{m}^{-2}\cdot\text{d}^{-1}$) is within the range of secondary release rates of other

elements. However, the secondary release rate for Na from the + 5 wt.% NaAlO₂ formulation (0.622 g.m⁻².d⁻¹) is more than double the next highest secondary release rate (0.280 g.m⁻².d⁻¹, Ba from + 5 wt.% NaAlO₂). The + 5 wt.% Na₂B₄O₇ formulation had Na mass loss which was more consistent with the release of elements, e.g. Ba, however the uncertainties are still very large. One possible cause is the high concentration of K in the leachate which caused severe ionisation issues during ICP and resulted in problems measuring Na.

There was no significant increase, decrease or trend in pH over the sampling period of 18 months in the aliquot taken from any of the formulations.

XRD data collected from the month 3 and month 12 sacrificial samples for each formulation (Figure 58) did not display any additional reflections associated with new phases, or any significant variation in the relative intensity of different peaks associated with different phases.

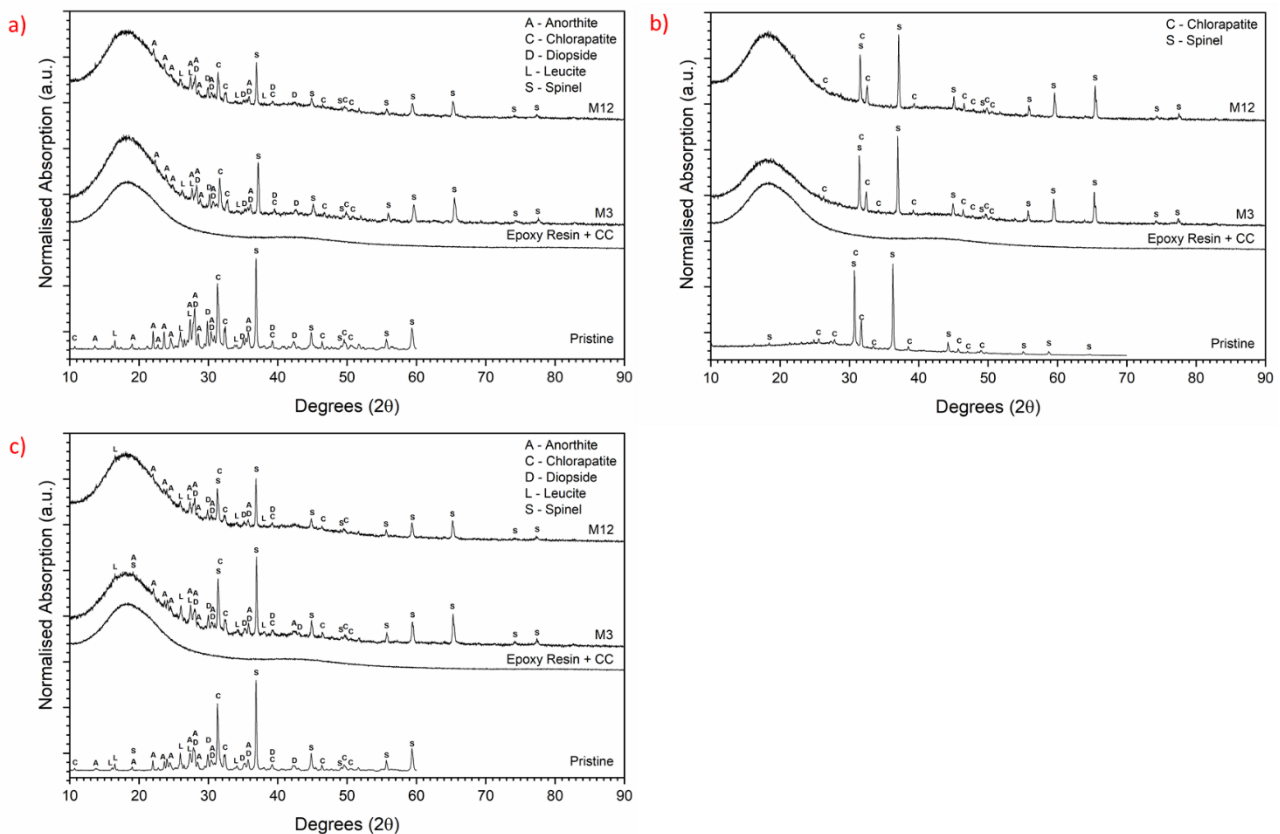


Figure 58. XRD data collected from pristine, month 3 and month 12 post dissolution samples of a) HIPed ground ash, b) HIPed ground ash + 5 wt.% Na₂B₄O₇ c) HIPed ground ash + 5 wt.% NaAlO₂.

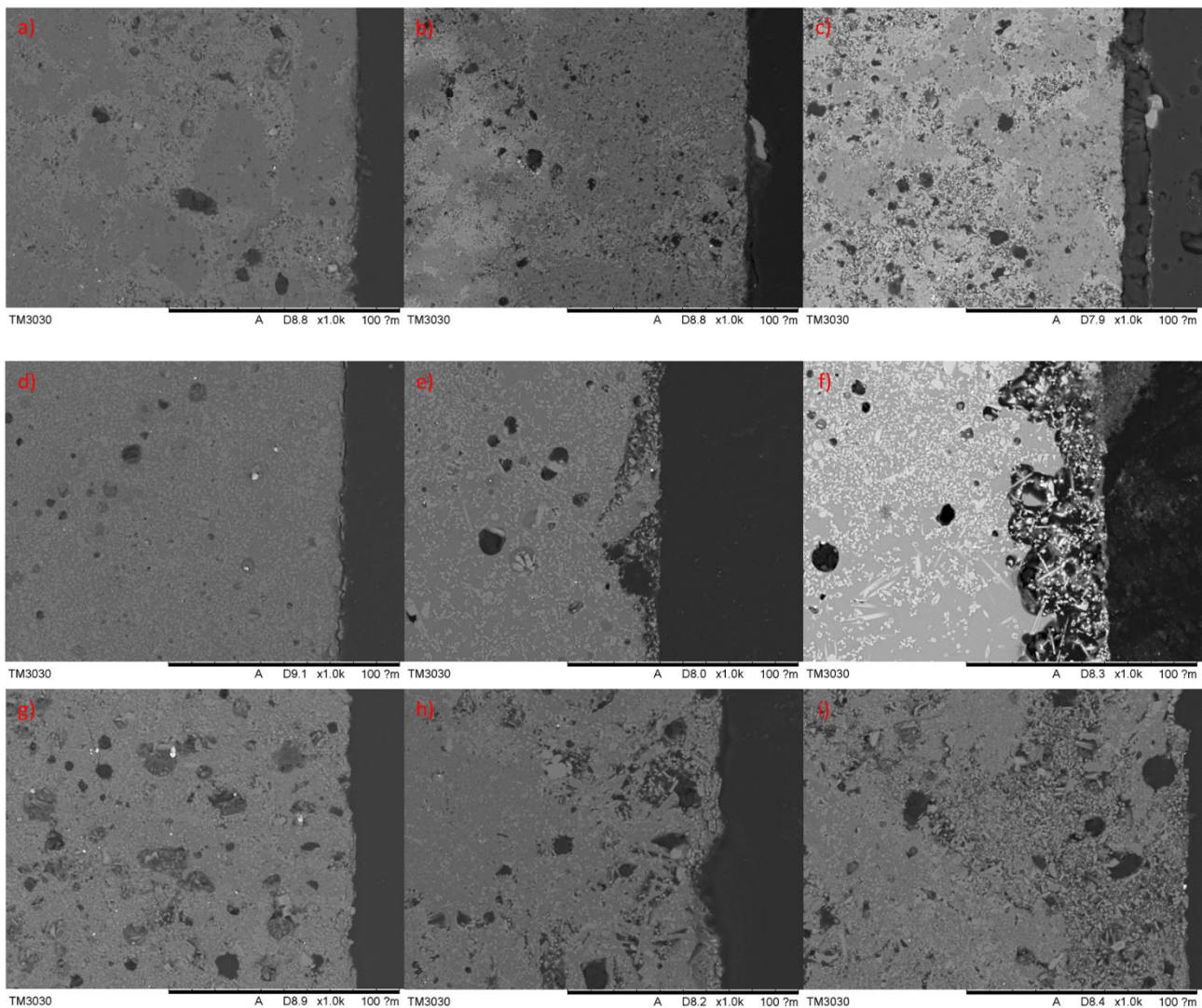


Figure 59. SEM BSE micrograph of monoliths of: HIPed ground ash a) pristine, b) 3 months and c) 12 months; HIPed ground ash + 5 wt.% $\text{Na}_2\text{B}_4\text{O}_7$ d) pristine, e) 3 months and f) 12 months; and ground ash + 5 wt.% NaAlO_2 g) pristine, h) 3 months and i) 12 months.

SEM data (Figure 59 a-c) collected from the no additions formulation shows a developing alteration region, which by month 12 was present along the exterior of the sample, with a consistent thickness ca. 10 μm . Brighter phases, possible precipitates can be seen on the exterior edge of the alteration region, at both month 3 and month 12. These have been identified by EDX as a K and S rich phase on the month 3 sample, and a Ca rich phase on the month 12 sample. XRD data did not indicate the presence of additional phases, so a specific structure cannot be attributed to these phases.

An alteration region can also be seen developing in the SEM images collected from the ground ash + 5 wt.% $\text{Na}_2\text{B}_4\text{O}_7$ formulation. The width of this alteration region varied significantly at both month 3 (5-20 μm) and month 12 (20-90 μm). EDX mapping (Figure 60) of the alteration region showed a decrease in Na, Al, Si, and Ca compared to the bulk, which appears to be associated with the loss of the glassy matrix. An increase in C concentration, is attributed to the penetration of epoxy resin into the alteration region. Crystals of a P, Cl and Ca rich phase, attributed to chlorapatite and smaller crystals of a Na and Al rich phase, thought to be some form of spinel, are still present within the altered region. There also is a Mg rich phase present at the outer edge of the alteration region, which has not been identified.

Examination of the SEM of the ground ash + 5 wt.% NaAlO₂ formulation revealed no indication of an alteration region for samples up to 12 months, and EDX mapping did not indicate any notable variation in element concentration at the edge of the monoliths.

Additional information on the post-mortem characterization of studied specimens and leachates analysis is available in [USFD Data collection Task6 form.xlsx](#). (available to PREDIS partners).

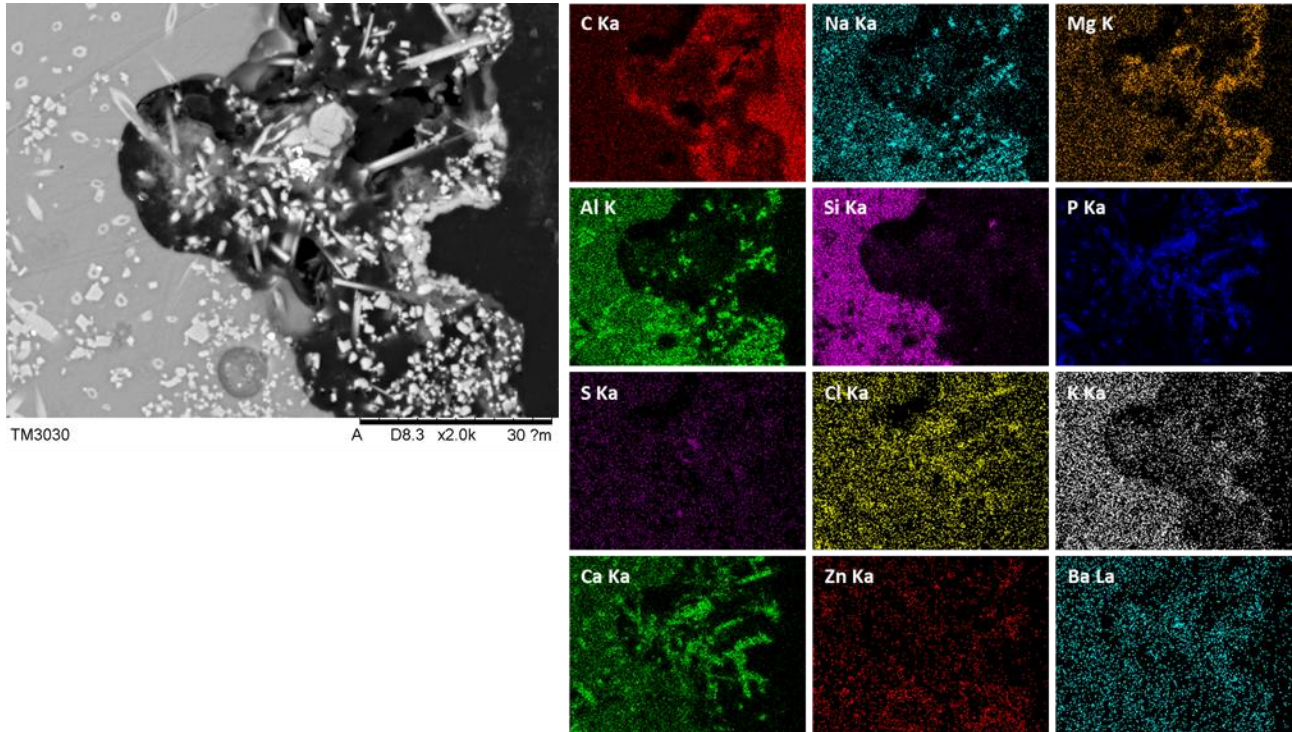


Figure 60. SEM BSE micrograph and EDX element maps of sacrificial sample of HIPed ground ash + 5 wt.% Na₂B₄O₇ removed at month 12.

9 SCK CEN CONTRIBUTION on HiPed samples

9.1 Samples preparation

9.1.1 Waste

IRIS ashes were characterized by CEA (SEM-EDX, XRD...) (see Chapter 7.1.1). The elemental composition is given in Table 37.

Table 37: IRIS ashes composition in weight %.

Element	Al	Si	Ca	Zn	K	Mg	P	Cl	Na	S	Ni, Ti, Fe, Ba, C, Bi, Cr
Weight %	15.1	13.7	9.7	5.8	3	2.7	1.8	1.7	0.7	0.6	<0.5 each

9.1.2 Matrix

95 wt.% of IRIS ashes were mixed with 5 wt.% of $\text{Na}_2\text{B}_4\text{O}_7$ to produce a glass-ceramic by Hot Isostatic Pressing (HIPing) at the University of Sheffield (UoS). (see Chapter 8.1.2)

9.1.3 Waste encapsulation protocol

HIPing was used as thermal treatment route to immobilize the waste. First, the welded cans were heated to 300 °C for ~12 hours under vacuum and sealed. Afterwards, they were HIPed at 250 °C and 100 MPa for 2 hours. The composition of the HIPed samples was not provided by UoS, so a theoretical composition was used for the calculations (Table 38).

Table 38: Theoretical composition of the HIPed ashes.

Element	Al	Si	Ca	Zn	Ba	Na	B
g element i / g sample	0.1435	0.1302	0.0922	0.0551	< 0.0047	0.0181	0.0107

9.2 Leaching protocols

For the leaching tests with the HIPed samples, the reference protocol described in the Milestone MS39 [5] was used. The elemental concentrations in the leachates were determined by ICP/MS. The unaltered and leached samples after 3 months, 1 year and 2 years were characterized by SEM-EDX and XRD.

9.3 Results

As requested in the reference leaching protocol, the temperature was constant at $22 \pm 2^\circ\text{C}$ throughout the tests. The pH was also constant at the reference pH value of 12.7 ± 0.1 between two samplings (or solution renewals). The K, Mg, Bi, Ca and SO_4^{2-} concentrations were similar to those measured in the PREDIS water. Many elements were not detected or their concentration was below the quantification limit (low t° , low SA/V, renewal of the leaching solution, dilution of the samples). Si, Al, B, Zn, Na, and Ba concentrations were used to calculate the cumulative normalized mass loss and the cumulated fraction release. Note that because the Ba content is below the value given in Table 38, the NL(Ba) values are higher than those reported; for Na the concentrations were close to that measured in the PREDIS water and sometimes even lower; for Zn some measurements were not consistent, so they were not used in the calculations. Figure 61 shows the cumulative normalized mass loss as a function of time for the elements measured in the leachates.

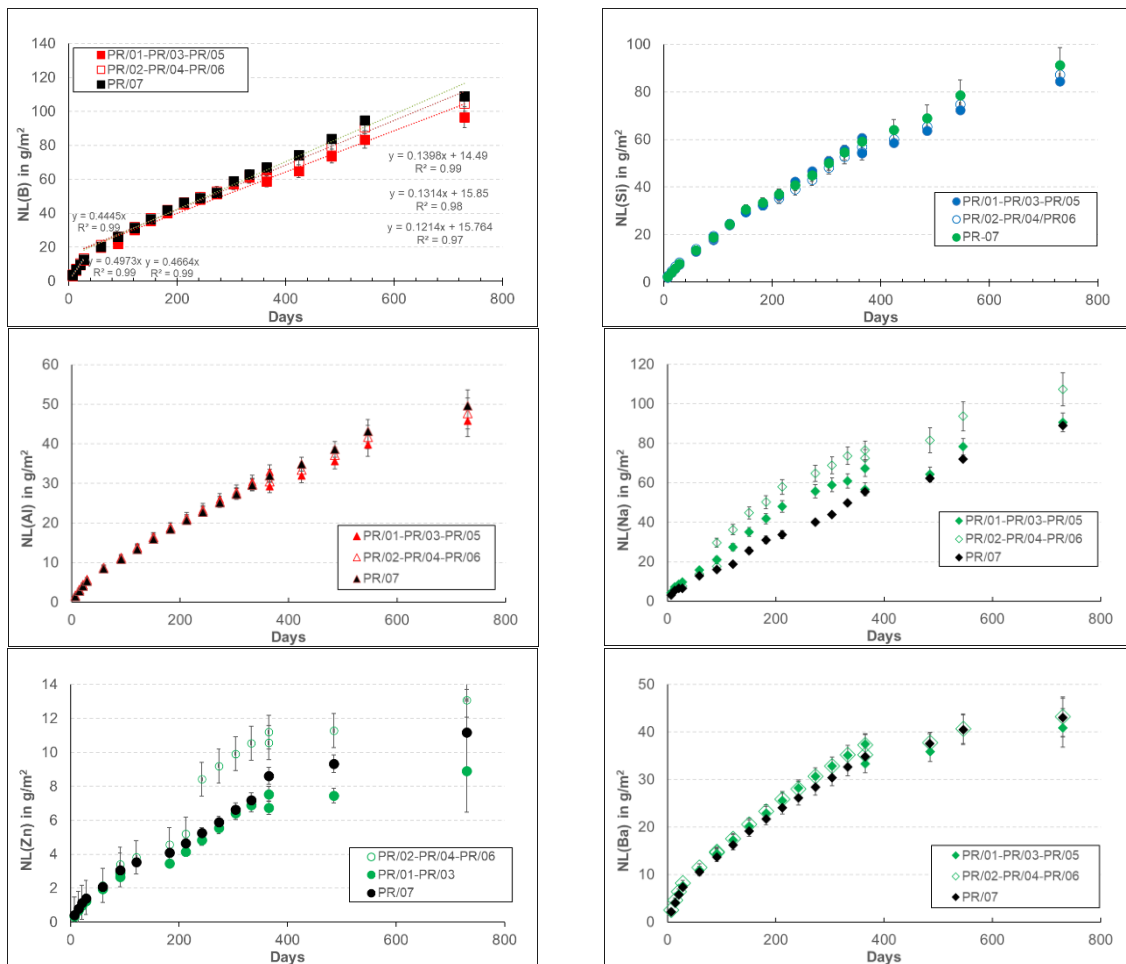


Figure 61: Cumulative normalized mass loss of B, Si, Al, Na, Zn and Ba as a function of time.

Dissolution rates are given by the slopes of the linear regressions from the NL(B) data, as shown in Figure 61. An average maximum dissolution rate of $(4.69 \pm 0.39) \times 10^{-1} \text{ g/m}^2\text{d}$ was found between 0 and 28 days. This rate is of the same order as that measured for borosilicate glass altered in KOH at pH 12.5 and 30 °C performing dynamic tests ($2 \times 10^{-1} \text{ g/m}^2\text{d}$). Between 28 and 730 days, the rate decreased slightly to $(1.31 \pm 0.14) \times 10^{-1} \text{ g/m}^2\text{d}$. Based on the ANSI/ANS-16.1-2019 standard [7], average effective diffusion coefficients and leachability indexes (LI) were determined; they were between 3.87×10^{-12} and $3.77 \times 10^{-10} \text{ cm}^2/\text{s}$ and 9.42 and 11.27, respectively. The lowest LI was obtained from the B data and the highest LI from the Zn data.

SEM pictures of the leached HIPed samples revealed the presence of an amorphous alteration layer in which crystalline phases with structures similar to those present in the unaltered samples were observed. From semi-quantitative EDX analysis a wide range of atomic percentages was measured both in the amorphous alteration layer and in the crystalline phases. Moreover, the high oxygen content in some analyses indicates the penetration of the epoxy resin in the alteration layer. SEM-EDX analysis suggests that the amorphous matrix of the unaltered HIPed sample was dissolved and then, the dissolved elements recondense to form an amorphous alteration layer, which still contains the crystalline phases originally present. This is consistent with the better chemical durability of the crystalline phases compared to amorphous phases. After 3 months, 1 year and 2 years of alteration, the peaks of the XRD patterns were attributed to calcium chloride phosphate and magnesium and zinc aluminium oxides. However, a few peaks were also present, but it was not possible to identify the corresponding crystalline phases (Figure 62).

While the alteration layer was not present on the whole surface of the sample after 3 months of alteration, it was observed on all sides of the sample after 2 years with a mean thickness of 45 μm , which was 1.7 times higher than that after 1 year (Figure 63). However, in some areas, the alteration

layer thickness was larger reaching up to 80 μm and even $\sim 190 \mu\text{m}$, occasionally. The areas where thick alteration layers were observed corresponds to areas where pores were originally present at the sample surface (or were very close to the sample surface), allowing the ingress of the leaching solution further in the sample.

Additional information on the post-mortem characterization of studied specimens and leachates analysis are in [SCK KFe Data collection Task6.6.xlsx](#). (available to PREDIS partners).

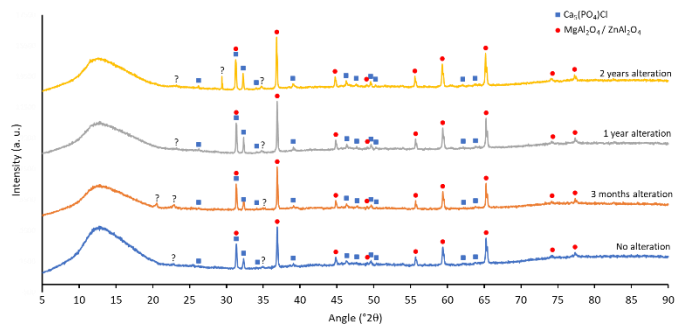


Figure 62: XRD patterns of the HIPed samples (unaltered and altered for 3 months, 1 year and 2 years).

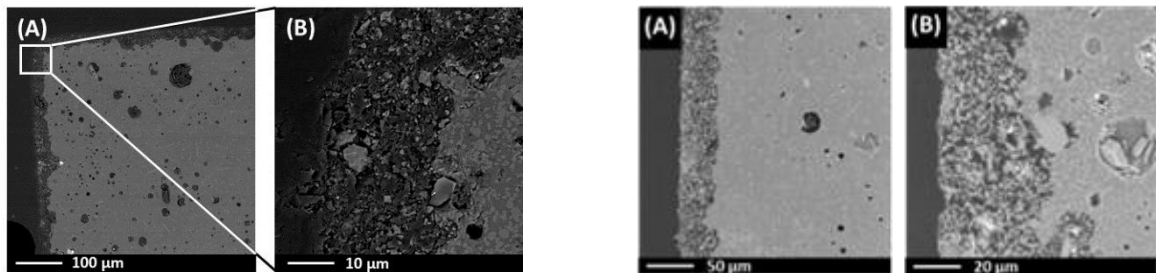


Figure 63: HIPed sample altered for 1 year (pictures on the left) and 2 years (pictures on the right).

10 SUMMARY

According to results obtained, glass-ceramic waste forms allow to immobilize the greatest waste loadings (up to 95%wt.), showing the greatest chemical stability in cementitious medium of the three types of the conditioning matrices studied. On the contrary, geopolymers exhibit the higher leaching rates for both, matrix constituents (e.g. Al and Si) and contaminants (above all B, Cs, and Sr).

Figure 64 illustrates the normalized mass loss for glass-ceramic and geopolymers waste matrices based on the data provided by different partners. The observed differences in leaching behaviour even between the same matrices (variation in the same plot) are mostly due characteristics of the pretreated waste and the formulations used to produce the final waste forms.

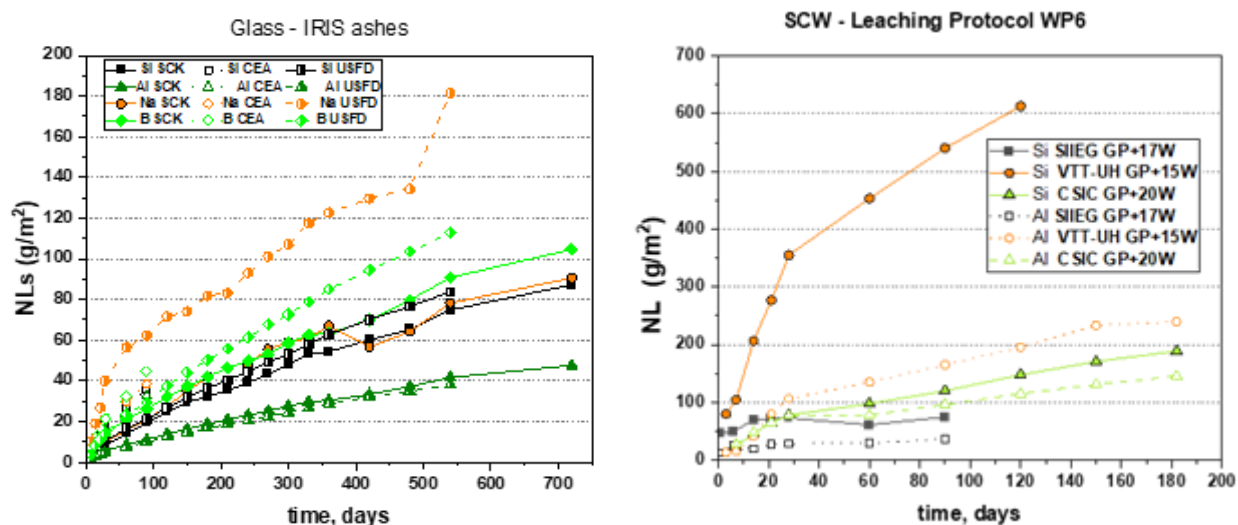


Figure 64. Comparison of leaching results of glass/ceramic matrixes (on left) and geopolymers matrixes in synthetic cementitious water.

In general, hyperalkaline medium ($\text{pH} > 12$) enhances Si and Al leaching in geopolymer-based waste forms. This alkaline-induced dissolution seems to result in a decrease of the retention capacity of the matrix, especially in the case of Cs.

These results highlight the importance of a tailor-made design of the conditioning matrix, considering issues such as physic-chemical nature of the waste or the long-term evolution of the waste/matrix system.

Regarding the type of waste and its compatibility with the cement and geopolymer formulations studied, it should be pointed out that MSO seems to be the most problematic type of waste to be conditioned. MSO waste forms showed poorer mechanical and chemical stability in alkaline medium than waste forms with immobilized thermally-treated wastes. For similar waste loadings, immobilization of ashes from thermal treatments (gasification, pyrolysis, incineration...) in geopolymer and cement produced waste forms with an improved leaching behavior. Thermal treatment increases the chemical stability of waste, not only obtaining a significant waste volume reduction but also improving its disposability.

Post-mortem analyses of the tested waste forms showed that no significant alteration had occurred, in both short- and long-term leaching tests. As an overall conclusion, cement and geopolymer of waste forms meet mechanical and leachability WACs in all cases. However, further studies need to be conducted in order to assess the long-term performance of these novel waste forms under realistic disposal conditions.

As an overall conclusion, cement and geopolymer waste forms tested in task 6 meet mechanical and leachability national WACs. However, further studies need to be conducted in order to assess the long-term performance of these novel waste forms under realistic disposal conditions.

Remarks for future research

On the basis of results obtained in the framework of PREDIS WP6, and in order to increase confidence in these new conditioning alternatives, several issues need to be addressed in the future, for example:

- Long-term compatibility with existing cementitious Engineered Barrier Systems, already in use;
- Impact of irradiation and temperature on the ageing of geopolymer waste forms;
- Extrapolation to long-term disposal (generally 300 years for LILW surface disposal facilities) by using numeral codes;
- Scaling-up: manufacturing of mock-ups and prototypes;
- Use of real waste.

REFERENCES

- [1] IAEA Safety Standards Series, Safety Guide No WS-G-2.5, 2003, Predisposal Management of Low and Intermediate Level Radiactive waste.
- [2] H. Nonnet [2023]. PREDIS Deliverable D6.1. "Summary report: Description of the thermal processes used for the thermal treatment of the RSOW and the physical properties and chemical composition of the resulting treated wastes"
- [3] V. Galek [2023] PREDIS Deliverable D6.2 "Conditioning of ashes of RSOW by geopolymer or cement-based encapsulation"
- [4] EURAD-ACED Deliverable 2.16: Conceptual model formulation for a mechanistic based model implementing the initial SOTA knowledge (models and parameters) in existing numerical tools.
- [5] E. Myllykylä, E. (2021). PREDIS Milestone 39. Definition of the leaching procedure for the short-term experiments and the long-term durability experiments. PREDIS internal report. 7 pp.
- [6] Standard test method for static leaching of monolithic waste forms for disposal of radioactive waste. ASTM standard American Society for Testing and Materials
<https://inis.iaea.org/search/searchsinglerecord.aspx?recordsFor=SingleRecord&RN=30031203>
- [7] ANSI/ANS-16.1-2019 (R2024): Measurement of the Leachability of Solidified Low Level Radioactive Wastes by a Short-Term Test Procedure
- [8] T. Vehmas, *et al.* [2020] 'Geopolymerisation of gasified ion-exchange resins, mechanical properties and short-term leaching studies', in *IOP Conference Series: Materials Science and Engineering*. Institute of Physics IOP, p. 012017. doi: 10.1088/1757-899X/818/1/012017.
- [9] W. R. Bower, *et al.* [2019] 'Metaschoepite Dissolution in Sediment Column Systems - Implications for Uranium Speciation and Transport', *Environmental Science and Technology*, 53(16), pp. 9915–9925. doi: 10.1021/acs.est.9b02292.
- [10] C. M. Fallon, *et al.* [2023] 'Vadose-zone alteration of metaschoepite and ceramic UO₂ in Savannah River Site field lysimeters', *Science of The Total Environment*, 862, p. 160862. doi: 10.1016/J.SCITOTENV.2022.160862.